Optimization of mechanical mixing of anaerobic digesters using computational fluid dynamics (CFD)

Master of Philosophy (MPhil)

Leonhard Wiedemann

Comprehensive parametric optimisation of stirrer based mechanical mixing in anaerobic digesters using experimental techniques and computational fluid dynamics (CFD)

Leonhard Wiedemann

A thesis submitted in partial fulfilment

of the requirements of

De Montfort University

for the degree of

Master of Philosophy (MPhil)

September 2018

Institute of Energy and Sustainable Development

De Montfort University, Leicester (UK)

Copyright

Abstract

To keep biogas production competitive against alternatives in the energy sector, reducing the operating costs is a major challenge for biogas applications. Up to 50 % of the energy consumption in biogas plants is contributed by the digester mixing. Therefore, the optimization of the digester mixing system is a promising approach to increase the overall efficiency of biogas plants. The main objective of the presented thesis is to optimize digester mixing to achieve the highest benefit at the lowest cost. Investigating the mixing process in digesters is a necessary precursor for successful design, operation, and increased efficiency in biogas plants. However, observation of mixing in digesters under real conditions is complex and cost intensive. With an adapted mixing system, a reduction of the operating costs of up to 30 % is possible. Process disturbance and maintenance costs can be minimized and the biogas production within a given digester volume can be maximized. The work shows the process and results of a simplified approach to simulate the mixing dynamic in a common cylindrical digester with computational fluid dynamics (CFD). The CFD simulation is verified by laboratory experiments. Based on the theory of similarity, at the Institute of new Energy Systems of the Technische Hochschule Ingolstadt, a 1:12 scale digester model was set up and an artificial chemical substrate was selected to mimic the rheology of real biomass. Different mixing regimes were configured using propellers and paddle stirrers located in varying positions. Optical and acoustic techniques were employed to observe the fluid dynamics in the laboratory experiment. In this thesis, the laboratory setup and the results on the flow velocity and torque on stirrer shaft developed during mixing are presented and discussed. The experimental are used to validate the similar numeric computational fluid dynamic study.

Keywords: Biogas digester, mixing, rheology, flow characteristic, computational fluid dynamics (CFD) simulation, laboratory digester, artificial chemical substrate, mixing process, stirring configurations, particle image velocimetry (PIV), acoustic doppler velocimetry (ADV).

Acknowledgements

Firstly, I must thank my supervisors at De Montfort University Leicester Professor Dr Bogumil Ulanicki, Professor Dr Adam Moroz, Professor Dr Rick Greenough and Dr Tomasz Janus for their comprehensive support and comprehensive insight throughout the research and thesis documentation. Additionally, the author would like to thank UTS Products GmbH in Dorfen (Germany) for cooperation. The work was financial supported by the German Federal Ministry of Education and Research within the program “Forschung an Fachhochschulen” under the grant number “BioOpt-Mix, 03FH031PX4”.

Furthermore, I am very thankful to my partner in life Anne and my two children Elena and Mathilda for their enduring support, encouragement and understanding when often the work rank first.

Moreover, I am very grateful to the students and colleagues who accompanied me during the years at the CENTRE OF EXCELLENCE FOR RENEWABLE ENERGY RESEARCH, especially to Matthias Sonnleitner, Georg Häring, Abdesammad Saidi and Dr Fosca Conti. They gave me support whenever needed and made the university in Ingolstadt much more than just a place to work.

Finally, I would like to thank my parents Maria and Leonhard as well as my brothers and sisters for their support and their encouragement throughout the work.

I declare that the content of this submission is my own work. The contents of the work have not been submitted for any other academic or professional award. I acknowledge that this thesis is submitted according to the conditions laid down in the regulations. Furthermore, I declare that the work was carried out as part of the course for which I was registered. I draw attention to any relevant considerations of rights of third parties.

Table of Contents

Appendix

Appendix A: CFD study parameter settings

Appendix B: CFD calculated flow velocities at subregions

Appendix C: CFD calculated flow velocities of digester overall, Thrust and Torque at mixer blades as well as Uniformity Index

Appendix D: List of Publications

List of Figures

List of Tables

Abbreviations

ADV	Acoustic Doppler Velocimetry
CFD	Computational Fluid Dynamics
CAD	Computer Added Design
DBFZ	Deutsches Biomasse Forschungszentrum
DM	Dry Matter
DoF	Degree of Fulfilment
EB	economic benefit
FNR	Fachagentur für Nachwachsende Rohstoffe
MRF	Moving Reference Frame
PBM	Parts Based Mesher
PIV	Particle Image Velocimetry
pTB	criterion individual technical benefit
RANS	Reynolds-Averaged-Navier-Stokes equations
TB	technical benefit
ΣTBS	individual technical score of a mixer setting
2D	two dimensional
3D	three dimensional

Symbols

λ	scale factor	[-]
d_R	the characteristic diameter	[m]
ρ	density of the fluid	[kg/m³]
η_a	dynamic viscosity	[kg/m*s]
N	rotational speed (stirrer)	rpm
Re	Reynolds number	[-]
$Re_{full\text{-}scale}$	Reynolds number full scale	[-]
$Re_{lab\text{-}scale}$	Reynoldsnumber laboratory scale	[-]
T_{air}	Torque stirrer without fluid	[Nm]
$T_{substrate}$	Torque with stirrer fluid immersed	[Nm]
T_{blades}	hydraulic effective torque at blades	[Nm]
UI_{mag}	Uniformity Index magnitude (velocity)	[-]
UI_x	Uniformity Index x-direction (velocity)	[-]
UI_y	Uniformity Index y-direction (velocity)	[-]
UI_z	Uniformity Index z-direction (velocity)	[-]
V_c	cell Volume	
α	horizontal orientation angle of mixer	[°]
β	vertical incline angle of mixer	[°]
y^+	wall distance (CFD specific)	[-]
u_*	“friction” velocity close to wall (CFD)	[m/s]
υ	fluids local kinematic viscosity (CFD)	[m²/s]
y	distance to wall (CFD)	[m]
v_m	average flow velocity	[m/s]
v_{msub}	average flow velocity subregion	[m/s]
k	consistency factor (power law fluid)	[Pa*s^n]
n	flow index (power law fluid)	[-]
P	power	[W]
P_{shaft}	power on the mixer shaft	[W]
P_{el}	electric power	[W], [kW]
z%	velocity vector component in the z direction	[%]
$\phi_c, \overline{\phi}$	value and average of a selected vector/scalar	

1 Introduction

1.1 Background and motivation

Growing energy demands require the continual development of strategies concerning renewable energies. Anaerobic digestion has received increased interest in the panorama of sustainable energies, especially in Germany according to FNR (2017) and DBFZ (2016). Anaerobic digestion is a method of breaking down organic substances with microbes produce biogas for use as renewable energy source. Anaerobic digestion starts with bacterial hydrolysis of organic materials, followed by a series of complex biological processes, and results in the production of a gas composed mostly of methane. The digestion process occurs within an enclosed vessel commonly called a fermenter or digester. These digesters are available in different shapes such as rectangular, egg-shaped, or cylindrical as stated by Subramanian et al. (2014; 2015). Cylindrical digesters with large diameter to height ratios (see figure 1) are most common in German biogas plants DBFZ (2012).

Figure 1: examples of biogas plants with cylindrical digesters. (Agrarheute 2016 u. 2017)

An overview of research achievements of bioconversion of organic waste to energy can be found in Mao et al. (2015) and Kiran et al. (2014). To maximize gas production and create optimal conditions for decomposition of organic materials in the digester mixing to homogenize the biomass volume is necessary.

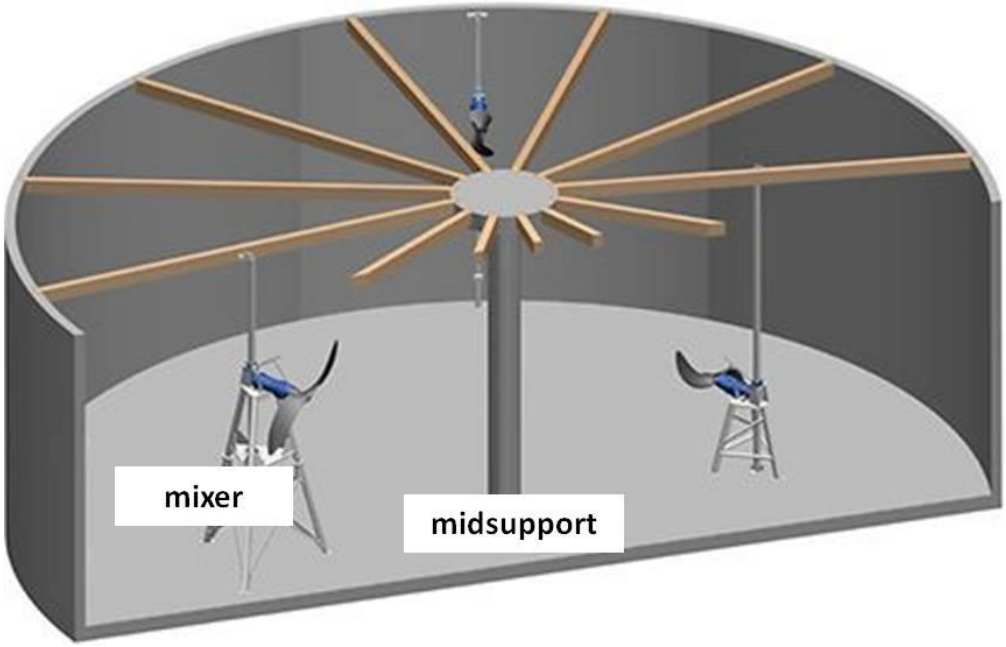

Figure 2: View inside a common cylindrical digester with midsupport and an example of propeller bladed mixers (KSB 2017)

Mixing creates a homogeneous substrate inside the digester and brings the freshly introduced biomass in contact with the microbes. Poorly mixed zones with concentration peaks and lows, as well as settling at the bottom of the digester and scum at the sludge surface are prevented. Mixing enables utilization of the entire digester volume for a maximum possible conversion of biomass and consequently maximum biogas production within a given digester. However, cost-benefit analyses indicates that mixing is the highest contributor to the total energy consumption in biogas plants as Sonnleitner (2012) and Poeschl et al. (2010) mentioned. Considering the total efficiency of biogas plants, the mixing energy is a parasitic contributor, which needs to be reduced. Thus, spatial and operational configurations of agitators are fundamental parameters to optimize. Testing of different mixing regimes is required to understand mixing characteristics in digesters and achieve high efficiency mixing. It is not economically feasible to perform these tests on an industrial scale biogas plant. Therefore, laboratory scale experiments emerge as a convenient and appropriate approach to investigate the mixing in full scale anaerobic digesters. Aivasidis et al. (1990) concluded that experiments in the laboratory on a scaled down digester can provide data to design industrial scale anaerobic digesters. Gallert et al. (2003) have confirmed the correspondence between a laboratory scale and a full scale digester.

More recently, Brunn et al. (2009) have explained that the application of laboratory scale experiments to industrial scale is critical in the case of anaerobic waste (municipal sludge) treatment.

Despite its importance, cases where excessive mixing have been detrimental to the biogas process have also been reported. In particular, continuous mixing is not necessarily required to achieve good digestion efficiencies, as Stroot et al. (2001) demonstrated, whilst intermittent and low intensity mixing is more likely to produce better efficiencies at lower energy inputs. In particular they showed that high intensity and continuous mixing, particularly at high digester loading rates, resulted in a decrease in the digestion efficiency. The authors mentioned two possible explanations on their observations: first it is likely that higher mixing intensities create high shear rates large enough to break up the microbial flocculation structure, and second, the continuous operation promotes a more rapid hydrolysis than methanogenesis with digestion leading up to accumulation of acids inhibitory to methanogenic bacteria.

Continuous vs. intermittent mixing was also analyzed and compared by Kowalczyk et al. (2013) in a digester of co-digesting cow slurry and dung with energy crops. The authors determined energy savings up to 29% with intermittent mixing compared to continuous operation. Dague et al. (1970) analyzed anaerobic digestion of liquid municipal sludge and observed significantly higher biogas production under discontinuous mixing compared to continuous mixing. The same outcome was stated by Balcha (2014), who investigated the flow dynamic conditions in anaerobic digesters. Subramanian et al. (2014, 2015) additionally showed that larger downtimes of between mixing periods lead to reduced scumming and less digestion process disturbance.

There are three types of mixing systems currently in use. The most used system is a mixer (stirrer) based mechanical mixing system. The other two mixing methods involve recirculation of digester substrate with pumps, and the removal and reinjection of biogas. The most efficient mixing device in terms of power consumed per mixed volume is the mechanical mixer reported by Sindall (2014). This report is focused on the most used mixing system on German biogas plants, a stirrer based mechanical mixing system.

For further assessment of mixer settings or comparison at various digester conditions and sizes some key figures are

- Dry matter (DM) feeding load (daily amount) per digester volume
    - kg(DM)/m³
- Daily energy consumption by digester volume or by daily feeding load
    - Wh/m³
    - Wh/kg(DM)
- Thrust per volume or Torque per volume
    - N/m³
    - Nm/m³

can be helpful.

Investigations on mechanical mixing can be made experimentally on real plants. But due to the immense efforts which are necessary for valuable investigations on real plants it is helpful to do experiments in laboratory scale plant or use simulation via PC with computational fluid dynamics (CFD).

With the use of a down scaled similar model it is possible to investigate the flow dynamic under reasonable effort. However, laboratory experiments are limited in flexibility rendering comprehensive parametric studies with numerous measurements challenging and time-consuming.

With the increase of computational capacity, numerical simulation with computational fluid dynamics (CFD) becomes an increasingly powerful tool for investigation of complex parametric studies (Craig et al., 2013; Ding et al., 2010; Wang et al., 2010). Laboratory experiments can be used as validation tool to the numerical CFD calculations (Conti et al., 2017).

The presented thesis illustrates the optimization of the mixers placement and orientation inside a cylindrical digester to achieve homogeneity. It gives an alternative and helpful way for determination and interpretation of the digesters flow dynamic with computational fluid dynamics CFD. The presented numerical approach contributes to a comprehensive parametric optimization methodology. This enables a practicable optimization to achieve proper mixing quality. The objective is to reduce operating cost for sludge digestion and increased competitiveness of biogas plants.

1.2 Objectives

The objective of the present evaluation consisted of determining the flow characteristics of mixing regimes used in practice in a laboratory scaled-down digester, deriving measurements for favourable operational conditions, and developing a method to monitor flow velocity and mixing power input. The gained data was used for validating a similar laboratory scale numeric computational fluid dynamics CFD simulation. Then the validated CFD simulation (laboratory scale) then is up scaled onto the initial conditions (real dimension) to optimize mixing flow patterns in the real digester.

1.3 Approach, materials and methods

A laboratory-scale digester was designed and constructed to replicate the digesters of full-scale biogas plants. The geometry of a full-scale digester and all ancillary equipment were scaled-down to 1:12. For the laboratory experiments biomass was substituted by an artificial substrate which mimics the rheology of biomass, but has the benefit of being highly transparent, inodorous, and easy and safe to handle (Wiedemann 2017a). Real feed stocks usually vary according to their different origins e.g. domestic, energy crops, wastewater effluents, etc...

The artificial substrate is mixed in the laboratory digester using propeller stirrers, which is the most common way of mixing on German biogas plants. Two mixing configurations were investigated. The fluid velocity of the artificial substrate was observed in the 3D space using particle image velocimetry (PIV) and acoustic Doppler velocimetry (ADV). Data obtained from the two experimental techniques were compared to a computational fluid dynamics (CFD) model. Additionally, flow characteristics were visualized by coloring and decoloring the fluid throughout mixing. Torque moment and power consumption of the propellers and paddle stirrers were recorded periodically to assess the mixers performance. The laboratory data was validated with data obtained from real biogas plants.

2 Reality similar laboratory experiment

First is the creation of a reality similar practical laboratory experiment. These practical experiments are necessary for validation of the subsequent CFD simulation. The method to validate a CFD by comparing the simulated velocities with literature based experimental data of a lab-scale digester was performed by Wu (2010, 2011) and Jacobsen (2015). In the current approach, new experimental data is collected.

As a starting point for the experimental configuration, a real cylindrical digester (see figure 3) with 18m diameter, a fluid filling level 5.50 m of height and a mid-support column is down scaled into laboratory scale with scale factor $\lambda = 12$.

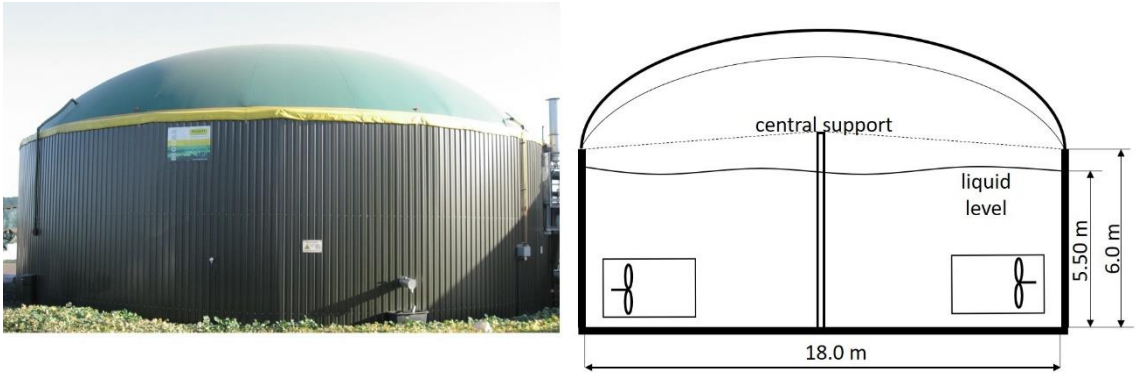

Figure 3: real cylindrical digester used as basis dimensions for the experimental configuration (Uni Mainz 2018)

The following figure 4 shows the downscaled cylindrical model. The model digester, made of polymethylmethacrylate (pmma → acrylic glass), was designed and constructed to maintain geometric similarity of the full-scale digester at a biogas plant (see figure 4). The transparency of pmma allowed for the optical observation of flow dynamics in the vessel.

The cylindrical laboratory digester had the following dimensions:

- 1.5 m in diameter,
- 0.7 m in height
- and total volume of ca. 1.2 m3.

The dimensions were derived from a ca. 2100 m³ total volume real digester (see figure 3) with a 1:12 size reduction in three dimensions. A wall thickness of 15 mm assured the mechanical stability of the laboratory digester. The lab-scale digester was filled to a liquid depth of 46 cm,

which corresponds to ca. 800 l of liquid.

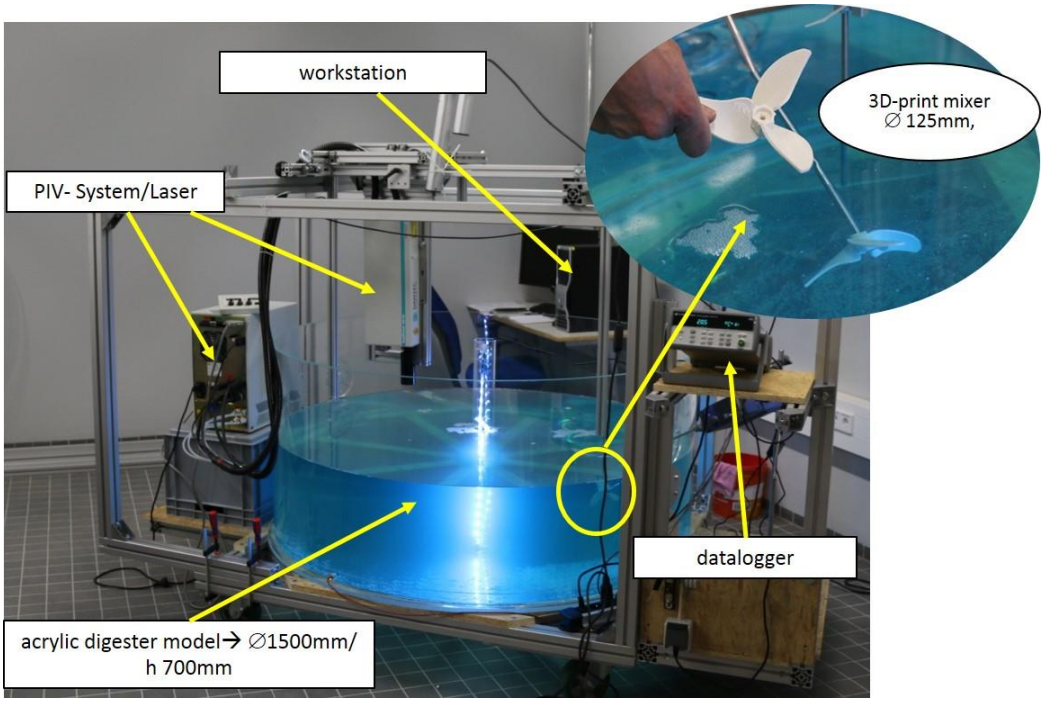

Figure 4: laboratory experimental setup

For the laboratory mixing configuration common types of mixers are chosen, in our case propeller-bladed mixers. Propeller-bladed mixers are mostly used in German biogas plants (German 2012, 2014). These mixers may be completely (plus engine) submersed or partially submerged with the engine mounted outside via a long rod to the propeller blades. Propeller blades of large diameter are increasingly used because of a favorable power input to effective mixing power relationship (Rostalski and Springer 2010).

The propeller mixers are in real use at plants of our project partner UTS. From the CAD drawings the propeller mixer is printed 1/12 scaled with a 3D-printer for the use in the laboratory experiment

Full scale	Laboratory scale (λ = 12)
• ∅1500mm, • rpm 80 – 150	• ∅125mm, • rpm 140

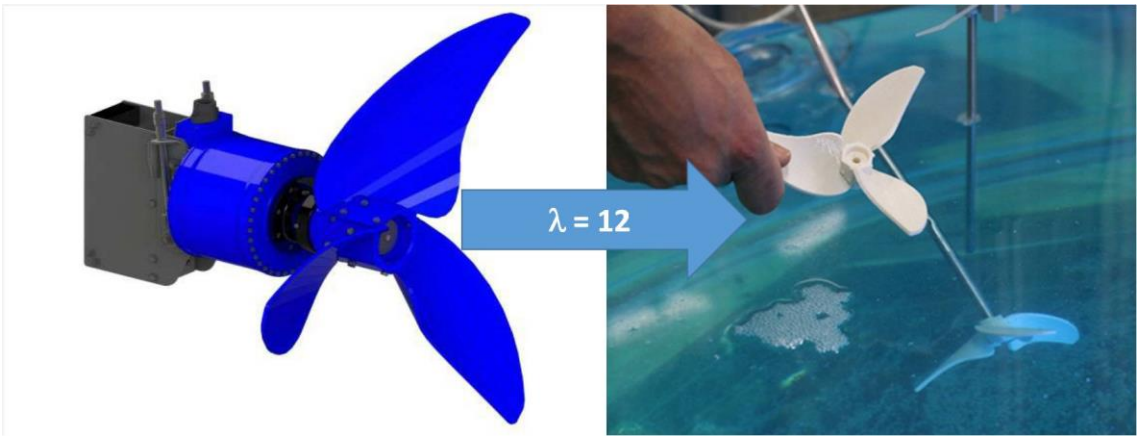

Figure 5: Propeller mixer big diameter (UTS Products GmbH); left: reality picture; right: downscaled 3D-print (laboratory scale)

2.1 Laboratory digester setup

All internal structures present in the real biogas digester were replicated in the scale-down model to the same size reduction factor. Thus, the laboratory tank was equipped with six access holes for insert the stirring shafts at different heights and angles. Mixing in the digester was achieved by two IKA Eurostar 100 control overhead stirrers. Motors for the mixer were placed opposite in the model digester and were equipped with variable speed drivers, for controlling the motor speed via motor input frequency.

Three tmg Gerabert GmbH Pt100 temperature sensors (T1-T3), with accuracy/resolution 1.0°C/0.1°C, were installed at different locations within the tank (see figure 6). The sensors were attached to a 34972A Keysight unit system, equipped with a 34901A 20 channels multiplexer module for data acquisition and logger switching.

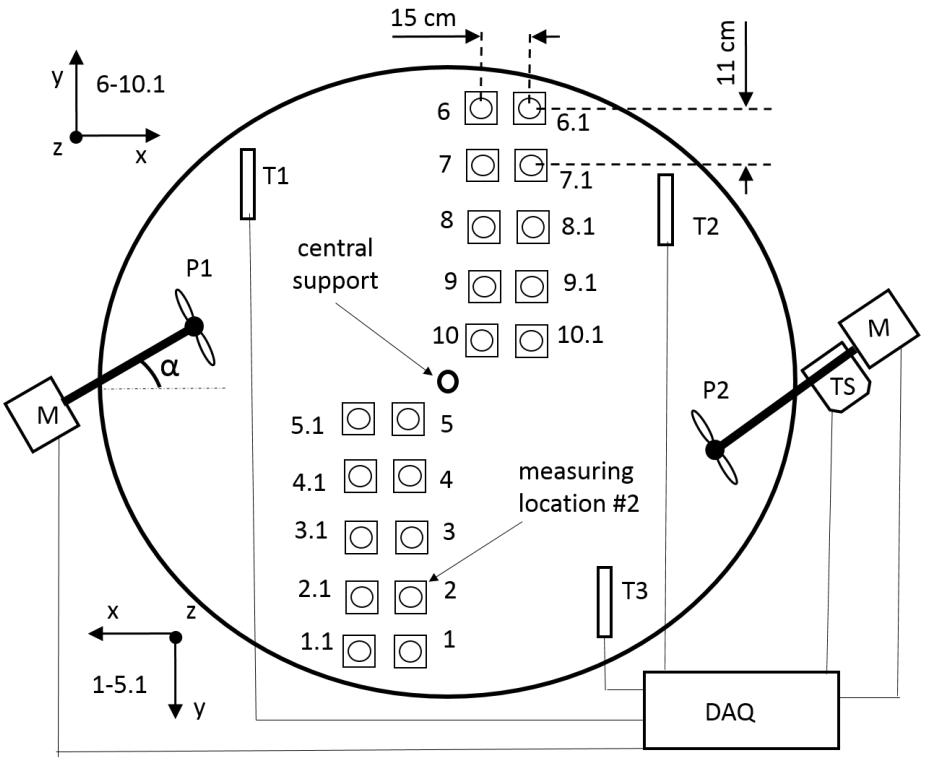

Figure 6: Home-made experimental setup, which is designed to investigate the mixing process.

2.2 Mixing setup and configuration for investigation

Different agitator height and angle configurations could be achieved using the six access holes placed on the wall of the acrylic laboratory tank. To model different flow characteristics with regard to a differentiated validation of the subsequent CFD calculation, various mixing configurations can be chosen for the investigative runs (see figure 9). The shaft of the propellers can be adjusted in various heights and angles α and β. In the following figure 7 two different mixing configurations are shown principally.

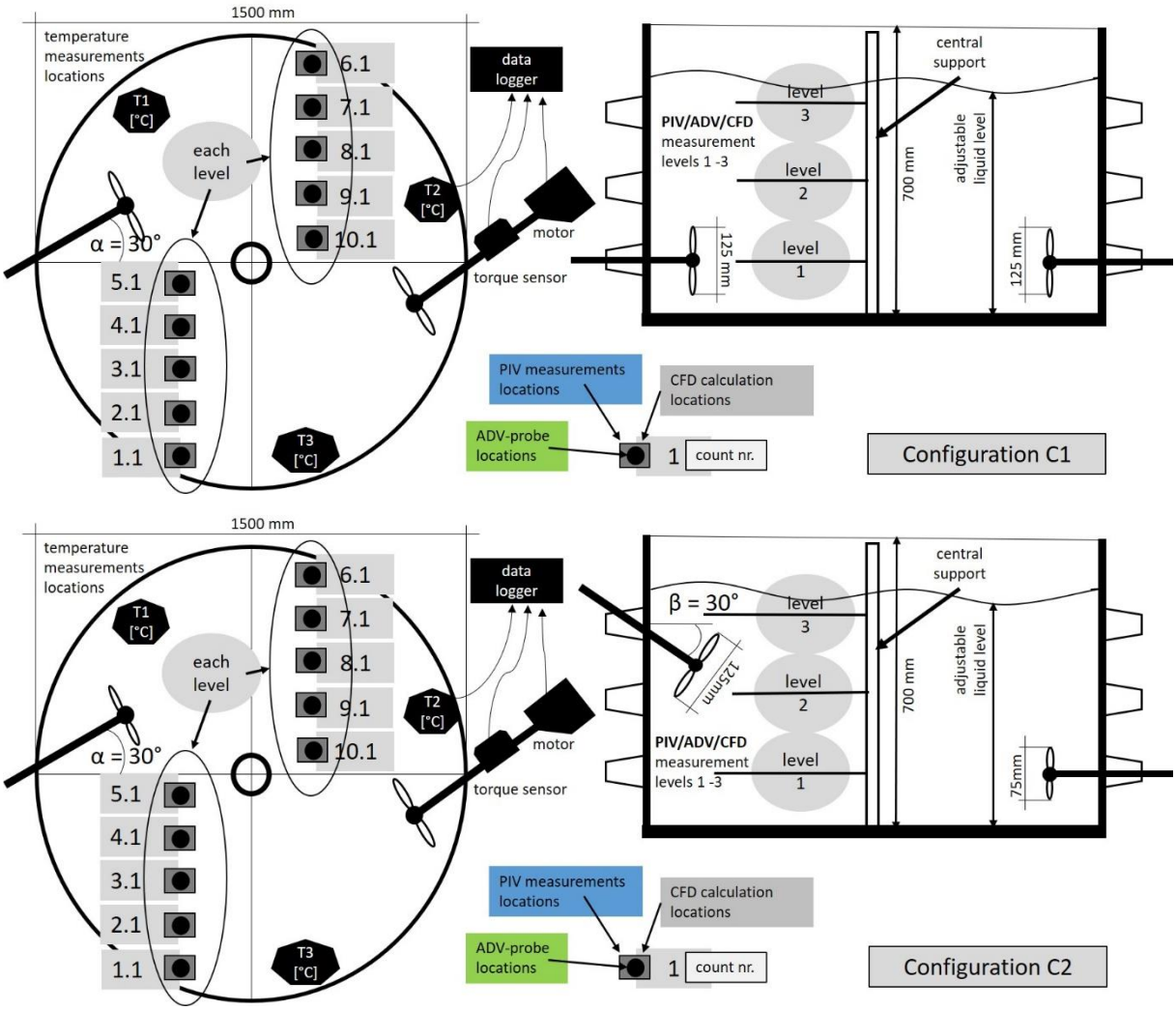

Figure 7 :Schematic representation of mixing configuration C1(above) and C2, which can be used for experimental investigation.

In Configuration C1 two large propellers mimic submersible mixers to simulate symmetrical flow with same propeller mixers and same positioning. The shafts are directed horizontally and located 15 cm from the bottom. In C2 asymmetrical flow with propeller mixer types is modeled. A small propeller is used as submersible mixer horizontally directed 15 cm from the bottom, and a large propeller inclined (simulating an immersed “blender” mixer) forming an angle β = 30° with the plane of the liquid surface. In the C1 and C2 configurations, the shaft of the propeller mixers is horizontally deflected by a deflection angle α = 30° with respect to a straight line through the center of the tank.

The further content of the thesis is focused on the mixing with configuration C1 (two big bladed propeller mixers). Big propeller blades provide more energy efficiency as mentioned by Rostalski and Springer (2010).

2.3 Substrate material for use in laboratory digester

A major impact on the flow dynamic in a digester is from the sludge or substrates rheology. The substrate inside a digester shows more or less shear thinning, non Newtonian behavior (Ratkovich et al., 2013), which strongly influences digester mixing. For the necessary flow some friction has to be overtaken to move the particles. The viscosity is changing during mixing and with mixing intensity. The viscosity and its characteristic is the important value to describe the substrates behavior, but hardly can be measured. Generally fresh material like corn silage is more difficult to mix then “predigested“ material like manure/slurry. The DM is a good measurable value for orientation, but you never know the substrates DM in advance precisely.

While the use of real biogas substrate in laboratory experiments is critical, the creation of a consistent model substrate for the laboratory experiments with similar physical properties to real substrates (see figure 8) is beneficial according to Wiedemann et al. (2017a, 2017b, 2017c, 2017d).

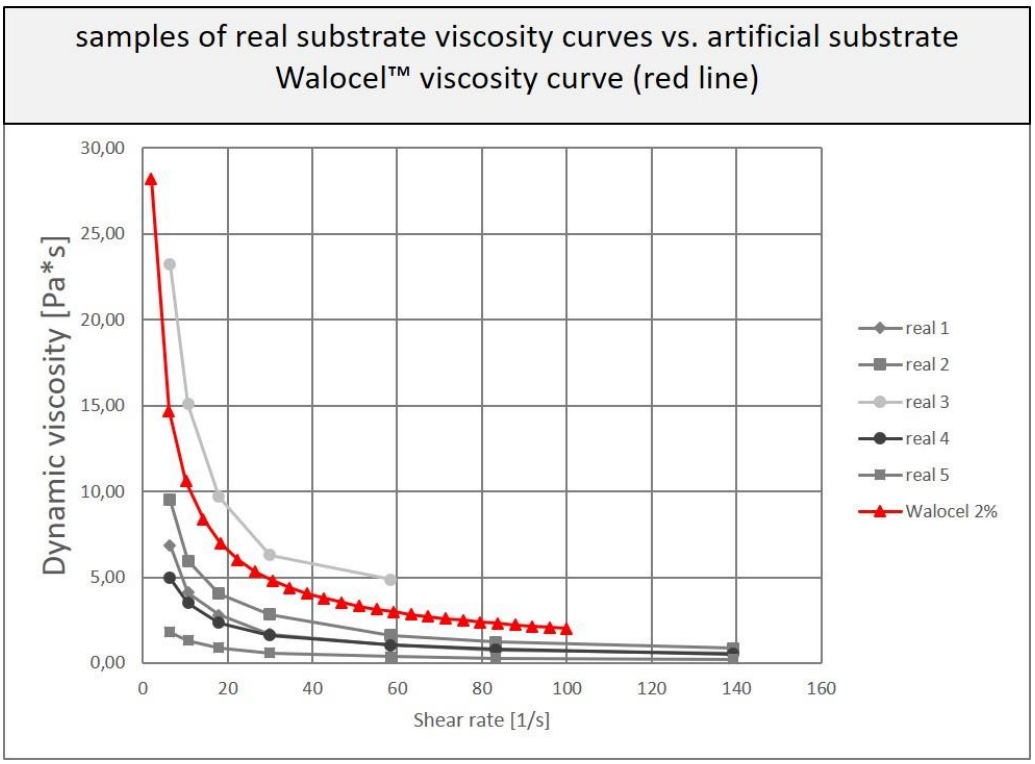

Figure 8: Comparison of real substrate with artificial substrate (Wiedemann et. al 2017a)

A comprehensive description of creating an artificial substrate is given from Wiedemann et al. (2017a).

In addition to the opaqueness and handling difficulties, major challenges in investigating real substrate are the constantly changing properties and conditions. The artificial substrate used in the laboratory experiments provides stable conditions to get comparable and reproducible results. To meet the requirements of the laboratory experiment an artificial substrate with 0.3% of Walocel™ suits best. The substrate provides a non Newtonian behavior, high transparency and fulfills the dynamic viscosity requirements of equal flow conditions from reality to lab-scale ($Re_{full\text{-}scale} = Re_{lab\text{-}scale}$) described in following section 3.1. The comparable behavior of 2,0% with 0.3% Walocel™ is shown in following figure 9.

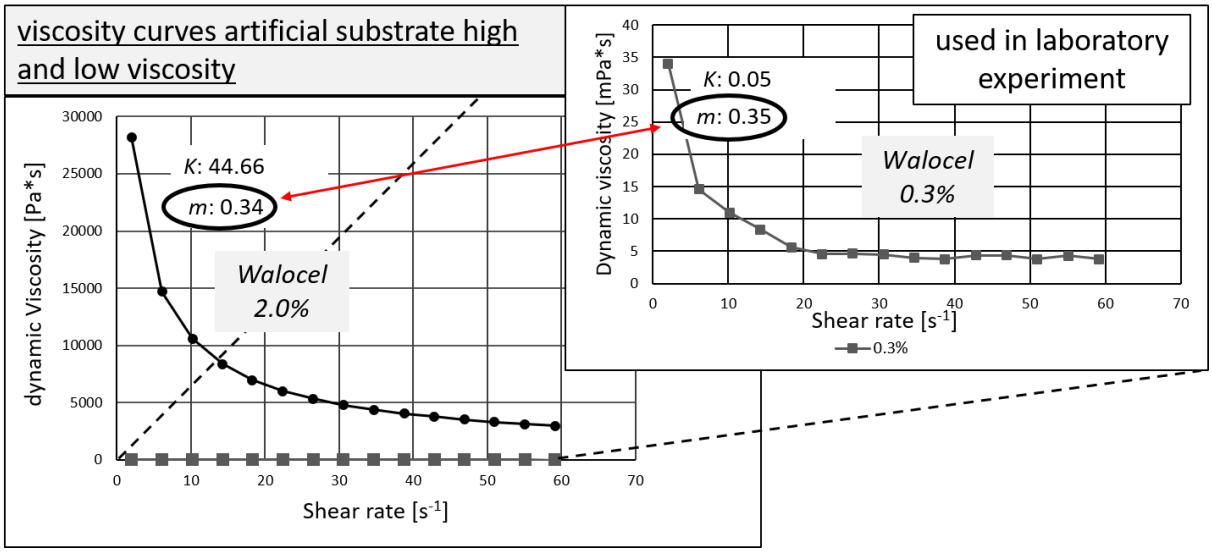

Figure 9: Comparison of viscosity 2,0% with 0.3% Walocel™ (Wiedemann et. al 2017a)

The artificial fluid temperature was maintained at 21°C throughout the study. At that temperature the viscosity characteristic of the chosen artificial substrate is comparable to real substrate characteristic at common mesophilic conditions (≈ 35° - 39°C) in digesters.

At defined locations inside the digester the flow velocity is captured as vector. A laser based Particle Image Velocimetry (PIV) and an ultrasonic based Acoustic Doppler Velocimetry (ADV) was used to measure the flow velocity (Conti et al., 2017). Additionally, the torque is measured on the mixers shaft.

2.4 Preparation of artificial substrate

The artificial substrate was prepared using a sodium carboxymethyl cellulose (NaCMC), which was purchased by Dow Wolff Cellulosics GmbH, Germany, with the commercial name of

Walocel 3000TM [WC]. Initially, the substance was a white powder with a viscosity of 3000 cps. A 0.3% water-cellulose mixture was prepared dissolving 2.5 Kg of Walocel in 800 l of water. To facilitate and speed up the dissolving process, the powder was previously distributed in five cans containing 25 l of water at 25°C. An electric drill equipped with a double spiral liquid stirrer with 20x600x10 mm hexagonal shaft was used for mixing. Afterwards, the five cans were emptied into the laboratory digester and water was added to reach the final liquid volume of 800 l. In the laboratory digester, the artificial substrate was mixed with the spiral liquid stirrer intermittently for three days until complete and homogeneous dissolution.

2.5 Configuration of coloring/decoloring process

The process of iodine / thiosulfate titration equilibrium was used to color and decolor the artificial water-cellulose mixture. The iodometric titration is to reduce iodine with the reduction agent thiosulfate. The intention is to define the time needed to mix fresh added biomass of a feeding cycle completely into the digester. The end point of the reaction, and therefore the mixing time, is the disappearance of the iodine.

Iodine was purchased from AppliChem GmbH (Darmstadt, Germany) as standard 0.5 M volumetric solution. Sodium thiosulfate 0.5 N was purchased from Bernd Kraft (Duisburg, Germany). 750ml iodine 0.5 M were diluted in 1250ml water. The final 2 l solution was used to brown the 800 l water-cellulose solution present in the digester. 500 ml of water was added to 1500ml of sodium thiosulfate 0.5 N. The final 2 l solution was used for decoloring iodine solution, in accordance to the chemical reduction of iodine to colorless iodide and oxidation of thiosulphate anions to tetrathionate (Equation 1):

$$I_2 + 2S_2O_3^{2-} \rightarrow 2I^- + S_4O_6^{2-} \qquad (1)$$

The injection point of the dye is close below the fluid surface, following the common feeding point of real digesters. The coloring and decoloring processes were recorded every 5 seconds by two Canon EOS 1200 D cameras with EF 50 mm lenses and in continuous modality using a GoPro Hero4 video camera.

2.6 Particle Imagine Velocimetry (PIV) configuration

The water-cellulose fluid velocity was measured using PIV technology. Seeding particles are

injected in the fluid and illuminated with a laser sheet. The trajectories of the particles are captured by a high-speed camera in consecutive images. By cross-correlating the images, the fluid velocity can be calculated. The seeding particles were microporous polyamide particles purchased by Dante Dynamics with an average particle diameter of 20 µm. For the 800 l of water-cellulose mixture, 5g of powder were used as tracers to generate light scattering and high visibility signals in the laboratory digester. The PIV setup was composed of a Nd-YAG laser light source (Dantec Dynamics, Erlangen, Germany) running in double-cavity (Q-switched) mode. The excitation wavelength was 1064 nm with pulse duration of 6 nsec. The laser was equipped with special optic components to generate light sheets, which were pulsed to produce a stroboscopic effect, freezing the movement of the seeding particles over time. The position of the illuminated seeding particles was captured by a Nikon AF Micro Nikkor 60mm camera, positioned at a right angle to the laser light sheet. The cameras capture the light reflecting particles with a double picture, synchronized to the double pulsed laser. As a result, particles appear as light specks on a dark background on each camera frame. For the given setup, the time separation between the two images of an image pair was set to 8000 µs. For each experimental run, 8 images were acquired at a trigger rate of 3 Hz. This provided velocity data for the two-dimensional velocity fields. The laser was placed at three different levels (at 14.5, 29.5 and 44.0 cm of height from the bottom of the tank) to illuminate different sections of the fluid in the digester (see the side view of the digester in figure 10-top). For each of the three levels, the movement of the seeding particles used to visualize the liquid flow was captured at 10 positions (1.1 – 10.1) at the camera locations depicted in the top view of the digester in previous figure 7. Indeed, to obtain velocity vector maps, statistics, and spatial correlations of the artificial substrate, 30 measurements positions were set up and investigated. A calibration procedure was conducted prior to each measurement.

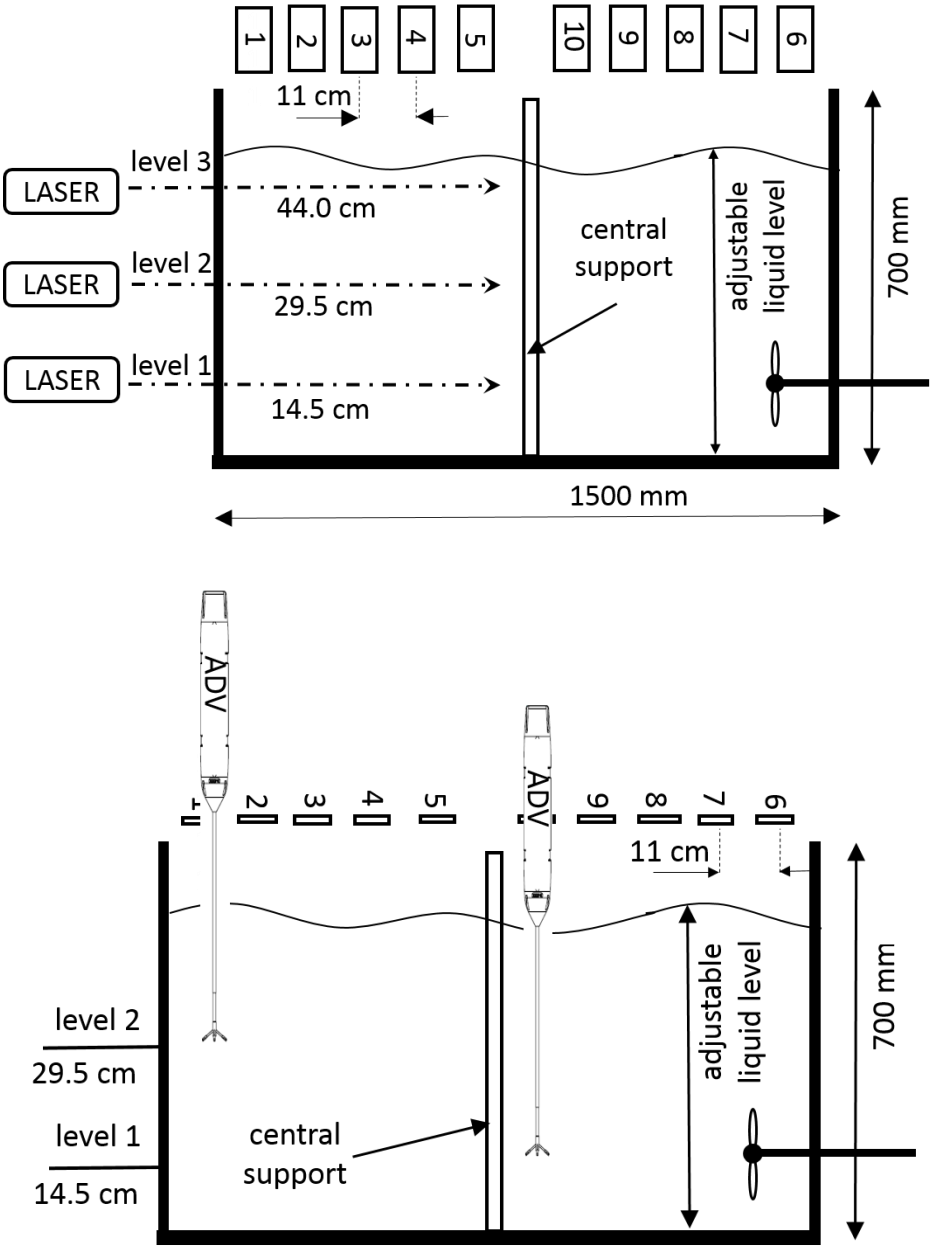

Figure 10: Schematic representation of the home-made laboratory digester setup (side view) for PIV (top figure) and ADV (bottom figure) measurements of the water-cellulose fluid.

2.7 Acoustic Doppler Velocimetry (ADV) configuration

Additionally, the water-cellulose fluid velocity was directly measured using a Vectrino Velocimeter (Nortek AS, Norway) operating with the Doppler effect principle and a bistatic sonar, i.e. the ADV velocimeter used separate transmit and receive beams, in contrast to standard Doppler profilers. The probe consisted of four receive transducers, each mounted inside a receiver arm, and a transmit transducer in the center. The transducers were each

covered with a hard epoxy and the probe was titanium. A pulse was transmitted from the central transducer, and the Doppler shift, introduced by the reflections (echo) from the particles suspended in the water, was picked up by the four receivers. Water velocity measurements had an accuracy of ±0.5% of measured value ±1mm/s. Doppler uncertainty at 25 Hz is estimated to be 1% of the velocity range. Inside the probe head, a temperature sensor is located with accuracy/resolution of 1°C/0.1°C. The ADV velocimeter was placed with the transducers at the levels 1 and 2 of the PIV configurations (i.e. at 14.5 cm and 29.5 cm of height from the bottom of the tank) and at the 10 positions corresponding to the light sheets generated by the laser in the PIV configuration (see figure 10-bottom).

2.8 Setup for torque and mixers power consumption determination

To evaluate the power consumption which was needed to mix the water-cellulose solution, the torque moment at the shaft was measured. An ETH DRFL-I-n rotating torque transducer with speed measurement was used. The maximal measurement error was 0.1 % of full scale and measurements between 0 and 1 Nm were possible with a maximum speed up to 10 000 min^{-1}. Figure 11 demonstrates the torque measurement setup with the used controllable mixer drive and the feedthrough of the shaft into the laboratory model digester.

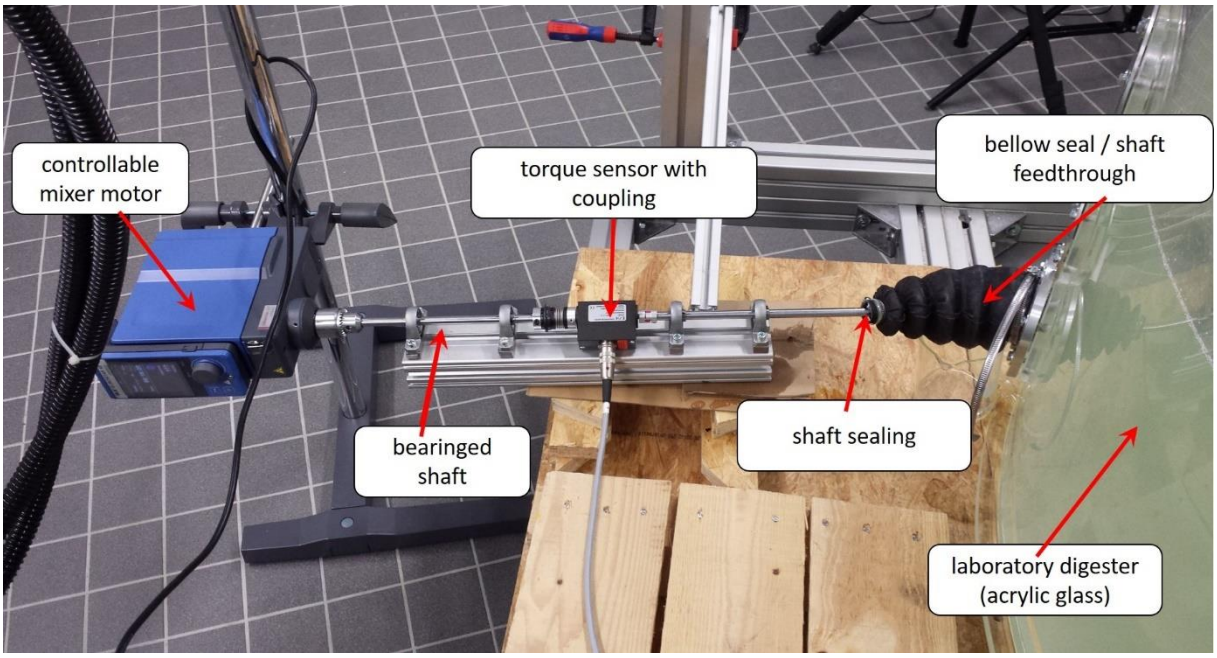

Figure 11: mixer drive and torque measurement setup at downscaled laboratory experiment

The torque sensor was attached to a 34972A Keysight unit system, equipped with a 34901A 20 channel multiplexer module for data acquisition and logger switching.

3 Results and discussion of laboratory investigation

Velocity of the water-cellulose fluid was investigated using three independent methods (Particle Image Velocimetry optical technology PIV, and Acoustic Doppler Velocimetry ADV and Computational Fluid Dynamics CFD) with the aim to compare the experimental results of the methods PIV, and ADV with the CFD computer simulations.

3.1 Digester model

Creating a dynamic similitude between reality and model is the basic concept on which the present study was structured. The scaling down process from the full-scale digester size used in biogas plants to laboratory-scale is formulated on the basis of rheological concepts. The Reynolds number (Re) is used to predict flow patterns in the fluid for both real biomass and the artificial substrate. In particular, for mixers the Re is expressed as:

$$Re = \frac{\rho N d_R^2}{\eta_a} \qquad (2)$$

In Equation (2), the parameter ρ represents the density of the fluid, N the rotational speed of the stirrer, d_R the characteristic diameter of the propeller mixer, and η_a the dynamic viscosity. To ensure the same flow characteristic in laboratory scale as in reality, an equal Reynolds number is used ($Re_{full\text{-}scale} = Re_{lab\text{-}scale}$).

As a result of maintaining an equal Re, the required propeller rotational speed N would be impossibly high to observe at laboratory scale dimension. But by adjusting of the rheological dynamic viscosity η_a in the denominator of Equation (2) too, for the laboratory experiment realizable and practical conditions can be set. Recently Wiedemann et al. (2017a, 2017b, 2017c, 2017d) and Conti et al. (2016) have investigated several artificial substrates on the basis of their viscosity to determine the conditions which can satisfy dynamic similarity.

The cellulose Walocel 3000TM dissolved in water at the concentration of 0.3% wt was chosen to ensure an equal Re between reality and model. Hence, the lab-scale digester can use a

practical rotational speed N of 238 rpm for the small propeller with diameter of 75 mm, 140 rpm for the big propeller with diameter of 125 mm (see table 1).

Table 1: Parameters used in the laboratory digester setup to fix the two different mixing configurations.

Configuration	**mixer type**		**height of shaft [mm]**		**rotational speed [rpm]**	
	mixer 1 (m1)	*mixer 2 (m2)*	*m1*	*m2*	*m1*	*m2*
C1	big propeller	big propeller	150	150	140	140
C2	big propeller (*)	small propeller	375	150	140	238

(*) This mixers shaft is vertically inclined. All other mixers are horizontally arranged

According to these considerations of similarity, the selected stirrers (small propeller and big propeller) suggest a series of possible combinations for mixing.

In the present work we have considered arrangements with two mixers, which are placed opposite in the model digester. Moreover, we have combined the two propellers arrangements to create two different basic configurations (C1 and C2). In Table 1, the configurations are schematically described. In general, the efficiency of the mixing process inside a digester depends on a large number of parameters which are related to the substrate rheology, design of the tank (geometry and size) and stirrers (quantity, locations, direction), as well as operational procedure (continuous or intermittent substrate feeding, bulk liquid temperature, mixing velocity, and continuous or intermittent mixing).

In the present investigation we have selected the configurations C1 and C2 on the basis of five factors: (i) the possibility to compare the resulting data with published results, (ii) the plan to start with a simple flow dynamic (in C1) and to increase its complexity (in C2) (iii) the concept to have symmetrical (C1) and asymmetrical (C2) flows inside the laboratory digester, (iv) the intention was to be not limited to a single mixer but to use different types of propeller blade mixers, which are normally used in biogas plants, and (v) the idea to use configurations comparable to full-scale applications to obtain results which may be valuable to the operational procedures in biogas plants. The aforementioned rationale also supported using an angle of 30° for the shafts of the stirrers. The α and β angles of 30° are generally used in the reality and studied in the literature.

3.2 Torque and power consumption

In Table 2, notable results of the developed torque and power consumption in laboratory experiment during mixing of the artificial substrate are presented.

Table 2: Power consumption and torque developed using the small and big propeller to mix the substrate in the laboratory digester.

measurement arrangement	**medium**	**P_{el} [W]**	**T_{tot} [Nm]**	**P_{shaft} [W]**	**T_{blades} [Nm]**
shaft without propeller	air	19.5	0.002		
shaft with small propeller	Walocel 0.3%	25.4	0.029	0.66	0.004
shaft with big propeller	Walocel 0.3%	23.1	0.027	0.36	0.006

To estimate the power consumption P_{shaft} the following equation is used:

$$P_{shaft} = \frac{2\pi N}{60}(T_{substrate} - T_{air}) \qquad (3)$$

where the parameter T indicates the torque developed during the mixing. To precisely calculate the contribution of mixing the substrate to the power consumption two torque measurements were recorded, with and without artificial substrate in the vessel. The torque of shaft rotation in the air was recorded as T_{air} in Equation (3) to get the rotational machine losses due to friction. Secondly, with the propellers connected to the shaft and the digester filled with artificial substrate, torque was recorded as $T_{substrate}$ in Equation (3). N indicates the rotational speed of the shaft per minute (rpm). In Table 2 P_{el} represents the total electrical power consumption and is directly obtained from the laboratory setup. The results demonstrated that the use of the smaller propeller required more energy and produced less hydraulic torque as already mentioned by Rostalski and Springer (2010). The consideration that a large propeller is less energy demanding is useful for mixing design and selection of stirring configurations in real digesters.

3.3 Flow velocity analyses

The use of Particle Image Velocimetry to quantify liquid flow properties is not novel. Very recently, Yan et al. (2015, 2016) have used PIV technology to confirm with velocity profile

measurements their CFD simulation results on the hydraulic optimization of a membrane bioreactor. On the contrary, the use of ADV technology is more restricted. In the present thesis, both methods are used to measure the fluid flow velocity and a discussion on the two modalities is presented on the basis of the experiences observed in the presented investigation. A first disadvantage of PIV against ADV is the necessity of using transparent materials. The laboratory digester was made of acryl glass because the measurement of fluid velocity by PIV required the tank to be transparent so that the substrate could be illuminated by laser.

For the same reason the artificial substrate needed to be transparent to assure that the camera could capture the light sheets from the top of the laboratory digester. This restricted the choice of artificial substrate since rheological properties needed to meet similarity requirements in addition to being colorless. Fluid tracing using PIV technology required seeding particles to be present in the substrate. The quantity of seeded particles needed to be limited to avoid any opacity and turbidity. Concomitantly, a sufficient amount of particles was mandatory for accurate tracing of the particle trajectories. Another disadvantage of PIV technology was the error in liquid velocity measurements. Jiang et al. (2014) estimated the error of PIV to be less than 5% via the experimental calibration of the velocity, which required the employment of standardization. Furthermore, since the trajectories of the particles are captured in the 2D plane, the third spatial component of the velocity is not determinable. Finally, PIV measurements require long periods of measurements since the determination of the velocity is not instantaneous, rather successive imagines must be captured and processed by a DynamicStudio™ software of Dantec Dynamics.

On the other hand, ADV measurements are much easier to perform since the complexity of the PIV setup (laser and consequently safety requirements, camera, corresponding supports, computer) is limited for ADV to the computer, the ADV probe (sensor) and its support. Data acquisition time of ADV is comparably shorter with respect to PIV technology since the sending of the acoustic pulse, the travel of the pulse through the substrate, the record of the echo and the processing of the echo to find the Doppler shift take place at a rapid rate. The simplest model of ADV measuring sensor assures a sampling rate (output) of 1-25 Hz, which reach the value of 1-200 Hz in non-standard models.

Another advantage of ADV over PIV is that calibration procedures are not required. The z-

component of the flow velocity is detectable, allowing 3D determination of velocity. The error in the measurements is estimated at ±0.5%, a magnitude lower than with PIV technology. Finally, the financial costs of the two techniques are very different making the ADV technology economically more convenient.

The flow velocity of the water-cellulose mixture measured with PIV and ADV in ten positions (see Figure 7) inside the laboratory digester is plotted in Figures 12 and 13. The results refer to the mixing configuration C1, where two large propellers are placed opposite in the tank and their shafts are at a height of 15 cm above the bottom of the digester. The velocity values measurements performed at level 1 in x-direction (see Figure 12), nearly at the same plane of the shafts, range in the interval ≈ 0.02 - 0.1 m/s.

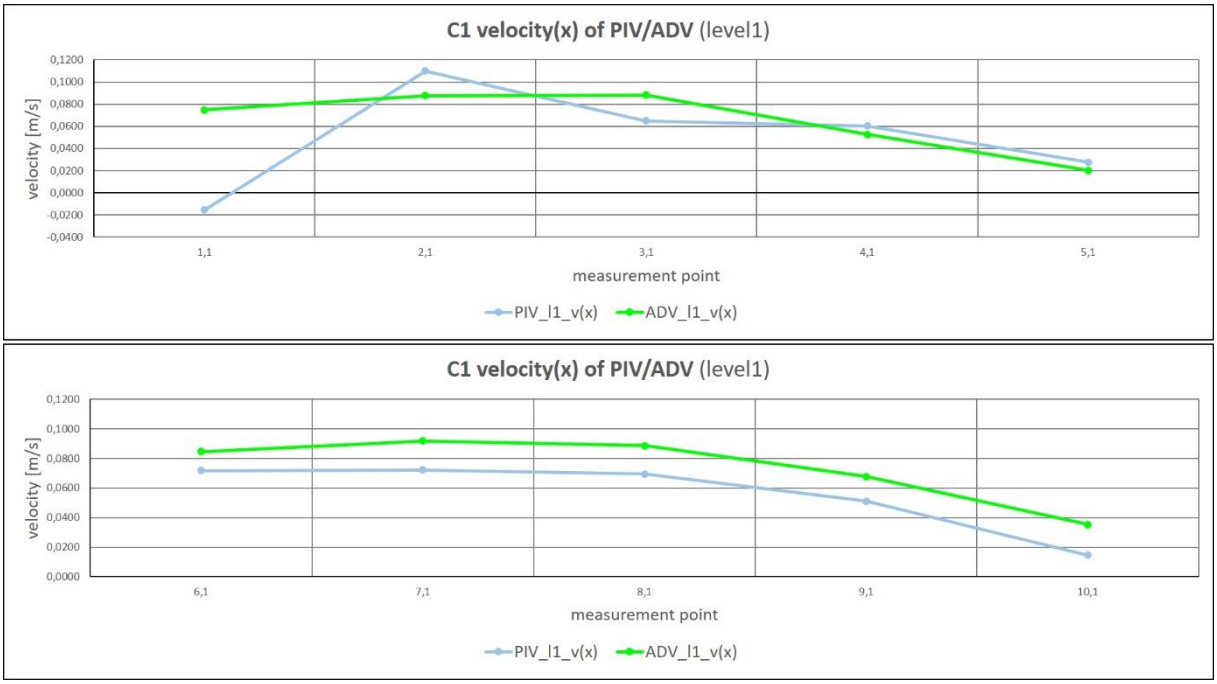

Figure 12: comparison of measured flow velocity in x-direction at level 1 with PIV and ADV at measurement points 1.1 to 10.1 (see figure 7) of lab scale mixing configuration c1

Lower fluid velocities were apparent near the center of the digester (positions 5.1 and 10.1). This suggests lower quality of the mixing within that region, since slow moving zones represent less mixed zones. This appearance is also present in level 1 y-direction (Figure 13). The velocity values measurements of the y-direction range in the interval 0.02 - 0.05 m/s (absolute).

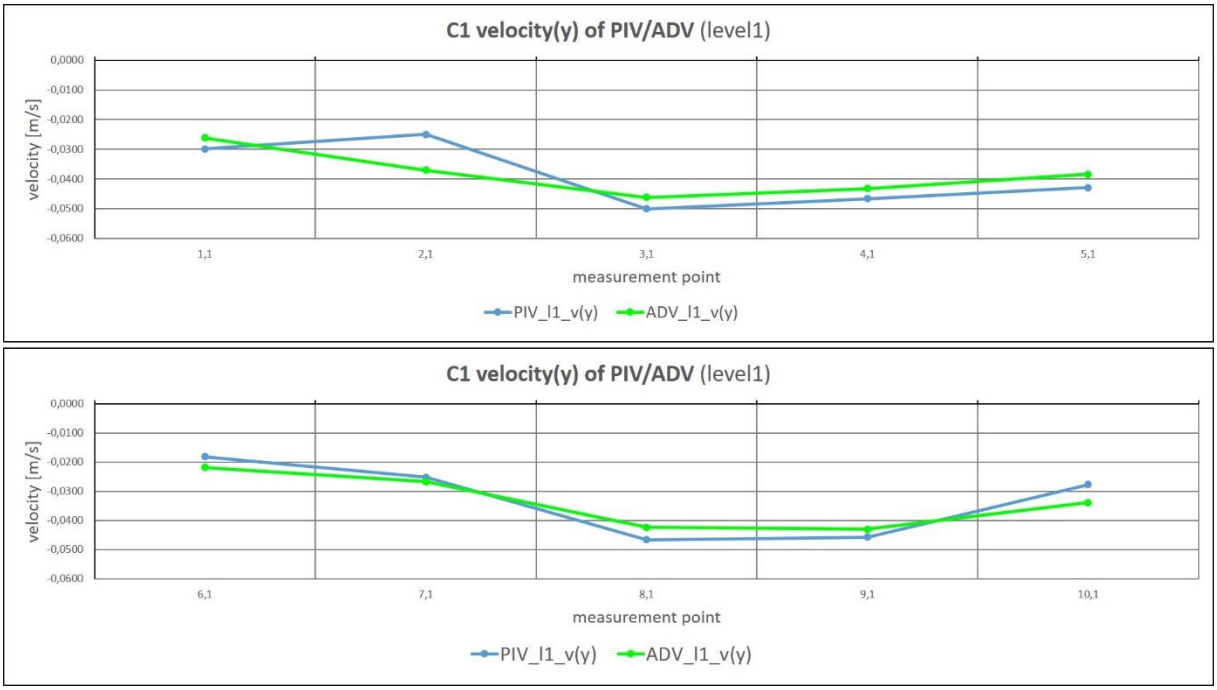

Figure 13: comparison of measured flow velocity in y-direction at level 1 with PIV and ADV at measurement points 1.1 to 10.1 (see figure 7) of lab scale mixing configuration c1

For the configuration C1 a symmetry in the flow dynamics is expected between the 1.1-5.1 (Figure 12/13-top) and 6.1-10.1 (Fig. 12/13-bottom) regions, so that the results in positions 1.1 and 6.1 should be comparable and also those of positions 5.1 and 10.1.

This expectation was validated by the experimental data, which confirm the precision of the used PIV and ADV setups. The similarity of PIV and ADV (see Figure 12 and 13) data suggest the possibility to limit the investigation to the ADV technology. Indeed, the accuracy is much higher due to the low error of the ±0.5% of the measurement value.

The results indicate a development of the flow velocity from wall of the digester to the center. The velocity is slower at the wall due to friction, then increases to a maximum of ca. 0.1 m/s and then nearly no flow is present in the central section. The presence of a dead zone in the center is related only to the movement of the flow in the plane parallel to the bottom of the digester (xy-plane). In the z-axis the flow appears slightly eddying and with up and down movement.

The conclusion of lower velocities in the center region is confirmed by the dyeing (coloring and decoloring) process, which is described in following paragraph 3.4 and depicted in Figure 14. Indeed, closer to the midsection the slower moving fluid is accompanied by less mixing dynamics, which is visible by the remaining colored zones (Figure 14-V).

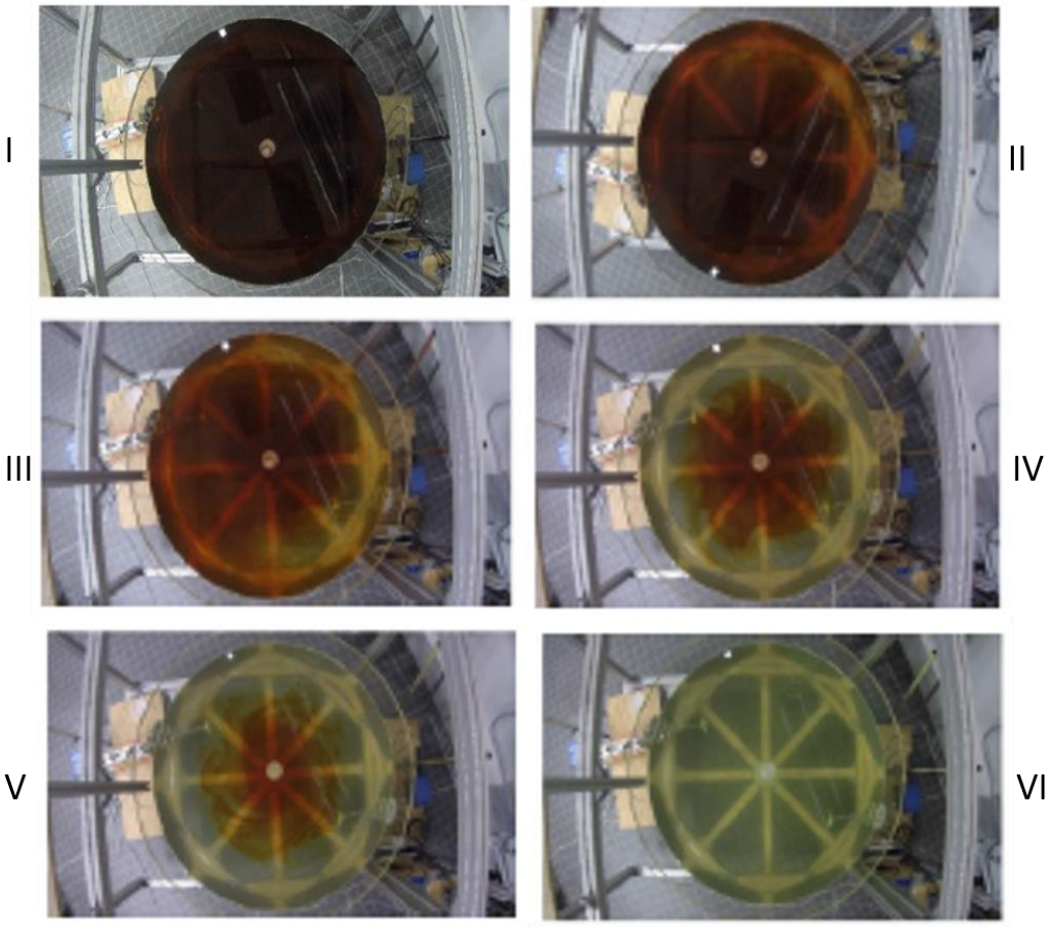

Figure 14: Photo sequence (I – VI) of the decoloring process (Configuration C1) used to estimate the mixing time in the 0.3% water-cellulose solution.

3.4 Mixing time

The dying process (coloring and decoloring) allows a qualitative visual investigation of the mixing dynamic as well as quantitative results in terms of mixing time. A sequence of the mixing pattern inside the digester is depicted in previous Figure 14. The water-cellulose mixture is fully brown due to the injected iodine solution. The decoloring process was initiated by adding thiosulphate, (following the chemical reaction reported in Equation (1)), which led to the production of colorless tetrathionate. During the decoloring process, zones with fast mixing dynamic are clearly visible and are in correspondence to the external ring (transparent

zone) where the flow induced by the agitator is stronger. The red-brown shaded zone remaining in the central part of the tank, indicated less dynamic, lower intensity mixing. For configuration C1 ≈ 8 min was necessary to completely decolor the mixture. For configuration C2 ≈ 5 min was necessary. It must be concluded that the iodometric titration serves just as a basis of a qualitative statement for the mixing process. The end point of the reaction, the iodine disappearance couldn´t identified precisely. Finally, dyeing can also be done with colored tracers, e.g. methylene blue, which are common in use.

3.5 Temperature effect

Several temperature dependent parameters were present in the study. Since dynamic viscosity is dominated by temperature effects, the artificial substrate needed to be thermostatic to maintain desired rheological conditions. Furthermore, the torque measurements required thermal equilibrium to avoid deformation (expansion) of the two shafts. To minimize thermal effects, all the laboratory experiments were performed constantly at fixed 21°C. As mentioned under 2.3 the chosen viscosity of the artificial substrate at 21°C is comparably to real substrate at mesophilic temperature conditions.

3.6 Validation of CFD model

One main purpose of the laboratory experiments was to obtain results which could be used to validate a corresponding CFD model developed because of optimising mixing systems. The CFD calculated flow velocities are graphically reported with the PIV and ADV experimental data in Figures 12 and 13. The correlation with the CFD simulation would be useful to support accuracy of investigations with CFD. CFD simulation is advantageous over laboratory experiments due to the drastically reduced timescale required to visualize flows. Experiments on the laboratory digester were time consuming and limited by the number of configurations and parameters to be checked. For example, the investigation of the flow dynamic in the 50-250 rpm range at steps of 50rpm needed weeks of measurements but only hours of computer simulation. The discrepancy in time required is also evident when changing the angle of the shaft of the stirrer from 30 to 60°. However, CFD simulations alone, without any validation from experimental results is risky and hardly be justified. Thus, a combination of the two methodologies must be applied.

4 Computational Fluid Dynamics (CFD)

As computational capacity increases, simulation with Computational Fluid Dynamics (CFD) becomes an increasingly powerful tool to model complex flow processes. In this project, the commercial software StarCCM+ from CD-Adapco Siemens was used to model the flow dynamic. The software tool StarCCM+ covers all simulation aspects from geometry design, grid generation, selection of physical models and solvers up to data evaluation and optimisation.

In particular CFD allows determination of the flow characteristics of sludge in digesters at a much lower cost. The CFD simulations can be used effectively to model the flow fields in a digester and to determine critical limitations and boundaries of the mixing process. Its advantages are even greater in applications where it is difficult to experimentally detect the mixing parameters, as it is in the case of biogas plant's anaerobic digesters. It should be mentioned that the application of CFD in anaerobic digesters is still limited. The prediction of gas mixing is betters for example is not possible with available CFD tools.

4.1 Hypothesis for numerical investigation

In the case of a continuous digestion, all steps of the conversion process take place in the digester. The operational efficiency of a continuously operated cylindrical anaerobic digester depends on the homogeneity of the substrate (active sludge and fed biomass) according to Sindall (2014). The hydrodynamics required to achieve substrate homogeneity is produced by mixing and ideally captures the available digestion volume.

The generated flow dynamic results in movement of the substrate at a certain velocity. With the assumption that an optimum homogeneity of the substrate is best for digestion, a near uniform distribution of flow velocity (evaluated as a multidimensional vector) indicates the substrate homogeneity. The flow velocity vector easily can be determined with CFD. With various evaluation criteria based on the velocity vector (e. g. average velocity, x-, y-, z-proportion) a comprehensive analysis of the velocity field is enabled, and mixing performance can be described.

With a subsequent benefit analysis, the various velocity criteria are weighted and summarized for an easy and understandable comparison of the various mixing systems. Accordingly, flow

anomalies can be identified, necessary key figures can be defined, and finally, the efficiency of mixing concepts can be assessed.

4.2 CFD model development

The geometry (digester, mixers, etc.), the artificial substrate rheology as well as the measuring points of the laboratory experiment are depicted in the CFD simulation set up. The downscaled CAD drawings of the mixers are imported into the CFD platform. With the 3D-CAD tool of StarCCM+ the geometries are drawn as necessary and then all parts are arranged in regions, with the related physics models. The measured results in laboratory are compared to the CFD calculated values to check the numeric models reliability. Later results show the numerical simulation model was in good accordance with the laboratory experiment.

4.3 CFD physics and settings

The flow patterns are analyzed under steady-state conditions to reduce the required computing capacity. The steady state simulation leads to similar results to the unsteady calculation. Within StarCCM+ the moving reference frame (MRF) frame approach incorporates the rotation of the mixers under steady state conditions. As the moving reference frame, an additional cylindrical rotating region around the mixers is created. The vast majority of the remaining fluid volume is static. The rotating region and the static fluid volume are connected via interfaces.

The Reynolds-Averaged-Navier-Stokes (RANS) equations are used along with the k-ε turbulence model and the Segregated Flow calculation model of StarCCM+. The realizable k-ε turbulence model as well as the standard k-ω model was also found by Wu (2011) to be more appropriate than other turbulence models.

The fluid rheology is based on the Non-Newtonian Generalized Power Law model of StarCCM+, which corresponds to Rheology models of Ostwald and de Waele and in their extension to Hershel-Bulkley.

On the walls and bottom no-slip conditions are set, whereas the fluids surface (transition to gas) is modeled with slip conditions as suitable simplification.

The mesh (see Figure 15) is generated automatically with the parts based mesher (PBM) of StarCCM+. The following meshers are chosen:

- Surface Remesher
- Automatic Surface Repair
- Polyhedral Mesher
- Advancing Layer Mesher

The basic cell size is set for laboratory geometry at 0.015 m diameter. Larger velocity gradients on walls and surfaces are solved with specific prism layers (see figure 15) created with the Advancing Layer Mesher.

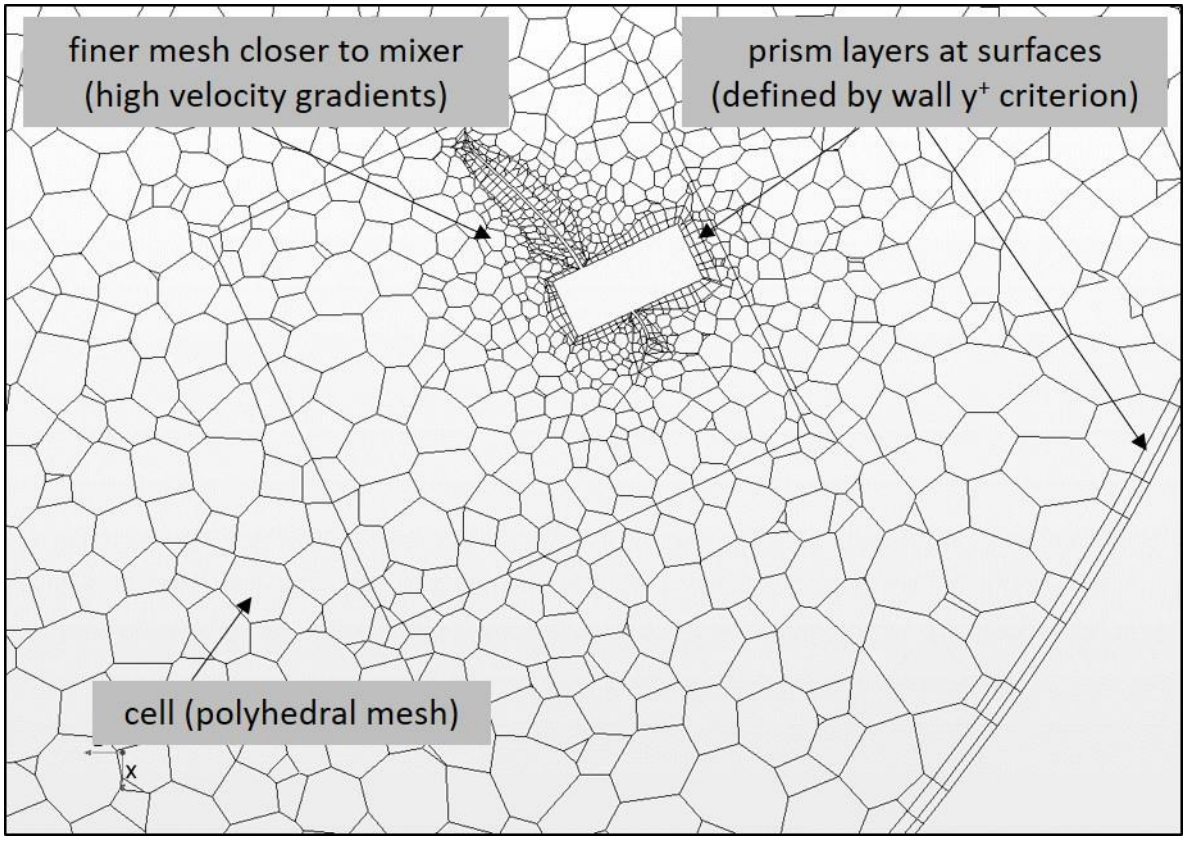

Figure 15: CFD mesh. Surfaces (digester wall, mixer) experience mesh refinement and prism layers

The visual appearance of the prism layers depends on a so called wall y^+value which should be < 1 as far as possible. The wall y^+ criterion of StarCCM+ is a non-dimensional CFD specific wall distance for wall bounded flows that can defined as:

$$y^+ = \frac{u_* \times y}{\upsilon} \qquad (4)$$

Where u_* is the shear velocity at the nearest wall, y the distance to the wall close by and υ represents a fluids local kinematic viscosity. The shear velocity captures the velocity profile close to a boundary (e.g. the wall). In fluid mechanics it helps for example to compare the velocity of a flow in a stream to a velocity that refers to shear between flow layers.

In order to minimize the computational effort of the complex investigation, various approaches for simplification of CFD simulation are applied (Basedau, 2015). The dependency of the cell sizes is also considered. With the above mentioned basic cell size the number of cells for Laboratory scale CFD calculation is 250.000 (calculation time ≈ 2h). The hardware used for calculation is a 6 core Intel Xeon Dell PC T5810 E5-1607 v3 8GB/1TB 3Y equipped with a Dell NVIDIA Quadro K4200 4GB graphical card, RAM-Storage Dell 64GB (8x8GB) DDR4 ECC and a Dell 512GB SSD Hard disk.

4.4 Validation of CFD

The validation of the CFD simulation with laboratory experimental results focuses on the mentioned mixing configurations C1 and C2. From the comparison of the flow velocity and the torque, validation of the CFD is obtained. The following diagrams (figures 16 to 18) show the flow velocity at levels 1 to 3 from mixing configuration C1 at measurement or calculation locations 1.1 - 10.1 calculated with CFD compared to the measured results of PIV and ADV. The flow velocity in the diagram is split to the individual scalar components of the velocity vector (x, y, z).

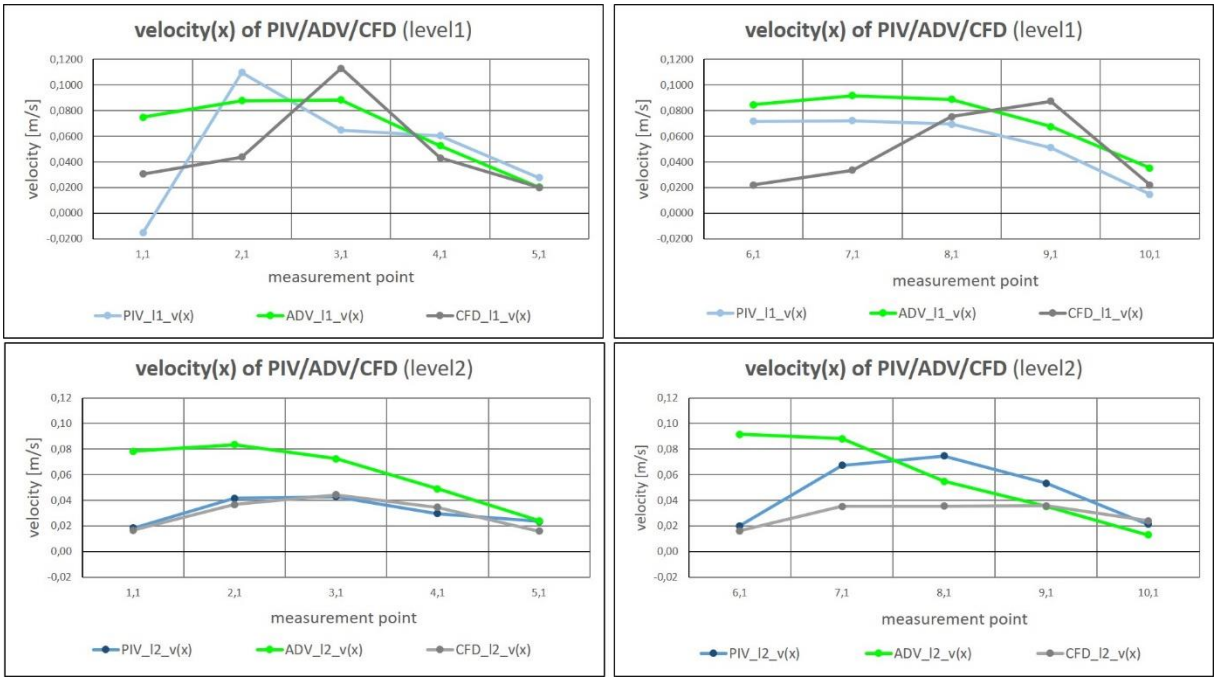

Figure 16: comparison flow velocity (x-component) measured by PIV/ADV and CFD of mixing configuration c1 at level 1 and 2 (see figure 7)

The diagrams show quite a good accordance of the flow velocity of the different methods, but not an exact match. This maybe a result of the many influences, as well as necessary simplifications for modelling and measurement errors. Previous figure 16 gives the vectors x-component of level 1 and level 2 and the following figure 17 shows the vectors y-component.

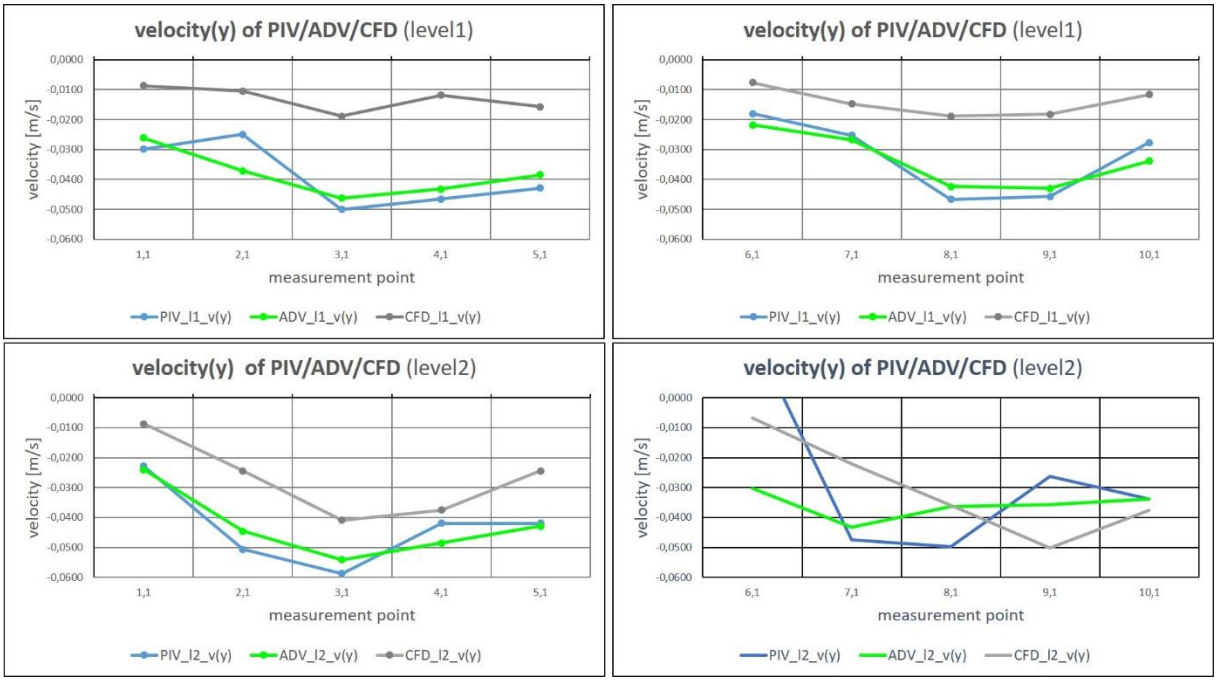

Figure 17: comparison flow velocity (y-component) measured by PIV/ADV and CFD of mixing configuration c1 at level 1 and 2 (see figure 7)

As mentioned in 3.3 the used PIV method is providing results only in 2 dimensions, the x- and y-component of the velocity vector. So, the following diagram of the z-component (figure 18) at level 1 and level 2 have just two lines.

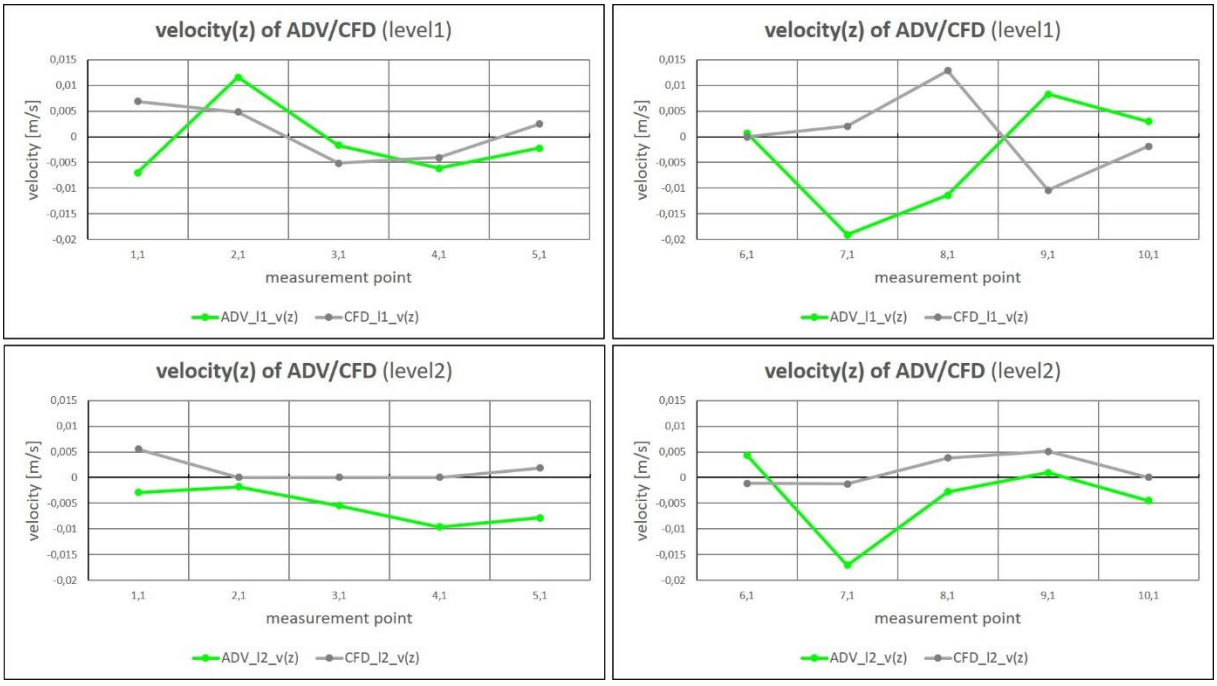

Figure 18: comparison flow velocity (z-component) measured by PIV/ADV and CFD of mixing configuration c1 at level 1 and 2 (see figure 7)

The velocities 3rd component, the z-component, is measured in laboratory just with the ADV system and calculated with CFD (the CFD calculation provides all three scalar components of the vector).

Two lines as well can be seen in figure 19. The diagram gives the velocities obtained at measurement points 1.1 to 10.1 at level 3, close to the surface liquid level.

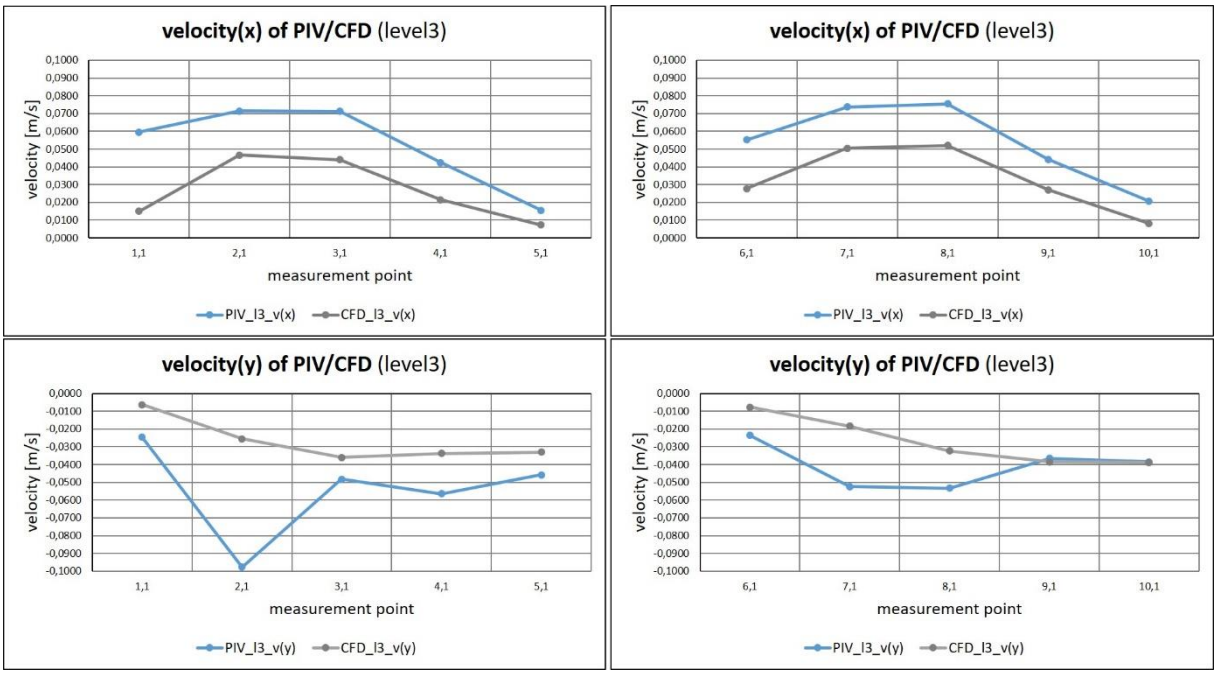

Figure 19: comparison flow velocity (x-/y-component) measured by PIV and CFD of mixing configuration c1 at level 3 (see figure 7)

There the ADV-Probe cannot be used, because it needs a minimum immersion depth. So just velocities measured with PIV and calculated by CFD are plotted in the diagrams of Figure 19.

4.5 Direction angle of velocity vector configuration c1

Furthermore, interesting is the direction angle of the velocity vectors measured (PIV, ADV) and calculated by CFD. Due to no z-component with PIV we concentrate in this analysis part on the plane of x- and y-dimension. Figure 20 gives some examples of 2D velocity vectors at selected measurement points.

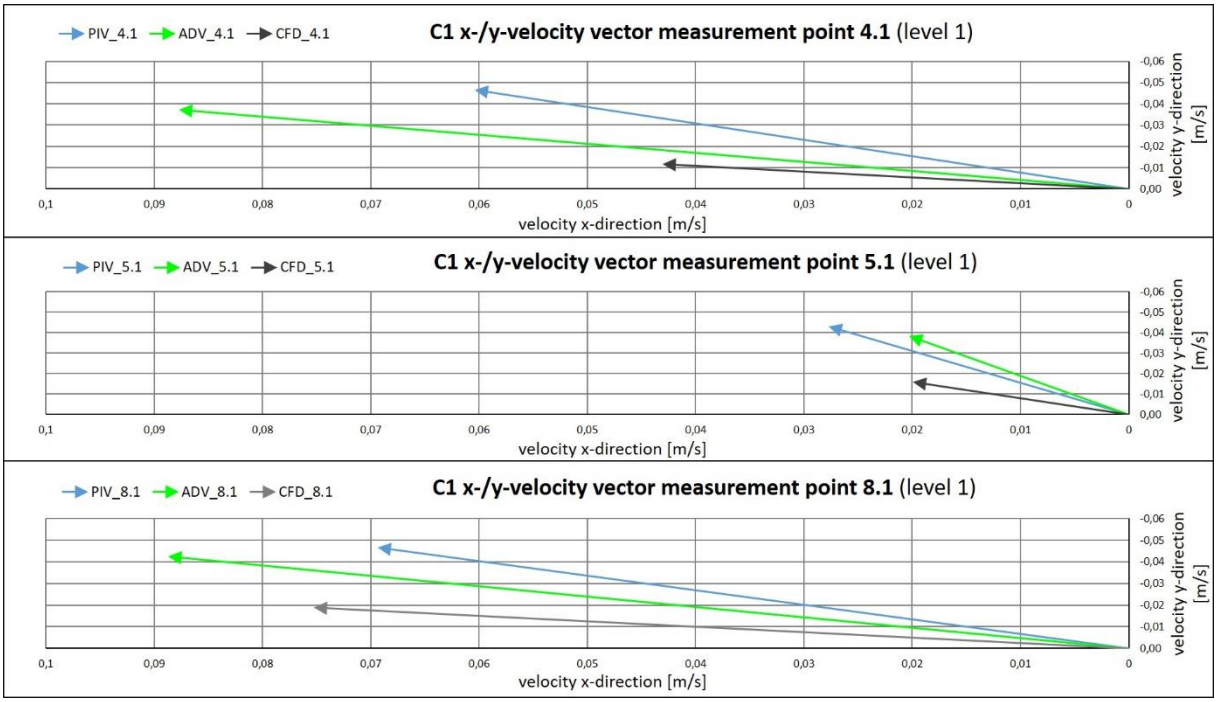

Figure 20: PIV, ADV and CFD comparison of direction of velocity vector 2D (x- and y-dimension) at selected measurement points of configuration C1 at level1

The axis to the left gives the velocity in x-direction and the upwards axis the velocity in y-direction. With the velocity scalars we then can calculate the 2 dimensions angle of the velocity vector.

The following diagram (figure 21) gives a summary of Configuration C1´s velocity vector angles at the measurement points 1.1 to 10.1 of level 1 and level 2. There is a very good accordance of the velocity vector direction at all levels given.

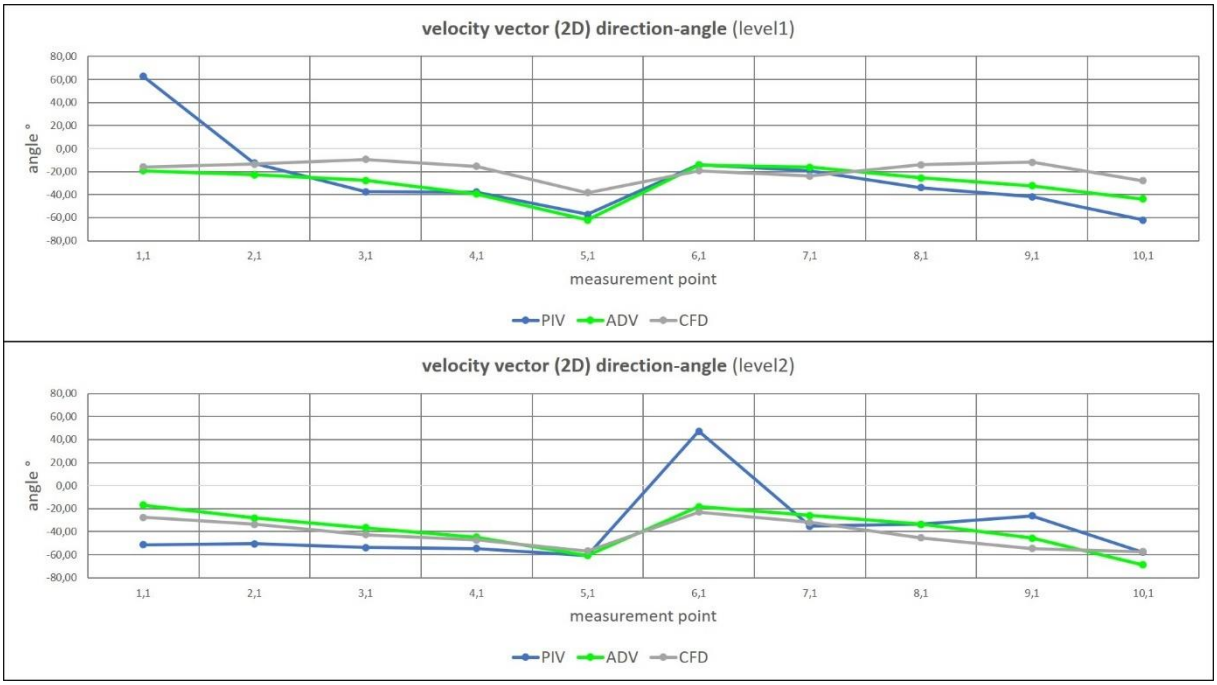

Figure 21: accordance of PIV, ADV and CFD velocity vector 2D (x,y) direction angle at the measurement points (see figure 7) of levels 1 and 2 of mixing configuration c1

Figure 22 gives the velocity vector angles at the measurement points 1.1 to 10.1 of level 3 measured by PIV and CFD close to the liquid surface where the ADV-Probe cannot be used due to low immersion depth.

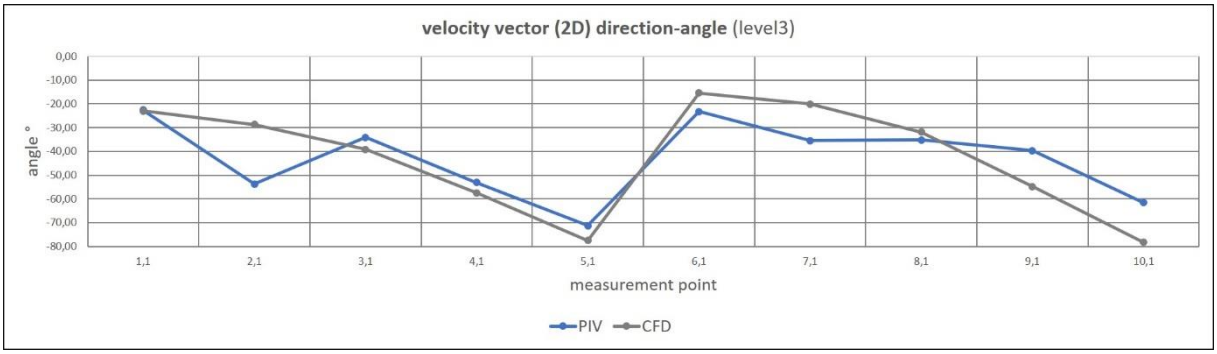

Figure 22: accordance of PIV and CFD velocity vector 2D (x,y) direction angle at the measurement points (see figure 7) of level 3 of mixing configuration c1

In summary we can see for the chosen mixing configuration C1 a good agreement of the measured (PIV, ADV) and calculated (CFD) values at lab-scale. But there are also a few discrepancies. This can be explained by the many influences and used models to simplify the complex nature of the mixing topic.

Corresponding results of experiment versus CFD calculation were also obtained for the mixing configuration C2 (one mixer vertical deflected and 2 different mixer blade sizes). The accordance there of the flow velocity (ADV and PIV measurement to CFD calculation) at the measurement points 1.1 to 10.1 is (example shown in following figures 23 to 27) not as good as it is at symmetric mixing configuration C1. However, to some extent this result is, due to the complexity of the task, acceptable.

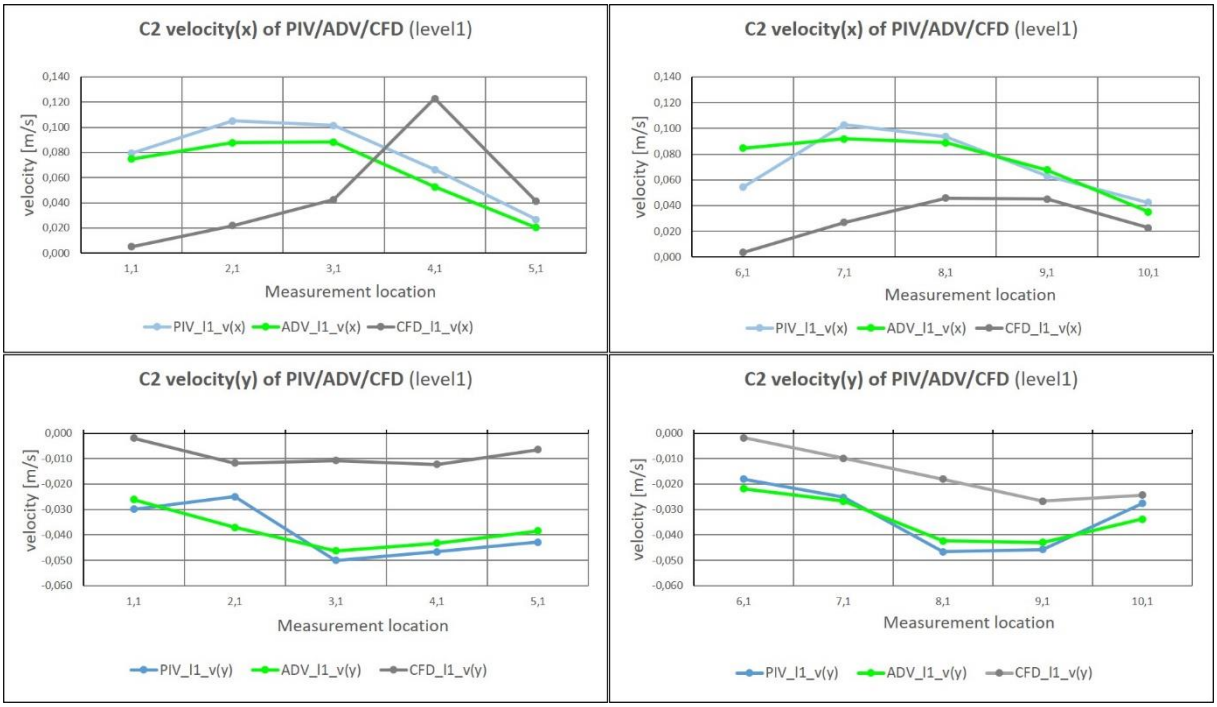

Figure 23: example flow velocity (x- and y-component) measured by PIV /ADV and CFD of mixing configuration c2 at level 1 (see figure 7)

As in previous figure 18 the velocity vector´s 3rd component, the z-component shown in following figure 24 is measured just with the ADV system and calculated by CFD.

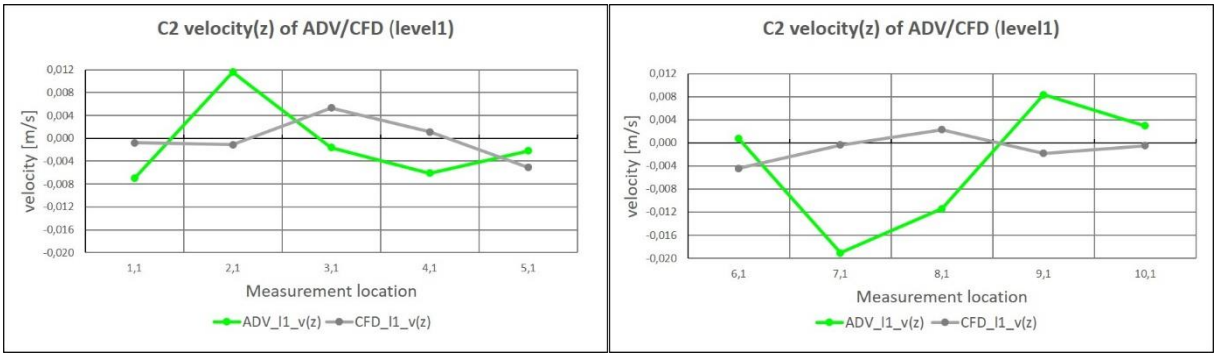

Figure 24: example flow velocity (z-component) measured by ADV and CFD of mixing configuration c2 at level 1 (see figure 7)

The asymmetric set-up of setting C2 seems to be much more complex to calculate with CFD. The flow velocity calculated with CFD is considerably lower than the measured. Nevertheless tendency of the mixing dynamic, illustrated by the flow velocity vector direction, is in good accordance what is demonstrated for some measurement points as example at figure 25.

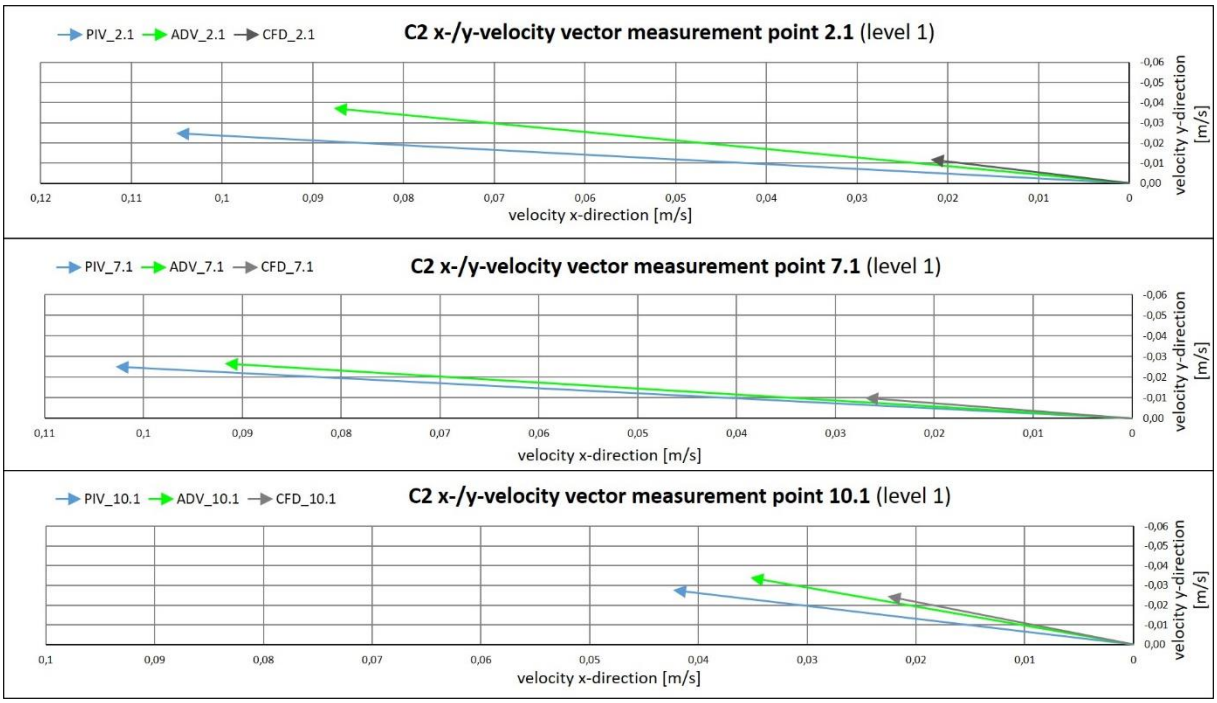

Figure 25: PIV, ADV and CFD comparison of direction of velocity vector 2D (x- and y-dimension) at selected measurement points of configuration C2 at level1

The following figures 26 and 27 give the summary of the flow velocity vector direction (2-dimensional x and y of PIV, ADV and CFD of configuration C2 at measurement points 1.1 to 10.1 and all 3 levels.

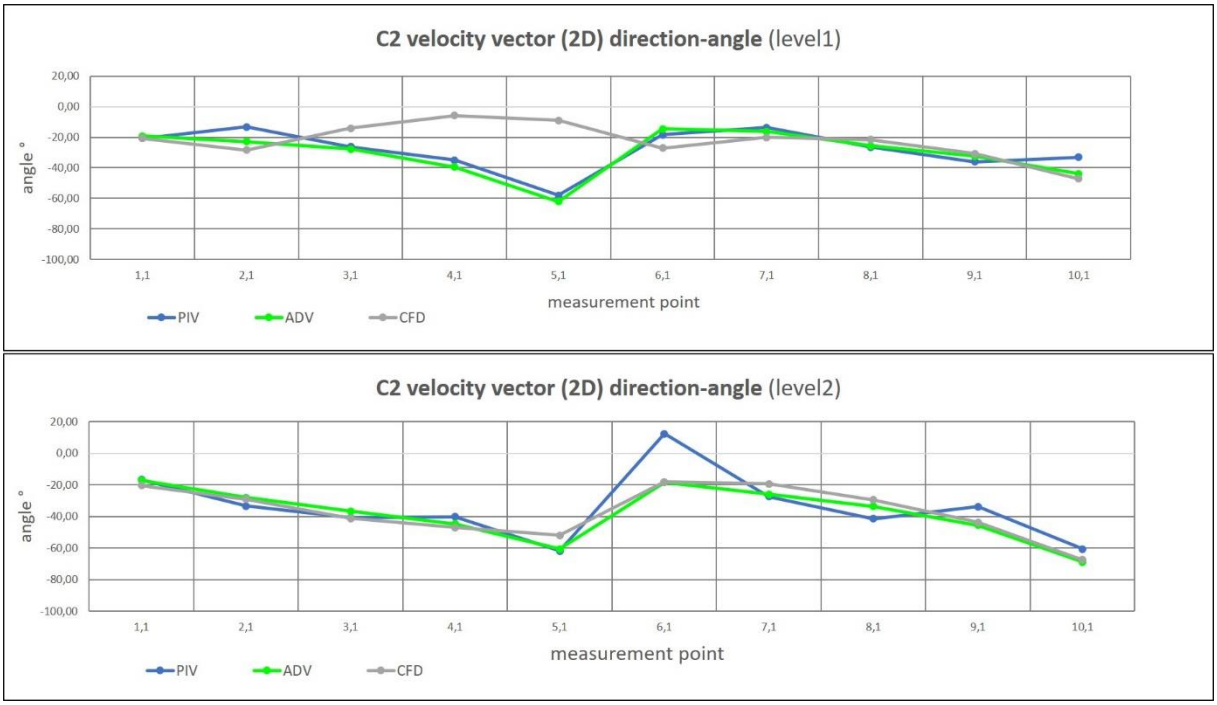

Figure 26: mixing configuration c2 velocity vector direction angle level 1 and 2

At level 3 the velocity vector direction is given just of PIV and CFD (see figure 27). The ADV-Probe cannot be used due to low immersion depth.

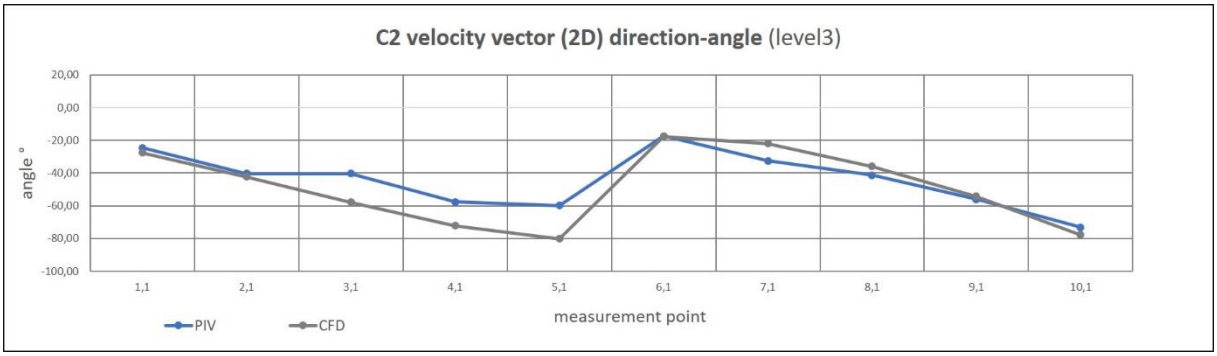

Figure 27: mixing configuration c2 velocity vector direction angle level 3

4.6 measured and calculated torque at mixer blades

Furthermore, the calculated torque in the CFD simulations for the propeller mixers between 0.0045Nm and 0.0065Nm is an additional feature consistent to measured (torque sensor) results at 0.004 Nm and 0.006 Nm (see table 2) in the laboratory experimentation (Conti et al., 2016, 2017). For the torque measurement set up see paragraph 2.8.

4.7 Summary CFD Validation

Thus, in summary, a reliable calculation of the CFD simulation is verified. The CFD provides a good reflection of the measured values (flow velocity, torque) in the laboratory experiment. The corresponding results from laboratory measurement and CFD calculation confirm the validity of the assumption that the numeric CFD calculation is working correctly.

Now it can be used for a comprehensive parametric optimization study. With the correct working of CFD at laboratory scale the assumption is that the CFD works properly at full scale (reality) too. No specific calibration of the CFD is needed. For the parametric study, the CFD simulation is first upscaled onto real conditions. Therefore the geometry, the rheology and the operational parameters are adjusted onto reality.

4.8 Upscale CFD simulation and Hardware resources

The geometry is upscaled as mentioned in Section 3.1 to a digester with 18 m diameter and 5.5 m fluid level (ca. 1400 m3 total volume). The upscaled numeric calculation under real scale conditions has a basic mesh size of 0.18m, i.e. number of cells ~1.000.000 and calculation time ~4h.

The hardware used for calculation is same as for CFD calculation of laboratory experiment:

- 6 core Intel Xeon Dell PC T5810 E5-1607 v3 8GB/1TB 3Y equipped with a Dell NVIDIA Quadro K4200 4GB graphical card, RAM-Storage Dell 64GB (8x8GB) DDR4 ECC and a Dell 512GB SSD Hard disk.

The fluid rheology is adapted to a real substrate mix with 12% of dry matter (dm). The Power law conditions are for consistency factor *k* 16.77 [Pa*s^n] and flow index *n* 0.35 [-] (Basedau, D., 2015).

5 CFD Study and analysis methodology

The goal of this research principally was to identify mixing systems that support digestion activity and improve biogas output whilst minimising the parasitic energy consumption.

The calculated results of the various parameter settings are compared among each other via a benefit analysis, what is new for a detailed specification/comparison of various mixing systems. The method of the benefit analysis is a multicriteria optimisation in our case based on functional Pareto principle related to the flow velocity vector as main aspect.

5.1 Benefit analysis

The methodology of the benefit analysis supports the comparison and decision-making of complex problems.

In our hypothesis the quality of the mixing (homogeneity) can be described by various evaluation criteria (see following table 3) related to the flow velocity vector:

- the direction → where flow dynamic goes
- the magnitude → flow dynamic intensity
- the distribution → homogeneity

With defined ranges for each criterion, a degree of fulfillment is determined and then multiplied by the criterion's corresponding weighting. These weighted criteria are summed up and the obtained score is related to an ideal score (best degree of fulfillment). The result is represented as a percentage of fulfillment what we call technical benefit (TB).

Table 3: defined evaluation criteria and weighting for benefit analysis

Criteria	Description	Weighting
Average flow velocity digester, $\mathbf{v_m}$	Indication of flow intensity	4
Uniform distribution of x-, y-, z- flow velocity vector components (∑33,$\overline{3}$ % each), **∑33⅓**	Indicates homogeneous mixing	3
Total amount of vertical (Up/Down) flow velocities of z-component, **z%**	Horizontal (circular) movement dominates in cylindrical digesters → vertical (up/down) amount of z-component indicates better mixing	2
Uniform amount (fifty-fifty) of positive (Up) and negative (Down) of the vertical z-component, $\mathbf{z^{+/-}}$	Avoidance of an up- or downward movement tendency	1

In order to assess the general flow dynamics in the digester, the average flow velocity in the vessel (v_m) is selected as the first evaluation criterion and considered to be the most important with a weight of '4'.

As an important criterion for good mixing dynamic the uniform distribution of the velocity in all three spatial directions (optimum 33% each) is assessed and weighted with '3'.

A further criterion is made by the vertical velocity vector component in the z direction (z%). In the worst case, flow dynamic just in the x- and y-directions only rotates the entire digester content around the mid-support (center) without producing proper mixing. Since an intensive mixing is achieved by an up and down movement of the fluid, the vertical z component of the velocity is determined as indication of good mixing. The weighting is set to '2'.

Furthermore, in the case of the vertical z-direction, it is necessary to avoid the tendency to float or to sink of the substrate solids. The proportion of z+ to z- should be as much as possible equal to 50%. However, since this situation contributes only marginally to a mixing optimization, just a weighting of '1' is defined.

5.2 Criteria range and Degree of fulfillment (DoF)

For a better scaling the degree of fulfilment is rated with a progressive evaluation scale (0, 1, 3, 5, 9). Table 4 gives the ranges for each criterion individual determination of the degree of fulfilment. The values are derived from the first CFD runs of the parametric study.

Table 4: Evaluation ranges of criteria to define degree of fulfilment (DoF)

Degree of fulfillment	**Criteria range (weighting)**			
	v_m (weighted 4)	∑33⅓ % (weighted 3)	$z_{\%}$ (weighted 2)	$z^{+/-}$ (weighted 1)
0	<0,10m/s	>30%	<21%	>16%
1	<0,11m/s	>25%	<24%	<16%
3	<0,12m/s	>20%	<27%	<12%
5	<0,13m/s	>15%	<30%	<8%
9	>0,13m/s	<15%	>30%	<4%

After evaluating the various simulated scenarios on the basis described in previous table 4, the applicable degree of fulfilment (DoF) is multiplied by the respective weighting. For example, if v_m is measured 0,1192 m/s the DoF is 3. With the associated weighting 4 an individual subtotal (pTB) of 12 (3 times 4) is scored.

The individual subtotals (pTB) of the defined criteria then are summed up to an individual utilizable tech score (ΣTBS) of each setting (run). This is then set in relation to the ideal scored scenario (highest possible degree of fulfilment) to determine the percentage of the technical benefit (TB). The percentage allows the comparison of the various mixer settings.

5.3 First CFD parametric optimization study

Various influences on the mixing characteristics such as the type, number, positioning, operation mode and geometry of the stirrer as well as the (influential) substrate rheology must be considered.

The goal of the parametric study is to achieve a homogeneous substrate with lowest energy input possible. In the following Table 5, a first CFD parametric study is summarized (CFD under real conditions) on the basis of the mixing configuration C1 using the 4 variables:

- a, the mixers horizontal angle [°] (orientation relative to midpoint of digester),
- b, the mixers height positioning [m] in the digester,
- c, the mixers vertical angle [°] (up-/down orientation)
- d, the mixers rotational speed [rpm].

A point in Table 5 shows the setting for each mixer. A number provided to a point outlines a different setting of the two mixers.

Table 5: Mixers settings of first parametric study on configuration C1 (see table 1)

setting nr. (run)	a **mixers orientation horizontal** *(deflection of orientation to the midpoint)*				b **mixers height positioning**		c **mixer orientation vertical** *(up-/down- angle)*		d **mixers rotational speed**		**technical Benefit %**
	0°	30°	60°	90°	1.8m	3.8m	0°	45°	60rpm	80rpm	TB
1.1	••				••		••			••	53.33%
1.2		••			••		••			••	50.00%
1.3			••		••		••			••	55.56%
1.4				••	••		••			••	32.22%
1.5	$•_1$	$•_2$			••		••			••	42.22%
1.6	$•_1$		$•_2$		••		••			••	48.89%
1.7	$•_1$			$•_2$	••		••			••	48.89%
1.8		$•_1$	$•_2$		••		••			••	60.00%
1.9		$•_1$		$•_2$	••		••			••	26.67%
1.10			$•_1$	$•_2$	••		••			••	55.56%
2.1	••				$•_1$	$•_2$	••			••	46,67%
2.2		$•_1$	$•_2$		$•_2$	$•_1$	••			••	48,89%
2.3		$•_1$	$•_2$		$•_1$	$•_2$	••			••	40,00%
2.4			••		$•_1$	$•_2$	••			••	31,11%
2.5			$•_1$	$•_2$	$•_2$	$•_1$	••			••	31,11%
2.6			$•_1$	$•_2$	$•_1$	$•_2$	••			••	64.44%
2.7	••					••	••			••	37.78%
2.8		$•_1$	$•_2$			••	••			••	62.22%
2.9			••			••	••			••	35.56%
2.10			$•_1$	$•_2$		••	••			••	51.11%
3.1			$•_1$	$•_2$	$•_1$	$•_2$	$•_1$	$•_2$		••	63.33%
4.1	••				••		••		••		33.33%
4.2		$•_1$	$•_2$		••		••		••		37.78%
4.3			$•_1$	$•_2$	••		••		••		22.22%
4.4			$•_1$	$•_2$	$•_1$	$•_2$	••		••		22.22%

Table 6: Benefit analysis, scoring of first parametric study C1 (settings see Table 6)

setting nr. (run)	average flow velocity v_m (weighted 4)		uniform vector components ∑33⅓% (weighted 3)		total amount of vertical component z % (weighted 2)		proportion up vs. down movement $z^{+/-}$ (weighted 1)		technical Benefit ∑ Score	technical Benefit %
	DoF	pTB	DoF	pTB	DoF	pTB	DoF	pTB	TB Score	TB %
1.1	9	36	1	3	3	6	3	3	48	53.33%
1.2	9	36	0	0	0	0	9	9	45	50.00%
1.3	9	36	3	9	1	2	3	3	50	55.56%
1.4	5	20	0	0	0	0	9	9	29	32.22%
1.5	5	20	3	9	3	6	3	3	38	42.22%
1.6	5	20	5	15	3	6	3	3	44	48.89%
1.7	5	20	5	15	3	6	3	3	44	48.89%
1.8	9	36	5	15	1	2	1	1	54	60.00%
1.9	3	12	1	3	0	0	9	9	24	26.67%
1.10	9	36	3	9	1	2	3	3	50	55.56%
2.1	5	20	1	3	9	18	1	1	42	46,67%
2.2	5	20	5	15	3	6	3	3	44	48,89%
2.3	5	20	3	9	1	2	5	5	36	40,00%
2.4	5	20	1	3	0	0	5	5	28	31,11%
2.5	5	20	1	3	0	0	5	5	28	31,11%
2.6	9	36	5	15	3	6	1	1	58	64.44%
2.7	5	20	1	3	5	10	1	1	34	37.78%
2.8	5	20	9	27	3	6	3	3	56	62.22%
2.9	3	12	3	9	1	2	9	9	32	35.56%
2.10	5	20	5	15	5	10	1	1	46	51.11%
3.1	5	20	9	27	5	10	0	0	57	63.33%
4.1	0	0	3	9	9	18	3	3	30	33.33%
4.2	0	0	9	27	3	6	1	1	34	37.78%
4.3	0	0	3	9	3	6	5	5	20	22.22%
4.4	0	0	3	9	3	6	5	5	20	22.22%

The previous table 6 shows the benefit analysis of the first handmade parametric study given with settings of Table 5. The study is not done automatically with a specific optimate tool. The settings are chosen by hand. The first study serves primarily for a better understanding of the parametric changes and the calculation effort. This then helps to prepare a more precise parametric optimization study, which then is done automatically with Optimate+, a specific optimization tool of Siemens StarCCM+. The tool offers some formal methods for optimization done automatically.

The best score of this first handmade study is setting 2.6 with a technical benefit of 64.44% in relation to the ideal score of 90.

Obviously, there is an enormous range on the overall results within the different parameter settings (TB from 22.22% to 64,44%). This clearly demonstrates the importance of proper placement and operation mode of the mixers in the digester. The configurations 4.1 to 4.4 with reduced mixers speed of 60 rpm resulted in a flow velocity too low, without exception.

The following figure 28 gives as example the CFD flow velocity plot of the upscale Configuration C1 with parameter setting 1.3 (TB = 55.56%).

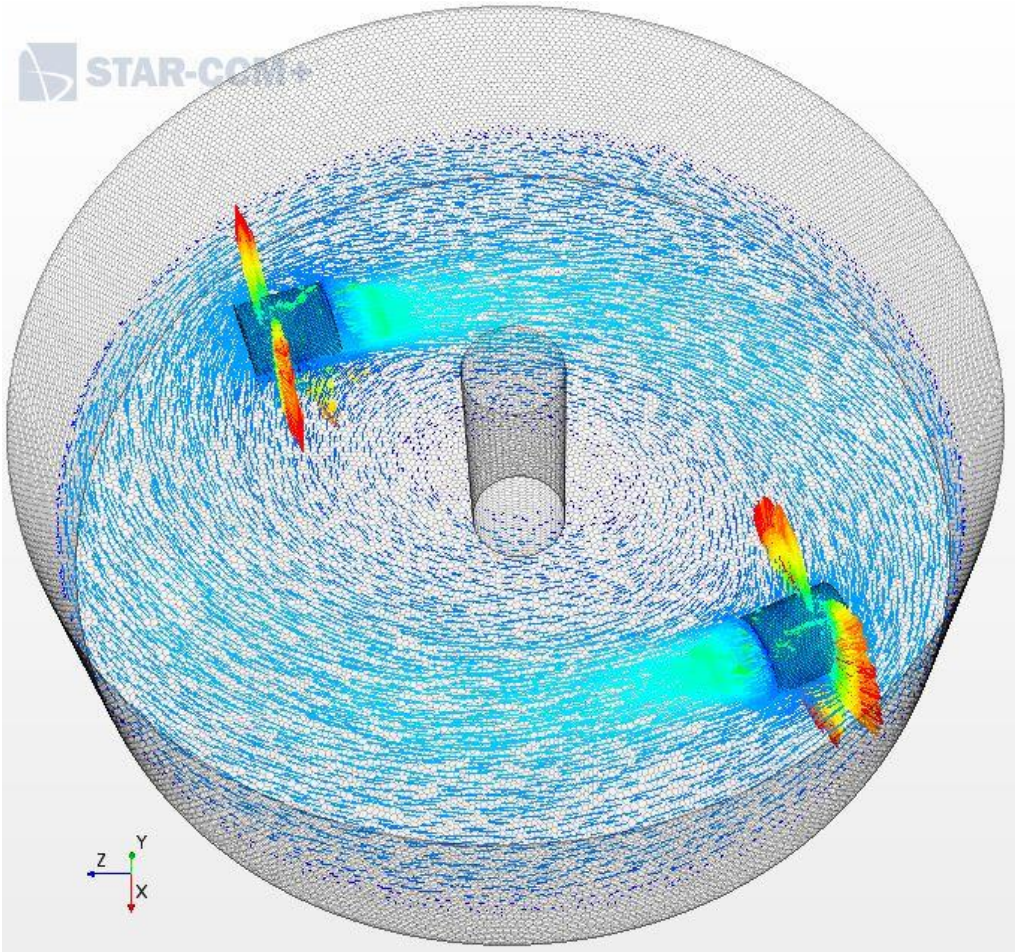

Figure 28: Parametric study flow velocity plot of setting 1.3 (data given in table 6). Vector scene flow velocity at mixers level

Clearly can be seen the poorly mixed zones around the center point and close to the wall as well as the well mixed zones with dense velocity vectors.

Furthermore if there are two or more mixers the placement at different heights could be advantageous. This corresponds to the comments made by Rostalski and Springer (2010). For flow improvement in the digester it is also found that, with the use of more than one propeller-bladed mixers, the horizontal operating direction (outgoing jet-stream) of each should be at different angles (relative to a straight line through the center). A change in the vertical angle (up and down) of one mixer of setting 2.6, done in parameterization 3.1 (see table 6) did not lead to a better mixing result, although an increased up and down movement, due to the incline, was expected.

The z+ criteria is not that important, so it is cancelled in favor of some other interesting criteria for the benefit-analysis, which is refined with more detailed criteria.

As a consequence of this first “handmade” benefit-analysis we have to limit the parameters kept variable. The effort for the CFD calculation gets several times higher with every additional variable and increment.

5.4 Refinement and extension of the parametric study

For a better significance of the gained results further criteria must be considered. As additional criteria a uniformity index UI (weighting 2) is used to identify uniformity of the digesters flow velocity and to exclude local peaks or lows.

The whole digesters Uniformity index UI is given by StarCCM+ as (Equation 5):

$$UI(\phi) = 1 - \frac{\sum_c |\phi_c - \overline{\phi}| V_c}{2|\overline{\phi}| \sum_c V_c} \qquad (5)$$

That index shows to what extent a homogeneous distribution of a selected scalar or vector (in our case the flow velocity → vector) is present in a selected volume (i. e. total substrate volume), by a value between 0 and 1. The closer to 1, the more homogeneous the distribution of that scalar/vector is. Where $\overline{\phi}$ is the average of the selected volume and ϕ_c is the value of the selected scalar/vector in a cell (from the mesh). V_c is the cell volume. The progress of mixing in a digester was quantified by Terashima, et al (2009) with a uniformity index (UI). Their developed model was applied to determine the required time for homogeneity in the digester.

The evaluation of subregions (Figure 29) helps to identify the uniformity (exclusion of lows or peaks) of the flow velocity vector in the digester. A high flow velocity at some sections can encourage misinterpretation of a setting as positive due to presumed proper dynamic, because there can be sections with critical less dynamic (dead zone) which are overlapped by the fast moving sections.

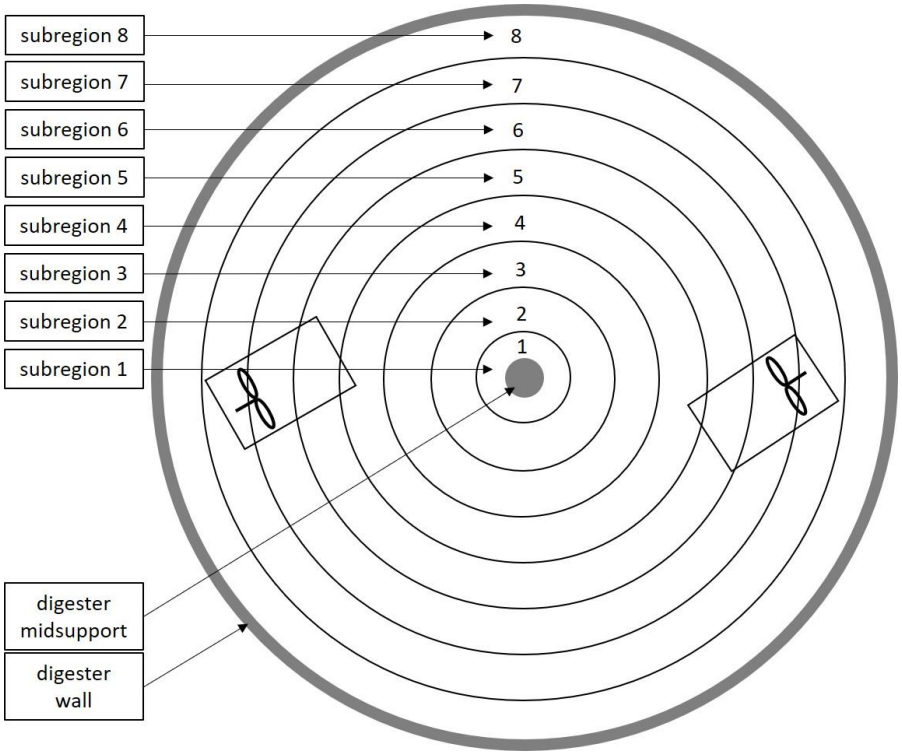

Figure 29: partitioning digester into subregions

Finally, the torque and generated thrust, calculated on the mixer heads (weighting 2) as indication of mixing power, completes the benefit analysis. The additional criteria are summed up in table 7.

Table 7: Additional evaluation criteria and weighting for refinement/improvement of benefit analysis

Criteria	**Description**	**Weighting**
Uniformity index UI	Uniformity of flow velocity inside digester. Exclusion of local peaks or lows	2
v_{msub}	average flow velocity of subregions	2
Torque (sum)	Indication of mixing power (force on mixers propeller-blade) as sum of the mixers	2
Thrust (sum)	Indication of mixing power (force onto the fluid) as sum of the mixers	2

This extended and refined analysis provides a more detailed evaluation. Results for the subsequent data analysis are calculated and monitored over the entire digester, as well as in several defined subregions of the digester (see table 8). The torque on mixer blades was calculated in order to get data for the necessary energy input.

The flow velocity evaluation over the entire digester indicates the mixing intensity. It gives an impression of a mixer settings ability to convert the supplied power into dynamic mixing.

Table 8: defined values calculated by CFD during the calculation runs

data collection location	**calculation parameter**	**unit**
entire digester	average flow velocity magnitude $\bar{v}$	[m/s]
	average flow velocity in x-direction $\bar{v}_x$	[m/s]
	average flow velocity in y-direction $\bar{v}_y$	[m/s]
	average flow velocity in z-direction $\bar{v}_z$	[m/s]
subregions of digester	average flow velocity magnitude $\bar{v}_{sr}$	[m/s]
	average flow velocity in x-direction $\bar{v}_{xsr}$	[m/s]
	average flow velocity in y-direction $\bar{v}_{ysr}$	[m/s]
	average flow velocity in z-direction $\bar{v}_{zsr}$	[m/s]
at propeller blades	$\text{torque}_{\text{Propeller}}$	[Nm]

The corresponding evaluation ranges for the degree of criterion fulfillment (DoF) are then defined on the results of the parametric study.

For the new parametric study, the StarCCM+ optimization tool Optimate was used. The tool provides various automated evaluation processes. The so-called Design Sweeps mode is used for the analysis, where the given variables (parameters) are set with a chosen increment. The variables and incremental settings must be chosen carefully, because of its influence on the total number of runs and the computational effort respectively. The Optimate tool then automatically chooses the settings and calculates them step by step at all possible combinations. The Optimate tool automatically changes the mixer arrangements and then

remeshes each runs geometry.

The available software resources enable up to 6 CFD evaluation runs in parallel. As resultant a .csv table with the calculated values is generated. This table then is analyzed with the chosen criteria.

5.5 Variables chosen for the new study

Due to the immense effort and time for running the CFD calculation, only the following variable parameters were considered in this refined study of the propeller mixers:

- horizontal orientation angle of the mixer → between 0° and 90°, anticlockwise (Figure 30 left)
- positioning mixer at various heights →3 levels at 1.8m, 2.8m, and 3.8m from the ground (figure 30 right)

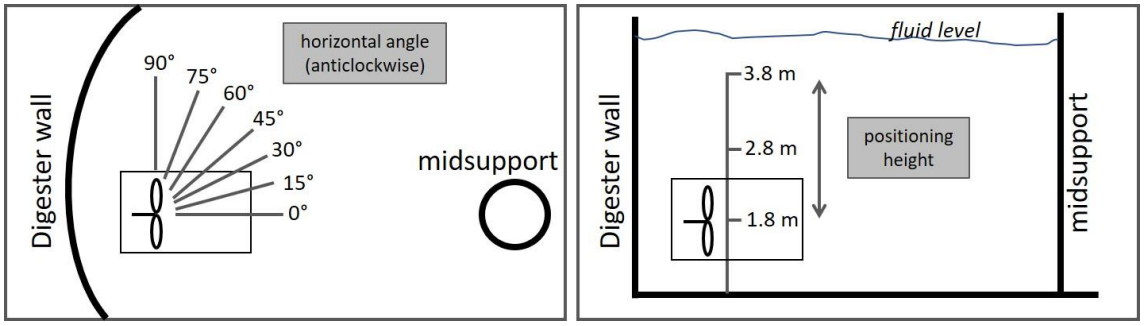

Figure 30: variable parameters in refined optimization study for the propeller mixers. Top view (left); side view (right)

After refinement of the optimization process for mixing configuration C1 was set with the following variables and incremental changes.

- AngleLRRR1 (mixer 1 orientation) → 0° to 90° with increment 15°
- AngleLRRR2 (mixer 2 orientation) → 0° to 90° with increment 15°
- TransRR1_Z (mixer 1 Height adjustment ↑↓) → 1.80m, 2.80m and 3.80m
- TransRR2_Z (mixer 2 Height adjustment ↑↓) → 1.80m, 2.80m and 3.80m

This means 441 (7x7x3x3) possible runs for CFD evaluation. With the given hardware resources (see 5.5) 6 runs can be done in parallel and the CFD calculation of one evaluation run takes about 4h. So, the study's duration is approximately 12 to 13 days. Other variable parameters

were kept constant for the optimization study. There were the rotational speed of the mixers, the mixers vertical incline at 0°, the mixers positioning at a 6.8m radius from the midpoint, the temperature and rheology of the substrate (consistency factor 16,77 [Pa*s^n] and flow index 0.35 [-]).

6 Results and discussion

Within the expected 13 days the CFD study was completed successfully. The generated .csv data were used for the analysis with Excel. As first step the chosen criteria individually are scored on the basis on their specific evaluation range. The criterion specific evaluation range was defined based on the gain in calculation values from the CFD study (see table 9).

Table 9: evaluation range for scoring of the defined criteria of benefit analysis

DoF (Subregion) / **criteria**	**0 (0)**	**1 (1)**	**3 (2)**	**5 (3)**	**9 (4)**
v_m (4) [m/s]	<0,1000	<0,1100	<0,1200	<0,1300	>0,1300
∑33% (3)	>80%	>75%	>70%	>65%	<65%
z% (2)	<14%	<18%	<20%	<22%	>22%
UI_{mag} [-]	<0,54	>0,54	>0,58	>0,62	>0,65
UI_x [-]	<0,50	>0,50	>0,54	>0,58	>0,625
UI_y [-]	<0,52	>0,52	>0,56	>0,58	>0,60
UI_z [-]	<0,435	>=0,435	>0,46	>0,48	>0,50
Torque [Nm]	>=1290	<1290	<1260	<1230	<1200
Thrust [N]	>=6000	<6000	<5700	<5500	<5300
v_{msub} [m/s]	>= 0,3178	>= 0,2255	>= 0,1333	>= 0,0410	< 0,0410

With the defined ranges of the criteria the Degree of fulfillment (DoF) of each criterion is determined and scored. For most criteria a progressive scoring is chosen (0,1,3,5,9). Just the Subregions evaluation (v_{msub}) has a linear DoF scoring (0,1,2,3,4) due to an avoidance of overvaluing higher velocities there.

The impact on flow velocity is included within the average flow velocity v_m of the entire digester.

This DoF then is multiplied by the assigned weighting of the criteria and results in the weighted score for each criterion (see table 10).

Table 10: criteria weighting and maximum possible weighted score

Criterion	**weighting**	**DoF maximum**	**weighted Score max**
v_m [m/s]	4	9	36
∑33%	4	9	36
z%	3	9	27
UI_{mag} [-]	2	9	18
UI_x [-]	2	9	18
UI_y [-]	2	9	18
UI_z [-]	2	9	18
Torque [Nm]	2	9	18
Thrust [N]	2	9	18
v_{msub}	2	4 (8 sections)	64
		ideal score (sum)	**271**

The weighted scores of the criteria are summed up to a total score of each setting (run). This total score is put into relation to the ideal score (sum of each criteria maximum weighted score) which is 271 for this study. The relation finally gives the technical benefit (TB) in %. The following tables 11 and 12 gives the top 25 settings after the benefit analysis (scoring DoF in relation to ideal score) of the 441 CFD calculation runs. Table 11 does not include consideration of subregions and table 12 includes the assessment of the subregion velocities. In both table

Table 11: top 25 ranking of the analysed 441 CFD calculation runs without consideration of subregions

Rank	Number of evaluation Run (CFD)	horizontal orientation mixer 1 [°]	horizontal orientation mixer 2 [°]	height (↑↓) [m]	height (↑↓) [m]	ΣTBS	TB %
1	369	75	75	3,80	3,80	159	76,81%
2	306	60	75	3,80	3,80	143	69,08%
3	305	60	75	3,80	2,80	139	67,15%
4	239	45	75	2,80	2,80	136	65,70%
5	241	45	75	3,80	1,80	133	64,25%
6	231	45	60	2,80	3,80	132	63,77%
7	284	60	45	2,80	2,80	132	63,77%
8	243	45	75	3,80	3,80	131	63,29%
9	352	75	60	1,80	1,80	131	63,29%
10	353	75	60	1,80	2,80	131	63,29%
11	308	60	90	1,80	2,80	129	62,32%
12	408	90	45	1,80	3,80	129	62,32%
13	222	45	45	2,80	3,80	128	61,84%
14	180	30	75	3,80	3,80	127	61,35%
15	188	30	90	3,80	2,80	127	61,35%
16	236	45	75	1,80	2,80	127	61,35%
17	287	60	45	3,80	2,80	127	61,35%
18	289	60	60	1,80	1,80	127	61,35%
19	315	60	90	3,80	3,80	127	61,35%
20	343	75	45	1,80	1,80	127	61,35%
21	360	75	60	3,80	3,80	127	61,35%
22	365	75	75	2,80	2,80	124	59,90%
23	171	30	60	3,80	3,80	123	59,42%
24	281	60	45	1,80	2,80	123	59,42%
25	291	60	60	1,80	3,80	123	59,42%

Table 12: top 25 ranking of the analysed 441 CFD calculation with consideration of subregions

Rank	Number of evaluation Run (CFD)	horizontal orientation mixer 1 [°]	horizontal orientation mixer 2 [°]	height (↑↓) [m]	height (↑↓) [m]	ΣTBS	TB %
1	369	75	75	3,80	3,80	203	74,91%
2	306	60	75	3,80	3,80	191	70,48%
3	305	60	75	3,80	2,80	185	68,27%
4	239	45	75	2,80	2,80	184	67,90%
5	231	45	60	2,80	3,80	180	66,42%
6	222	45	45	2,80	3,80	178	65,68%
7	284	60	45	2,80	2,80	178	65,68%
8	243	45	75	3,80	3,80	177	65,31%
9	233	45	60	3,80	2,80	175	64,58%
10	241	45	75	3,80	1,80	175	64,58%
11	287	60	45	3,80	2,80	175	64,58%
12	353	75	60	1,80	2,80	175	64,58%
13	360	75	60	3,80	3,80	173	63,84%
14	171	30	60	3,80	3,80	171	63,10%
15	180	30	75	3,80	3,80	171	63,10%
16	188	30	90	3,80	2,80	171	63,10%
17	343	75	45	1,80	1,80	171	63,10%
18	352	75	60	1,80	1,80	171	63,10%
19	356	75	60	2,80	2,80	171	63,10%
20	365	75	75	2,80	2,80	170	62,73%
21	162	30	45	3,80	3,80	169	62,36%
22	236	45	75	1,80	2,80	169	62,36%
23	408	90	45	1,80	3,80	169	62,36%
24	179	30	75	3,80	2,80	167	61,62%
25	281	60	45	1,80	2,80	167	61,62%

Considering the results overall (see appendix) there is an enormous range on the overall results within the different parameter settings of the runs, as already noted in the first handmade study.

The top 25 ranking of the study shows that apparently a mixers placement in the upper area or at different heights of a digester is advantageous, as stated already in the previous “handmade” parametric study and mentioned by Rostalski and Springer (2010). The mixers horizontal orientation with an angle (line mixer through midsupport) larger than 45 degrees was shown to be beneficial too. The consideration of the subregions flow velocities in the evaluation (see table 12) results just in a slight shift of the settings ranking. The top 4 rated evaluation runs (369, 306, 305, 239) are the same in both tables 11 and 12.

The mixers orientation in particular show a significant influence onto the flow dynamics inside a digester. A more detailed view onto the mixing dynamics of some settings show that the flow velocity development from the inside (mid support) to the outside (wall) strongly depends on the mixer orientation. An angle of 0° of both mixers (see figure 31) provides the highest flow velocity towards the midsupport. From subregions 1 to 6 the velocity remains nearly stable, and just towards the wall a significant decline of the dynamic can be seen. The low dynamic close to the wall favors the appearance of inhomogeneity there.

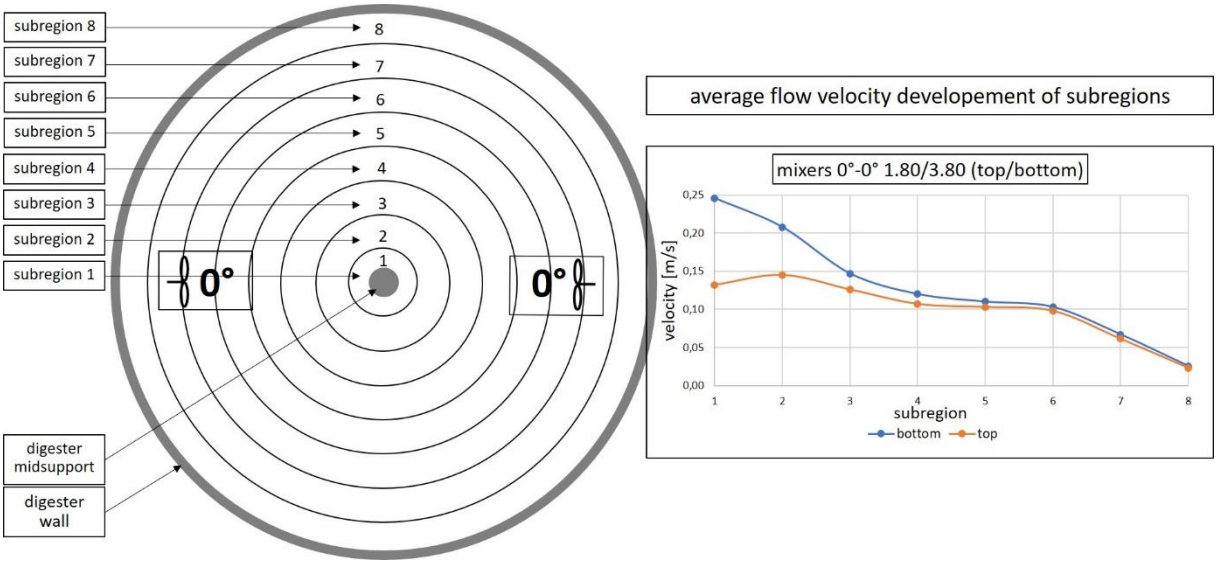

Figure 31: average flow velocity development at digester bottom half and top half and of subregions with mixers both at 0° and height 1.80m and 3.80m

Much different is the flow velocity development with both mixers orientation at 75° (see following figure 32). The lowest flow speed is given at the inner regions close to the midsupport. Towards the digester wall the flow velocity increases significantly until subregion 7. Just the outer subregion 8 (close to wall) show a drop of the flow velocity.

There is an enormous range between lowest and highest flow speed. The very low velocity close to the midsection can be critical in generating poorly mixed zone. When considering the results of the whole CFD study where a horizontal orientation angle larger than 45° is indicated as beneficial, figure 32 shows that this requires a differentiated consideration of the total score in respect of the ranking of a mixer setting. On the one hand there could be a very high flow dynamic (flow velocity) in some sections (i.e. subregions 6 and 7) and on the other hand there are sections (i.e. 1 and 2) with little or nearly critical flow velocity.

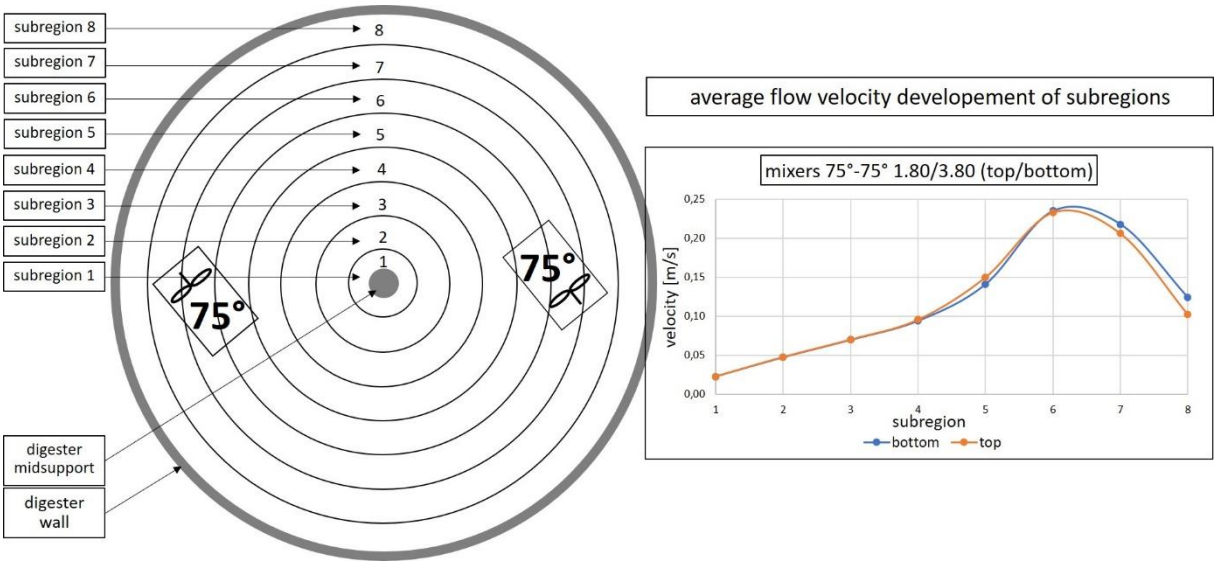

Figure 32: average flow velocity development at digester bottom half and top half and of subregions with mixers both at 75° and height 1.80m and 3.80m

With different mixers orientation, one at 0° and one at 90°, the development of the flow speed from inside to the outside is like the previous (mixers at 75°) but with a slight increase and fall in the velocity from inside to outside (see following figure 33). There is less velocity dynamic on the whole but not a significant range from lowest to highest flow speed, and the lowest flow speed was high enough to prevent poorly mixed zones.

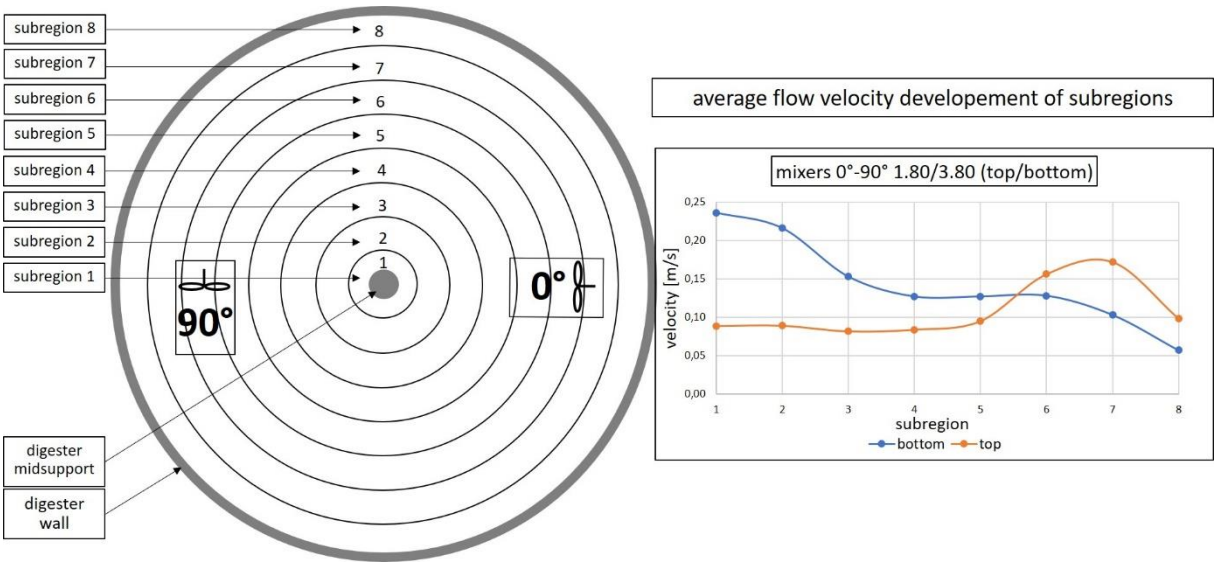

Figure 33: average flow velocity development at digester bottom half and top half and of subregions with mixers at 90° and 0° and height 1.80m and 3.80m

The horizontal orientation of the mixers has a significant influence on the flow dynamic inside the digester. It influences the substrates homogeneity as well as a rougher or more gentle treatment of the microbes. Both aspects are important for a stable and efficient biomass conversion process. Furthermore, the height arrangement of the mixers is essential too. A proper mixer orientation and placement prevents poorly mixed zones and the occurrence of harmful velocity peaks.

The following figures 34 to 36 illustrate the flow velocity development in a digester from the midsupport to the wall at selected horizontal orientation angles and placement at different heights. Both mixers at 0° (see figure 34) show less, potentially critical dynamic in velocity close to the digester wall. With mixers placed closer to the bottom the inner sub sections point out a significant high flow velocity what indicates high mixing dynamic there.

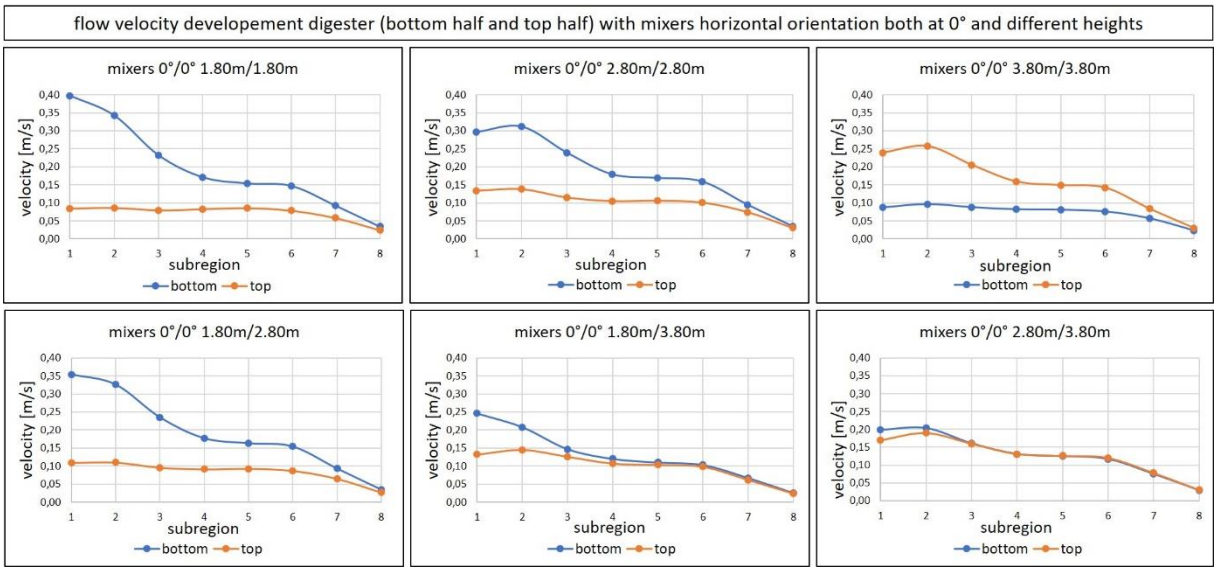

Figure 34: flow velocity development digester (bottom half and top half) with mixers horizontal orientation both at 0° and different heights

When the mixers orientation is larger than 45° we see the typical development with less dynamic close to the midsupport and close to the wall illustrated in figure 35. In between there are sections with high flow velocities. A placement of the mixers at different heights compensates this difference partially.

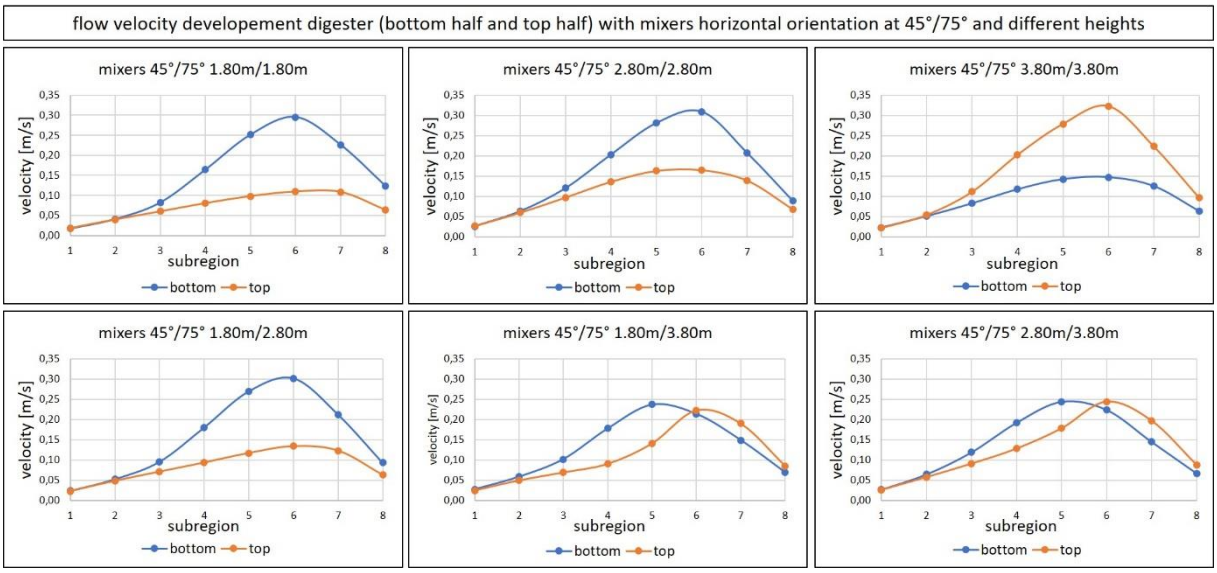

Figure 35: flow velocity development digester (bottom half and top half) with mixers horizontal orientation at 45°/75° and different heights

The most balanced dynamic appearance gives the following figure 36 with mixers orientation at 15° and 75°. This mixer setting shows hardly sections with very less and very high dynamic. A clear difference of the mixers horizontal orientation angles seems to be beneficial.

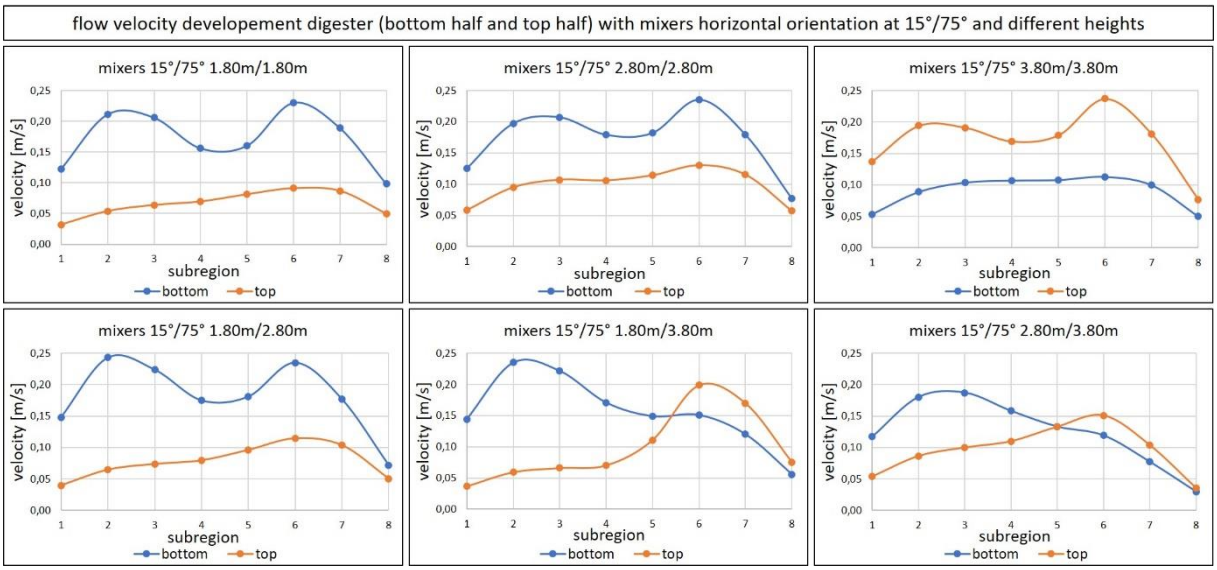

Figure 36: flow velocity development digester (bottom half and top half) with mixers horizontal orientation at 15°/75° and different heights

Furthermore, the previous figures 34-36 illustrate that a placement of the mixers at different heights is helpful for a digesters balanced dynamic and additionally a more gentle biomass treatment can be assumed due to less velocity peaks.

Regarding the energy consumption the CFD study show some savings with proper placement of the mixers too. The possible energy savings of the study range mainly at about 200Watts [W] (0.2 kilowatts [kW]) to 800W (0.8 kW) in total for the two mixers. The power P can be calculated from the measured torque T and rotational speed N with following expression (Equation 6)

$$P = 2\pi \times N \times T \qquad (6)$$

The optimisation of the mixers placement and orientation helps also to optimise the whole mixing operation strategy. A better homogeneity of the substrate achieved by the optimised mixers placement helps to reduce the length of mixers operation regarding an intermittent operation strategy. With an optimised intermittent operation mode (reduction of the operation periods) additional cost savings can be generated. A first impression gives the following Table 13, which illustrates the energy savings by an optimised mixer placement/orientation in combination to energy savings with an optimisation of an intermittent mixing (shortened operation period) mode. The savings of optimising the intermittent mixing time can be a multiple.

Based on the realistic assumption of a mixing configuration with 2 mixers, with an energy consumption of 18000W (18kW) in total and an operation time of 30min per hour at an intermittent mixing operation mode an energy consumption saving of 1.71kWh per hour can be achieved with a mere reduction of 5 min operation time per hour.

Table 13: rough consideration of energy input savings of digester mixing with an optimised mixers placement and intermittent operation

rough consideration of possible energy input savings *(combination of optimising mixers operation time as well as placement/orientation)*					
total operating mixers power [kW]	18	*presumed initial data (2 mixers)*			
initial intermittent operation time [min]/h	30				
energy consumption [kWh]/h	9				
power savings [kW] *(optimised mixers placement/orientation)*	0.5	*presumed from optimisation study (mean value)*			
operation time [min]/h *(reduced intermittent operation)*	29	28	27	26	25
savings energy consumption [kWh]/h *(of reduced mixers operation time)*	0.30	0.60	0.90	1.20	1.50
savings energy consumption [kWh]/h *(of optimised mixers placement/orientation)*	0.24	0.23	0.23	0.22	0.21
savings in total energy consumption [kWh]/h *(optimised intermittent operation and placement/orientation)*	**0.54**	**0.83**	**1.13**	**1.42**	**1.71**

The focus regarding the mixers placement and orientation must be on the flow dynamic inside a digester to get a homogenous substrate as far as possible. A homogeneous flow dynamic is highly dependent on the mixers placement and orientation as seen in previous figures 31 to 36. Digester homogeneity is important for stabilization of the digestion process and it supports the gas production according to Sindall (2014). As a result, the overall efficiency of the biogas digestion process increases. In summary this clearly demonstrates the importance of proper placement, orientation and operation mode (i.e. intermittent mixing) of the mixers in the digester.

7 Conclusions and recommendations

7.1 Conclusions of the research project

To find a proper mixing system investigation is necessary, but this research is difficult to perform due to the various and complex influences:

- rheology of biomass cannot be precisely defined
- the active biomass rheology often varies
- opacity of real substrate
- large geometrical dimensions in reality
- lack of proper (sensitive, precise, etc.) measurement equipment for use in real digesters.

Therefore, as an alternative approach computational fluid dynamics CFD (e.g. Siemens StarCCM+) can be beneficial for the optimisation. But the promising approach of CFD (savings in time, effort and cost) must be checked. To validate the accuracy of a computational fluid dynamics model a reality similar downscaled laboratory digester equipped with mixing systems and optical as well as acoustic setups was designed for investigation.

As important factor an artificial substrate, which properly mimicked the rheology of biomass was found in the cellulose Walocel™. Besides power consumption, torque at mixer blades and mixing time the flow velocity as main investigation parameter was determined in different mixing configurations.

The similarity of the experimental results and the values obtained from the CFD simulations validated the correctness of the method and confirmed the accuracy of computational fluid dynamics (CFD). The flow dynamics of a digester mixing system could there be confidently evaluated shown by the validated CFD. The accuracy of the computational fluid dynamics was found to depend on:

- precise geometry model with defined system boundaries and transition zones
- accuracy of physical boundary conditions

- a suitable flow model (turbulence, laminar) → in our case k-ε turbulence model
- appropriate meshing (type and size) → particularly at surfaces prism layers and at sections or components (e.g. mixer) with high velocity gradients a finer mesh
- proper reproduction of fluid behaviour (power law, etc.)

CFD supports suitable positioning of the mixers and helps to identify both, the well mixed zones and the poorly mixed zones inside a digester.

Furthermore, CFD modelling and analysis is not restricted to the presented project. Indeed, it is an appropriate tool to model other types of digester mixing like the recirculation of digester substrate or the removal and injection of biogas. Alternative digester construction such as an egg-shaped tank or in relation far more lean and tall digesters then the digester with large diameter and low height described in the project can be modelled with CFD. The analysis of further digester design and operation can be handled properly as well, like a gas-lift digester, the common UASB (upflow anaerobic sludge blanket) reactor, anaerobic filters, expanded- or fluidized- bed reactors, and others. In modern multistage digestion (separation of the digestion phases) different substrate viscosities of the individual phases must be handled in several tanks during the whole digestion process. With the presented method optimum settings can be found for each stage.

For CFD calculation commercial software tools like StarCCM+ seem easier to handle because of integrated CAD design tools (geometry preparing), automated meshing, preconfigured physics, defined calculation methodology (solvers) and given display options as well as a software support team in the background. Commercial CFD however are relative expensive compared to open source CFD software approaches like openFoam™, but these tools need more experience and additional programming skills. But both types are suitable tools.

Optimising digester mixing systems will be beneficial for the biogas process. It was concluded that the efficiency of a digester mixing system can be improved by:

- a proper placement of the mixers → We found in the study that the homogeneity of the substrate can be improved. Poorly mixed zones as well as vigorous mixed sections can be identified, to improve digester stability and efficiency.
- a proper intermittent mixing operation mode → Intermittent mixing was shown to support a calm biomass conversion process and provides significant energy savings.

Efficient intermittent mixing operation revenues proper mixers placement too.

- the use of bigger bladed propeller mixers → Bigger mixer blades have an efficient mixing impulse onto the mass to be moved (substrate) and support a gentle treatment of microbes and bacteria for substrate conversion due to lower rotational speed. The laboratory experiments confirmed also less energy consumption compared to smaller bladed propeller mixers

The CFD study case reported, indicated an increase in the digester efficiency that can be expected with the following mixers placement/orientation

- at different heights (with two or more mixers)
- preferably in upper regions
- at a horizontal orientation angle (referred to a straight line through midpoint) larger than 45° but by two or more mixers with a significant difference in orientation must be noted

However, it was also helpful to occasionally vary the mixer´s arrangement to change the flow dynamic inside a digester.

Due to the many and various influences on mixing a general optimisation function on the parameters/variables would not be derived now. But with the evidence that CFD accurately represented the hydrodynamics a benefit analysis on mixing relevant parameters derived from a CFD mixing study could be a functional method to assess and realise appropriate digester mixing solutions. This derived guidance will help to build up more efficient biogas plants.

7.2 Suggestions for further work steps

The results of the research suggest it would be interesting to carry out practical tests at laboratory scale and full scale on this CFD studies. Tests at full scale in particular help to determine the actual savings of a mixer settings energy consumption and the rewarded increase in the digester efficiency.

To improve CFD efficiency it would be helpful to deepen the investigation of meshing strategies. The meshing of a model has significant influence on the accuracy, calculation effort,

and calculation time needed. It is also worthwhile to have a closer look at asymmetrical mixer arrangements.

Besides the technical issues, better cost of ownership models using economics must also be defined which incorporate the costs generated by a mixer setting: power consumption, maintenance, process stability, substrate conversion rates, etc. Like the technical issues these economic aspects could be summed up in an economic benefit (EB).

A possible portfolio example is shown in figure 37 where technical (TB) and economic benefit (EB) are compared, the most efficient way of mixing in a cylindrical digester can be obtained. The blue points (examples of mixer settings) should be improved technically and economically onto the ideal field. As minimum a technical value (TB) of 50% and economic value (EB) of 50% is required.

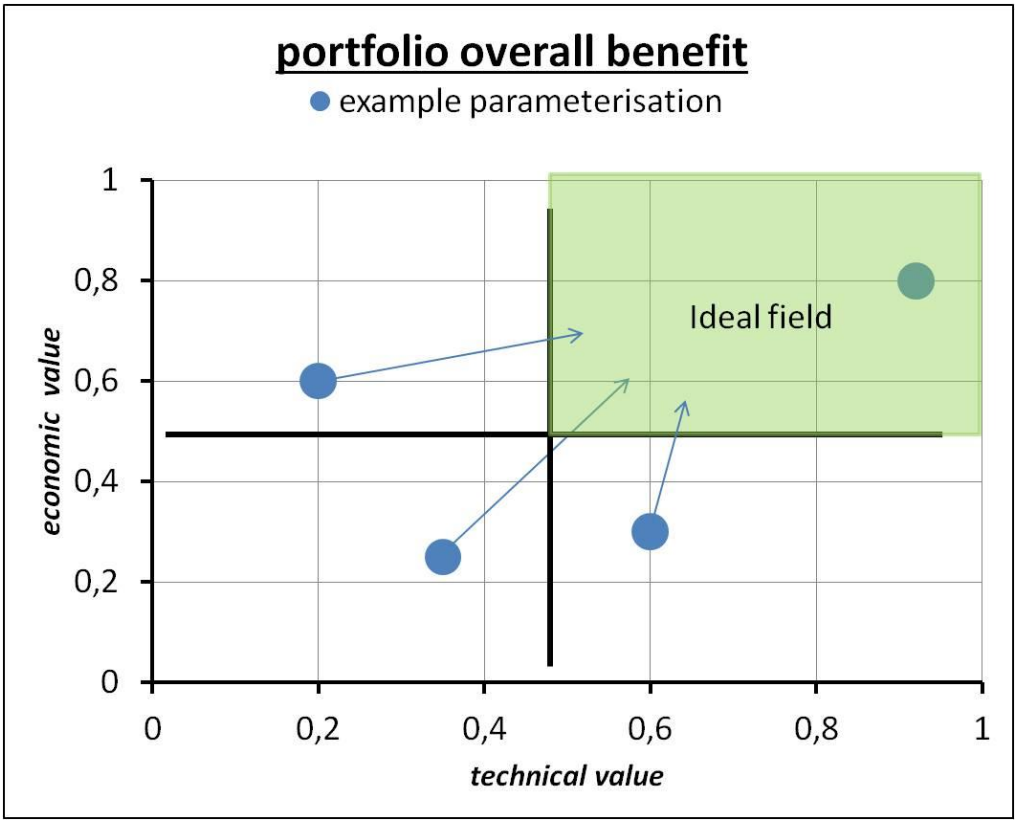

Figure 37: Portfolio comparison of technical and economic benefit for rating of mixer settings

Finally, it would be helping substantially for the complex multicriteria optimisation of digester mixing systems to find a function which covers the decision parameters.

References

AGRARHEUTE (2017), Available from: https://www.agrarheute.com/joule/biogas/biogas-flexibilisierung ueberschaubaren-kosten-532267, access 2017/11/5

AGRARHEUTE (2016), Available from: https://www.agrarheute.com/dlz/energie/bioga/mehr-energie-besten-substrat-530169, access 2017/11/5

AIVASIDIS, A., WANDREY, C. (1990). Development and Scaleup of a high-rate biogas process for treatment of organically polluted effluents, Annals of the New York Academy of Sciences 589, 599-615.

BALCHA, D.A., (2014). Ph.D. Thesis, University of Manitoba, Winnipeg Canada.

BASEDAU, D., (2015). Untersuchung von Strömungsvorgängen eines Zweiphasengemisches unter Berücksichtigung der Verortung dezentraler Rühraggregate und Betriebsparametervariationen innerhalb eines Fermenters einer Biogasanlage, PhD thesis, Leibniz Universität Hannover, ISBN 978-3-95900-050-5.

BIOGASTECHNIK SÜD GMBH (2017), *Datenblatt Paddelrührwerk RT-PRW_EN*, https://www.biogastechnik-sued.de/index.php?Paddelruehrwerk-Varibull#technischedaten

BENBELKACEM H., GARCIA-BERNET D., BOLLON J., LOISEL D., BAYARD R., STEYER J.-P., GOURDON R., BUFFIERE P., ESCUDIE R., (2013). Liquid mixing and solid segregation in high-solid anaerobic digesters, Bioresource Technol. 147, 387-394.

BRUNN, L., DORNACK, C., BILITEWSKI, B., (2009). Application of laboratory scale experiments to industrial scale in case of anaerobic waste treatment, Fresenius Environmental Bulletin 18 (2), 196-203.

CHU C. Y., WU S. Y., WU Y. C., LIN C. Y., (2011). Hydrodynamic behaviours in fermentative hydrogen bioreactors by pressure fluctuation analysis, Bioresource Technol. 102, 8669-8675.

CONTI, F., WIEDEMANN, L., JANUS, T., SONNLEITNER, M., ZÖRNER, W., GOLDBRUNNER, M., (2016). Mixing in biogas digesters: correlation between laboratory experiments on artificial

substrate and simulations with computational fluid dynamics. Proceeding of 10. Rostock Bioenergy Forum, Rostock, ISBN: 978-3-86009-433-4, 58, 445-450.

CRAIG, K.J., NIEUWOUDT, M.N., NIEMAND, L.J., (2013). CFD simulation of anaerobic digester with variable sewage sludge rheology. Wat. Res., 47, 4485-4497.

DANTEC DYNAMICS (2017). Available from: https://www.dantecdynamics.com/current-software-versions, access 2017/10/9

DAGUE, R.R., MCKINNEY, R.E., PFEFFER, J.T., (1970). Journal Water Pollution Control Federation, 42 (2) R29–R46.

DBFZ DEUTSCHES BIOMASSEFORSCHUNGSZENTRUM (2016). Collection of methods for biogas. 1st ed., Fischer Druck, Leipzig, Vol. 7, ISSN: 2364-897X.

DING J., WANG X., ZHOU X-F., REN N.-Q., GUAO W.-Q., (2010). CFD optimization of continuous stirred-tank (CSTR) reactor for biohydrogen production, Bioresource Technol. 101, 7016-7024.

FNR FACHAGENTUR FÜR NACHWACHSENDE ROHSTOFFE (2017). Bioenergy in Germany: Facts and figures. 3rd ed., Gülzow-Prüzen.

GALLERT, G., HENNING, A, WINTER, J., (2003). Scale-up of anaerobic digestion of the biowaste fraction from domestic wastes, Water Research 37, 1433-1441.

DBFZ DEUTSCHES BIOMASSEFORSCHUNGSZENTRUM, (2012). Monitoring zur Wirkung des Erneuerbare-Energien-Gesetz (EEG) auf die Entwicklung der Stromerzeugung aus Biomasse, Fischer, Leipzig, Report Nr. 12. ISSN: 2190-7943 (Online).

DBFZ DEUTSCHES BIOMASSEFORSCHUNGSZENTRUM, (2014). Entwicklung der Förderung der Stromerzeugung aus Biomasse im Rahmen des EEG, Fischer, Leipzig, Report Nr. 21, ISSN: 2197-4632 (Online).

JACOBSEN, F. (2015). CFD Modelling of Mesophilic Sludge Digester, Journal of Water Resource and Hydraulic Engineering, Vol. 4(2), pp. 162-170.

JIANG, J., WU J., ZHANG J., PONCIN S., LI H. Z., (2014). Multiscale hydrodynamic investigation to intensify the biogas production in upflow anaerobic reactors, Bioresource Technol. 155, 1-

7.

JOHANNES-GUTENBERG-UNIVERSITÄT MAINZ (2018). Available from: http://www.unimainz.de/eng/bilder_presse/10_mikrobiologie_biogasanlage_fermenter.jpg, access 2018/09/18

KIRAN, E. et al. (2014). Bioconversion of food waste to energy: A review. Fuel 134, 389-399.

KOWALCZYK, A., HARNISCH, E., SCHWEDE, S., GERBER, M., SPAN, R., (2013). Different mixing modes for biogas plants using energy crops, Applied Energy, 112, 465-472.

KSB SE & Co. KGaA, (2017), Available from: https://www.ksb.com/ksb-de/Produkte_Leistungen/Abwassertechnik/Biogas/ Messe_EuroTier/, access: 2017/01/23

LIN L., YAN R., LIU Y., JIANG W., (2010). In-depth investigation of enzymatic hydrolysis of biomass waste based on three major components: cellulose, hemicellulose and lignin, Bioresource Technol. 101, 8217-8223.

MAO, C., FENG, Y., WANG, X., et al., (2015). Review on research achievements of *biogas* from anaerobic digestion Renew. Sustain. Energy Reviews 45, 540-555.

POESCHL, M., WARD, S., OWENDE, P., (2010). Evaluation of energy efficiency of various *biogas* production and utilization pathways Appl. Energy 87, 3305-3321.

RATKOVICH, N., HORN, W., HELMUS, F.P., ROSENBERGER, S., NAESSENS, W., NOPENS, I., BENTZEN, T.R., (2013). Activated sludge rheology: A critical review on data collection and modelling, Water Research, 47, 463-482.

ROSTALSKI, K., SPRINGER, P., (2010). Tauchmotorrührwerke – ein Beitrag zur Anlageneffizienzsteigerung, Vortrag Seminar für Betreiber von Biogasanlagen 24/02/2010 Beratungszentrum Nachwachsende Rohstoffe des DLR-Eifel http://www.dlr.rlp.de/internet/global/themen.nsf/ALL/1046BD1C8B1B6DD3C12576DA00245B49?OpenDocument.

SAMANIUK J. R., SCOTT C. T., ROOT T. W., KLINGENBERG D. J., (2011). The effect of high intensity mixing on the enzymatic hydrolysis of concentrated cellulose fibre suspensions, Bioresource Technol. 102, 4489-4494.

SINDALL, R.C., (2014). Increasing the efficiency of anaerobic waste digesters by optimising flow

patterns to enhance biogas production, Ph.D. Thesis, University of Birmingham.

SONNLEITNER, M., (2012). Ecological and economic optimization of biogas plants. MPhil thesis, De Montfort University, Leicester.

STROOT, P.G., MCMAHON, K.D., MACKIE, R.I., RASKIN, L., (2001). Anaerobic codigestion of municipal solid waste and biosolids under various mixing conditions – I. digester performance, Wat. Res., 35(7), 1804–1816.

SUBRAMANIAN, B., MIOT, A., JONES, B., KLIBERT, C., PAGILLA, K.R., (2015). A full-scale study of mixing and foaming in egg-shaped anaerobic digesters, Bioresource Technol. 192, 461-470.

SUBRAMANIAN, B., PAGILLA, K.R., (2014). Anaerobic digester foaming in full-scale cylindrical digesters – effects of organic loading rate, feed characteristics, and mixing. Bioresource Technol. 159, 182–192.

THE DOW CHEMICAL COMPANY, (2018). *WALOCEL™ CRT* [WWW] available from: https://www. dow.com/dowwolff/en/industrial_solutions/product/walocel.htm, access 2018/09/27.

TERASHIMA, M., GOEL, R., KOMATSU, K., YASUI, H., TAKAHASHI, H, LI, Y.Y., NOIKE, T., (2009). CFD simulation of mixing in anaerobic digesters, Bioresource Technology 100 (7), 2228-2233.

WANG, X., DING J., GUO W.-Q., REN N.-Q., (2010). A hydrodynamics-reaction kinetics coupled model for evaluating bioreactors derived from CFD simulation, Bioresource Technol. 101, 9749-9757.

WIEDEMANN, L., CONTI, F., JANUS, T., SONNLEITNER, M., ZÖRNER, W., GOLDBRUNNER, M., (2017a). Mixing in biogas digesters and development of an artificial substrate for laboratory-scale mixing optimization. Chem. Eng. Technol. 40, 238-247.

WIEDEMANN, L., CONTI, F., JANUS, T., SONNLEITNER, M., ZÖRNER, W., GOLDBRUNNER, M., (2017b). Investigation of fluid dynamic in a scale-down laboratory digester. Proceeding of International Conference Progress in Biogas IV, Stuttgart, ISBN: 978-3-940706-09-6, 112.

WIEDEMANN, L., CONTI, F., JANUS, T., SONNLEITNER, M., ZÖRNER, W., GOLDBRUNNER, M.,

(2017c). Optimization of the mixing system in biodigesters with computational fluid dynamics (CFD). Proceeding of International Conference Progress in Biogas IV, Stuttgart, ISBN: 978-3-940706-09-6, 147.

WIEDEMANN, L., CONTI, F., SONNLEITNER, M., SAIDI, A., GOLDBRUNNER, M., (2017d). Investigation and optimization of the mixing in a biogas digester with a laboratory experiment and an artificial model substrate. Proceeding of 25th European Biomass Conference EUBCE, Stockholm, in press.

WU, B., (2010). Computational fluid dynamics investigation of turbulence models for non-Newtonian fluid flow in anaerobic digesters. Environmental Science and Technology 44 (23), 8989-8995.

WU, B., (2011). CFD investigation of turbulence models for mechanical agitation of non-Newtonian fluids in anaerobic digesters, Wat. Res., 2011, 45, pp. 2082-2094, Elsevier science Ltd.

YAN X., WU Q., SUN J., LIANG P., ZHANG X., XIAO K., HUUANG X., (2016). Hydrodynamic optimization of membrane bioreactor by horizontal geometry modification using computational fluid dynamics, Bioresource Technol. 200, 328-334.

YAN X., XIAO K., LIANG S., LEI T., LIANG P., XUE T., YU K., GUAN J., (2015). Hydraulic optimization of membrane bioreactor via baffle modification using computational fluid dynamics, Bioresource Technol. 175, 633-637.

Appendix A

CFD study parameter settings

The following Table gives the 441 mixer settings (evaluation runs) of the CFD study done with the OPTIMATE tool of Siemens StarCCM+ with parameters variable:

- AngleLRRR1 → mixer1 horizontal orientation angle [°]
- AngleLRRR2 → mixer2 horizontal orientation angle [°]
- TransRR1_Z → mixer1 height adjustment [m]
- TransRR2_Z → mixer2 height adjustment [m]

Evaluation Run CFD	AngleLRRR1	AngleLRRR2	TransRR1_Z [m]	TransRR2_Z [m]
1	0	0	1,80	1,80
2	0	0	1,80	2,80
3	0	0	1,80	3,80
4	0	0	2,80	1,80
5	0	0	2,80	2,80
6	0	0	2,80	3,80
7	0	0	3,80	1,80
8	0	0	3,80	2,80
9	0	0	3,80	3,80
10	0	15	1,80	1,80
11	0	15	1,80	2,80
12	0	15	1,80	3,80
13	0	15	2,80	1,80
14	0	15	2,80	2,80
15	0	15	2,80	3,80
16	0	15	3,80	1,80
17	0	15	3,80	2,80
18	0	15	3,80	3,80
19	0	30	1,80	1,80
20	0	30	1,80	2,80
21	0	30	1,80	3,80
22	0	30	2,80	1,80
23	0	30	2,80	2,80
24	0	30	2,80	3,80
25	0	30	3,80	1,80
26	0	30	3,80	2,80
27	0	30	3,80	3,80
28	0	45	1,80	1,80
29	0	45	1,80	2,80
30	0	45	1,80	3,80
31	0	45	2,80	1,80
32	0	45	2,80	2,80
33	0	45	2,80	3,80
34	0	45	3,80	1,80
35	0	45	3,80	2,80
36	0	45	3,80	3,80
37	0	60	1,80	1,80
38	0	60	1,80	2,80
39	0	60	1,80	3,80
40	0	60	2,80	1,80
41	0	60	2,80	2,80
42	0	60	2,80	3,80
43	0	60	3,80	1,80
44	0	60	3,80	2,80
45	0	60	3,80	3,80
46	0	75	1,80	1,80

Evaluation Run CFD	AngleLRRR1	AngleLRRR2	TransRR1_Z [m]	TransRR2_Z [m]
47	0	75	1,80	2,80
48	0	75	1,80	3,80
49	0	75	2,80	1,80
50	0	75	2,80	2,80
51	0	75	2,80	3,80
52	0	75	3,80	1,80
53	0	75	3,80	2,80
54	0	75	3,80	3,80
55	0	90	1,80	1,80
56	0	90	1,80	2,80
57	0	90	1,80	3,80
58	0	90	2,80	1,80
59	0	90	2,80	2,80
60	0	90	2,80	3,80
61	0	90	3,80	1,80
62	0	90	3,80	2,80
63	0	90	3,80	3,80
64	15	0	1,80	1,80
65	15	0	1,80	2,80
66	15	0	1,80	3,80
67	15	0	2,80	1,80
68	15	0	2,80	2,80
69	15	0	2,80	3,80
70	15	0	3,80	1,80
71	15	0	3,80	2,80
72	15	0	3,80	3,80
73	15	15	1,80	1,80
74	15	15	1,80	2,80
75	15	15	1,80	3,80
76	15	15	2,80	1,80
77	15	15	2,80	2,80
78	15	15	2,80	3,80
79	15	15	3,80	1,80
80	15	15	3,80	2,80
81	15	15	3,80	3,80
82	15	30	1,80	1,80
83	15	30	1,80	2,80
84	15	30	1,80	3,80
85	15	30	2,80	1,80
86	15	30	2,80	2,80
87	15	30	2,80	3,80
88	15	30	3,80	1,80
89	15	30	3,80	2,80
90	15	30	3,80	3,80
91	15	45	1,80	1,80
92	15	45	1,80	2,80
93	15	45	1,80	3,80
94	15	45	2,80	1,80
95	15	45	2,80	2,80
96	15	45	2,80	3,80
97	15	45	3,80	1,80
98	15	45	3,80	2,80
99	15	45	3,80	3,80
100	15	60	1,80	1,80
101	15	60	1,80	2,80
102	15	60	1,80	3,80
103	15	60	2,80	1,80
104	15	60	2,80	2,80
105	15	60	2,80	3,80
106	15	60	3,80	1,80
107	15	60	3,80	2,80
108	15	60	3,80	3,80
109	15	75	1,80	1,80
110	15	75	1,80	2,80
111	15	75	1,80	3,80
112	15	75	2,80	1,80
113	15	75	2,80	2,80

Evaluation Run CFD	AngleLRRR1	AngleLRRR2	TransRR1_Z [m]	TransRR2_Z [m]
114	15	75	2,80	3,80
115	15	75	3,80	1,80
116	15	75	3,80	2,80
117	15	75	3,80	3,80
118	15	90	1,80	1,80
119	15	90	1,80	2,80
120	15	90	1,80	3,80
121	15	90	2,80	1,80
122	15	90	2,80	2,80
123	15	90	2,80	3,80
124	15	90	3,80	1,80
125	15	90	3,80	2,80
126	15	90	3,80	3,80
127	30	0	1,80	1,80
128	30	0	1,80	2,80
129	30	0	1,80	3,80
130	30	0	2,80	1,80
131	30	0	2,80	2,80
132	30	0	2,80	3,80
133	30	0	3,80	1,80
134	30	0	3,80	2,80
135	30	0	3,80	3,80
136	30	15	1,80	1,80
137	30	15	1,80	2,80
138	30	15	1,80	3,80
139	30	15	2,80	1,80
140	30	15	2,80	2,80
141	30	15	2,80	3,80
142	30	15	3,80	1,80
143	30	15	3,80	2,80
144	30	15	3,80	3,80
145	30	30	1,80	1,80
146	30	30	1,80	2,80
147	30	30	1,80	3,80
148	30	30	2,80	1,80
149	30	30	2,80	2,80
150	30	30	2,80	3,80
151	30	30	3,80	1,80
152	30	30	3,80	2,80
153	30	30	3,80	3,80
154	30	45	1,80	1,80
155	30	45	1,80	2,80
156	30	45	1,80	3,80
157	30	45	2,80	1,80
158	30	45	2,80	2,80
159	30	45	2,80	3,80
160	30	45	3,80	1,80
161	30	45	3,80	2,80
162	30	45	3,80	3,80
163	30	60	1,80	1,80
164	30	60	1,80	2,80
165	30	60	1,80	3,80
166	30	60	2,80	1,80
167	30	60	2,80	2,80
168	30	60	2,80	3,80
169	30	60	3,80	1,80
170	30	60	3,80	2,80
171	30	60	3,80	3,80
172	30	75	1,80	1,80
173	30	75	1,80	2,80
174	30	75	1,80	3,80
175	30	75	2,80	1,80
176	30	75	2,80	2,80
177	30	75	2,80	3,80
178	30	75	3,80	1,80
179	30	75	3,80	2,80
180	30	75	3,80	3,80

Evaluation Run CFD	AngleLRRR1	AngleLRRR2	TransRR1_Z [m]	TransRR2_Z [m]
181	30	90	1,80	1,80
182	30	90	1,80	2,80
183	30	90	1,80	3,80
184	30	90	2,80	1,80
185	30	90	2,80	2,80
186	30	90	2,80	3,80
187	30	90	3,80	1,80
188	30	90	3,80	2,80
189	30	90	3,80	3,80
190	45	0	1,80	1,80
191	45	0	1,80	2,80
192	45	0	1,80	3,80
193	45	0	2,80	1,80
194	45	0	2,80	2,80
195	45	0	2,80	3,80
196	45	0	3,80	1,80
197	45	0	3,80	2,80
198	45	0	3,80	3,80
199	45	15	1,80	1,80
200	45	15	1,80	2,80
201	45	15	1,80	3,80
202	45	15	2,80	1,80
203	45	15	2,80	2,80
204	45	15	2,80	3,80
205	45	15	3,80	1,80
206	45	15	3,80	2,80
207	45	15	3,80	3,80
208	45	30	1,80	1,80
209	45	30	1,80	2,80
210	45	30	1,80	3,80
211	45	30	2,80	1,80
212	45	30	2,80	2,80
213	45	30	2,80	3,80
214	45	30	3,80	1,80
215	45	30	3,80	2,80
216	45	30	3,80	3,80
217	45	45	1,80	1,80
218	45	45	1,80	2,80
219	45	45	1,80	3,80
220	45	45	2,80	1,80
221	45	45	2,80	2,80
222	45	45	2,80	3,80
223	45	45	3,80	1,80
224	45	45	3,80	2,80
225	45	45	3,80	3,80
226	45	60	1,80	1,80
227	45	60	1,80	2,80
228	45	60	1,80	3,80
229	45	60	2,80	1,80
230	45	60	2,80	2,80
231	45	60	2,80	3,80
232	45	60	3,80	1,80
233	45	60	3,80	2,80
234	45	60	3,80	3,80
235	45	75	1,80	1,80
236	45	75	1,80	2,80
237	45	75	1,80	3,80
238	45	75	2,80	1,80
239	45	75	2,80	2,80
240	45	75	2,80	3,80
241	45	75	3,80	1,80
242	45	75	3,80	2,80
243	45	75	3,80	3,80
244	45	90	1,80	1,80
245	45	90	1,80	2,80
246	45	90	1,80	3,80
247	45	90	2,80	1,80

Evaluation Run CFD	AngleLRRR1	AngleLRRR2	TransRR1_Z [m]	TransRR2_Z [m]
248	45	90	2,80	2,80
249	45	90	2,80	3,80
250	45	90	3,80	1,80
251	45	90	3,80	2,80
252	45	90	3,80	3,80
253	60	0	1,80	1,80
254	60	0	1,80	2,80
255	60	0	1,80	3,80
256	60	0	2,80	1,80
257	60	0	2,80	2,80
258	60	0	2,80	3,80
259	60	0	3,80	1,80
260	60	0	3,80	2,80
261	60	0	3,80	3,80
262	60	15	1,80	1,80
263	60	15	1,80	2,80
264	60	15	1,80	3,80
265	60	15	2,80	1,80
266	60	15	2,80	2,80
267	60	15	2,80	3,80
268	60	15	3,80	1,80
269	60	15	3,80	2,80
270	60	15	3,80	3,80
271	60	30	1,80	1,80
272	60	30	1,80	2,80
273	60	30	1,80	3,80
274	60	30	2,80	1,80
275	60	30	2,80	2,80
276	60	30	2,80	3,80
277	60	30	3,80	1,80
278	60	30	3,80	2,80
279	60	30	3,80	3,80
280	60	45	1,80	1,80
281	60	45	1,80	2,80
282	60	45	1,80	3,80
283	60	45	2,80	1,80
284	60	45	2,80	2,80
285	60	45	2,80	3,80
286	60	45	3,80	1,80
287	60	45	3,80	2,80
288	60	45	3,80	3,80
289	60	60	1,80	1,80
290	60	60	1,80	2,80
291	60	60	1,80	3,80
292	60	60	2,80	1,80
293	60	60	2,80	2,80
294	60	60	2,80	3,80
295	60	60	3,80	1,80
296	60	60	3,80	2,80
297	60	60	3,80	3,80
298	60	75	1,80	1,80
299	60	75	1,80	2,80
300	60	75	1,80	3,80
301	60	75	2,80	1,80
302	60	75	2,80	2,80
303	60	75	2,80	3,80
304	60	75	3,80	1,80
305	60	75	3,80	2,80
306	60	75	3,80	3,80
307	60	90	1,80	1,80
308	60	90	1,80	2,80
309	60	90	1,80	3,80
310	60	90	2,80	1,80
311	60	90	2,80	2,80
312	60	90	2,80	3,80
313	60	90	3,80	1,80
314	60	90	3,80	2,80

Evaluation Run CFD	AngleLRRR1	AngleLRRR2	TransRR1_Z [m]	TransRR2_Z [m]
315	60	90	3,80	3,80
316	75	0	1,80	1,80
317	75	0	1,80	2,80
318	75	0	1,80	3,80
319	75	0	2,80	1,80
320	75	0	2,80	2,80
321	75	0	2,80	3,80
322	75	0	3,80	1,80
323	75	0	3,80	2,80
324	75	0	3,80	3,80
325	75	15	1,80	1,80
326	75	15	1,80	2,80
327	75	15	1,80	3,80
328	75	15	2,80	1,80
329	75	15	2,80	2,80
330	75	15	2,80	3,80
331	75	15	3,80	1,80
332	75	15	3,80	2,80
333	75	15	3,80	3,80
334	75	30	1,80	1,80
335	75	30	1,80	2,80
336	75	30	1,80	3,80
337	75	30	2,80	1,80
338	75	30	2,80	2,80
339	75	30	2,80	3,80
340	75	30	3,80	1,80
341	75	30	3,80	2,80
342	75	30	3,80	3,80
343	75	45	1,80	1,80
344	75	45	1,80	2,80
345	75	45	1,80	3,80
346	75	45	2,80	1,80
347	75	45	2,80	2,80
348	75	45	2,80	3,80
349	75	45	3,80	1,80
350	75	45	3,80	2,80
351	75	45	3,80	3,80
352	75	60	1,80	1,80
353	75	60	1,80	2,80
354	75	60	1,80	3,80
355	75	60	2,80	1,80
356	75	60	2,80	2,80
357	75	60	2,80	3,80
358	75	60	3,80	1,80
359	75	60	3,80	2,80
360	75	60	3,80	3,80
361	75	75	1,80	1,80
362	75	75	1,80	2,80
363	75	75	1,80	3,80
364	75	75	2,80	1,80
365	75	75	2,80	2,80
366	75	75	2,80	3,80
367	75	75	3,80	1,80
368	75	75	3,80	2,80
369	75	75	3,80	3,80
370	75	90	1,80	1,80
371	75	90	1,80	2,80
372	75	90	1,80	3,80
373	75	90	2,80	1,80
374	75	90	2,80	2,80
375	75	90	2,80	3,80
376	75	90	3,80	1,80
377	75	90	3,80	2,80
378	75	90	3,80	3,80
379	90	0	1,80	1,80
380	90	0	1,80	2,80
381	90	0	1,80	3,80

Evaluation Run CFD	AngleLRRR1	AngleLRRR2	TransRR1_Z [m]	TransRR2_Z [m]
382	90	0	2,80	1,80
383	90	0	2,80	2,80
384	90	0	2,80	3,80
385	90	0	3,80	1,80
386	90	0	3,80	2,80
387	90	0	3,80	3,80
388	90	15	1,80	1,80
389	90	15	1,80	2,80
390	90	15	1,80	3,80
391	90	15	2,80	1,80
392	90	15	2,80	2,80
393	90	15	2,80	3,80
394	90	15	3,80	1,80
395	90	15	3,80	2,80
396	90	15	3,80	3,80
397	90	30	1,80	1,80
398	90	30	1,80	2,80
399	90	30	1,80	3,80
400	90	30	2,80	1,80
401	90	30	2,80	2,80
402	90	30	2,80	3,80
403	90	30	3,80	1,80
404	90	30	3,80	2,80
405	90	30	3,80	3,80
406	90	45	1,80	1,80
407	90	45	1,80	2,80
408	90	45	1,80	3,80
409	90	45	2,80	1,80
410	90	45	2,80	2,80
411	90	45	2,80	3,80
412	90	45	3,80	1,80
413	90	45	3,80	2,80
414	90	45	3,80	3,80
415	90	60	1,80	1,80
416	90	60	1,80	2,80
417	90	60	1,80	3,80
418	90	60	2,80	1,80
419	90	60	2,80	2,80
420	90	60	2,80	3,80
421	90	60	3,80	1,80
422	90	60	3,80	2,80
423	90	60	3,80	3,80
424	90	75	1,80	1,80
425	90	75	1,80	2,80
426	90	75	1,80	3,80
427	90	75	2,80	1,80
428	90	75	2,80	2,80
429	90	75	2,80	3,80
430	90	75	3,80	1,80
431	90	75	3,80	2,80
432	90	75	3,80	3,80
433	90	90	1,80	1,80
434	90	90	1,80	2,80
435	90	90	1,80	3,80
436	90	90	2,80	1,80
437	90	90	2,80	2,80
438	90	90	2,80	3,80
439	90	90	3,80	1,80
440	90	90	3,80	2,80
441	90	90	3,80	3,80

Appendix B

CFD calculated flow velocities at subregions

The following Table gives the calculated flow velocity oft he 441 CFD study runs at the 8 subregions devided into the digesters top half (t) and bottom half (b).

Eval. Run CFD	AvMag1b [m/s]	AvMag1t [m/s]	AvMag2b [m/s]	AvMag2t [m/s]	AvMag3b [m/s]	AvMag3t [m/s]	AvMag4b [m/s]	AvMag4t [m/s]	AvMag5b [m/s]	AvMag5t [m/s]	AvMag6b [m/s]	AvMag6t [m/s]	AvMag7b [m/s]	AvMag7t [m/s]	AvMag8b [m/s]	AvMag8t [m/s]
1	0,3970	0,0847	0,3420	0,0863	0,2320	0,0796	0,1710	0,0827	0,1540	0,0857	0,1470	0,0784	0,0923	0,0579	0,0342	0,0239
2	0,3540	0,1090	0,3260	0,1100	0,2350	0,0959	0,1770	0,0910	0,1630	0,0926	0,1540	0,0870	0,0932	0,0650	0,0346	0,0269
3	0,2460	0,1320	0,2080	0,1450	0,1470	0,1260	0,1200	0,1070	0,1100	0,1030	0,1030	0,0979	0,0669	0,0612	0,0254	0,0232
4	0,3370	0,1120	0,3220	0,1130	0,2320	0,0962	0,1750	0,0910	0,1620	0,0922	0,1510	0,0860	0,0913	0,0639	0,0339	0,0265
5	0,2960	0,1340	0,3110	0,1380	0,2390	0,1150	0,1790	0,1050	0,1690	0,1060	0,1590	0,1010	0,0950	0,0747	0,0354	0,0308
6	0,1990	0,1700	0,2040	0,1900	0,1610	0,1600	0,1310	0,1310	0,1250	0,1260	0,1170	0,1200	0,0750	0,0780	0,0291	0,0303
7	0,2840	0,2490	0,2330	0,2190	0,1600	0,1540	0,1280	0,1240	0,1150	0,1140	0,1040	0,1010	0,0667	0,0623	0,0251	0,0230
8	0,2040	0,2030	0,2060	0,2130	0,1600	0,1680	0,1300	0,1340	0,1250	0,1270	0,1160	0,1200	0,0756	0,0786	0,0293	0,0300
9	0,0870	0,2390	0,0961	0,2570	0,0876	0,2050	0,0817	0,1590	0,0806	0,1490	0,0758	0,1420	0,0568	0,0836	0,0235	0,0303
10	0,3720	0,0718	0,3690	0,0764	0,2720	0,0710	0,1890	0,0731	0,1590	0,0789	0,1500	0,0774	0,0979	0,0625	0,0385	0,0277
11	0,2910	0,0836	0,3060	0,0983	0,2410	0,0916	0,1770	0,0835	0,1490	0,0818	0,1390	0,0762	0,0854	0,0573	0,0323	0,0239
12	0,3080	0,1960	0,2390	0,2090	0,1640	0,1720	0,1270	0,1350	0,1100	0,1130	0,1000	0,0983	0,0642	0,0603	0,0244	0,0223
13	0,2570	0,0878	0,3220	0,0967	0,2630	0,0862	0,1840	0,0816	0,1590	0,0840	0,1500	0,0828	0,0955	0,0662	0,0370	0,0286
14	0,2560	0,1100	0,3030	0,1250	0,2540	0,1120	0,1900	0,0989	0,1660	0,0985	0,1530	0,0957	0,0928	0,0725	0,0351	0,0303
15	0,1960	0,1850	0,2090	0,2110	0,1670	0,1820	0,1310	0,1450	0,1200	0,1260	0,1100	0,1150	0,0702	0,0742	0,0273	0,0284
16	0,1860	0,2260	0,2430	0,2060	0,2030	0,1500	0,1480	0,1180	0,1260	0,1080	0,1140	0,0997	0,0763	0,0656	0,0291	0,0262
17	0,1660	0,2310	0,2050	0,2250	0,1840	0,1740	0,1450	0,1350	0,1240	0,1210	0,1110	0,1110	0,0706	0,0720	0,0268	0,0277
18	0,1030	0,3100	0,1110	0,3280	0,1020	0,2630	0,0922	0,1970	0,0900	0,1650	0,0848	0,1490	0,0637	0,0892	0,0265	0,0330
19	0,2030	0,0461	0,2300	0,0566	0,2350	0,0568	0,2250	0,0584	0,1750	0,0640	0,1460	0,0659	0,0946	0,0540	0,0364	0,0238

Eval. Run CFD	AvMag1b [m/s]	AvMag1t [m/s]	AvMag2b [m/s]	AvMag2t [m/s]	AvMag3b [m/s]	AvMag3t [m/s]	AvMag4b [m/s]	AvMag4t [m/s]	AvMag5b [m/s]	AvMag5t [m/s]	AvMag6b [m/s]	AvMag6t [m/s]	AvMag7b [m/s]	AvMag7t [m/s]	AvMag8b [m/s]	AvMag8t [m/s]
20	0,3210	0,0687	0,2720	0,0812	0,2450	0,0902	0,2230	0,0891	0,1780	0,0808	0,1420	0,0744	0,0863	0,0586	0,0331	0,0252
21	0,2510	0,0746	0,2070	0,1260	0,1500	0,1590	0,1210	0,1600	0,1040	0,1330	0,0961	0,0988	0,0660	0,0614	0,0266	0,0243
22	0,2260	0,0940	0,2570	0,0926	0,2680	0,0779	0,2470	0,0722	0,1930	0,0763	0,1580	0,0798	0,1030	0,0675	0,0411	0,0307
23	0,1550	0,0799	0,2140	0,1010	0,2270	0,1050	0,2080	0,0977	0,1720	0,0888	0,1430	0,0847	0,0870	0,0668	0,0339	0,0289
24	0,1070	0,0702	0,1380	0,1410	0,1390	0,1920	0,1240	0,1920	0,1120	0,1550	0,1080	0,1160	0,0728	0,0760	0,0302	0,0307
25	0,0889	0,2530	0,1330	0,2130	0,1840	0,1490	0,2050	0,1160	0,1630	0,1080	0,1280	0,1060	0,0880	0,0733	0,0349	0,0305
26	0,0948	0,2460	0,1420	0,2150	0,1840	0,1700	0,1890	0,1400	0,1510	0,1200	0,1120	0,1080	0,0713	0,0722	0,0281	0,0289
27	0,0915	0,2560	0,1020	0,2790	0,1030	0,2680	0,0994	0,2350	0,0914	0,1920	0,0843	0,1530	0,0655	0,0919	0,0282	0,0356
28	0,2590	0,0485	0,2100	0,0554	0,1560	0,0537	0,1900	0,0571	0,2280	0,0648	0,1890	0,0689	0,1150	0,0620	0,0495	0,0311
29	0,2770	0,0614	0,2110	0,0717	0,1690	0,0775	0,1900	0,0888	0,2050	0,0909	0,1680	0,0751	0,0855	0,0567	0,0337	0,0257
30	0,2930	0,0601	0,2230	0,0705	0,1530	0,1130	0,1320	0,1750	0,1210	0,1960	0,1080	0,1480	0,0722	0,0714	0,0296	0,0278
31	0,2080	0,0818	0,2030	0,0839	0,1690	0,0728	0,1990	0,0718	0,2380	0,0793	0,1970	0,0846	0,1160	0,0732	0,0493	0,0347
32	0,1970	0,0844	0,1990	0,0912	0,1820	0,0888	0,2010	0,0943	0,2200	0,0983	0,1770	0,0878	0,0880	0,0672	0,0345	0,0298
33	0,2080	0,0873	0,2030	0,0903	0,1530	0,1180	0,1300	0,1740	0,1250	0,2000	0,1110	0,1580	0,0736	0,0814	0,0306	0,0323
34	0,0808	0,2310	0,0815	0,1980	0,0944	0,1390	0,1550	0,1110	0,2020	0,1080	0,1630	0,1080	0,1030	0,0805	0,0471	0,0371
35	0,0805	0,2220	0,0911	0,1980	0,1170	0,1560	0,1620	0,1420	0,1840	0,1340	0,1440	0,1170	0,0759	0,0771	0,0318	0,0325
36	0,0790	0,2370	0,0867	0,2070	0,0851	0,1760	0,0894	0,2050	0,0906	0,2190	0,0807	0,1780	0,0613	0,0886	0,0270	0,0341
37	0,2690	0,0497	0,2200	0,0569	0,1400	0,0568	0,1220	0,0606	0,1850	0,0700	0,2280	0,0759	0,1440	0,0697	0,0683	0,0378
38	0,2660	0,0613	0,2110	0,0724	0,1400	0,0718	0,1370	0,0765	0,1840	0,0890	0,2030	0,0869	0,1090	0,0632	0,0376	0,0277
39	0,2800	0,0568	0,2130	0,0650	0,1420	0,0636	0,1170	0,0871	0,1170	0,1440	0,1130	0,1640	0,0745	0,0892	0,0294	0,0286
40	0,2140	0,0828	0,2020	0,0826	0,1390	0,0719	0,1250	0,0713	0,1880	0,0797	0,2250	0,0851	0,1370	0,0743	0,0588	0,0367
41	0,1820	0,0834	0,1870	0,0945	0,1450	0,0893	0,1440	0,0897	0,1920	0,1010	0,2100	0,0998	0,1140	0,0746	0,0400	0,0332
42	0,2220	0,1020	0,2100	0,1030	0,1550	0,0836	0,1280	0,1060	0,1340	0,1820	0,1320	0,2110	0,0906	0,1240	0,0380	0,0437
43	0,0678	0,2120	0,0751	0,1890	0,0689	0,1370	0,0812	0,1130	0,1460	0,1120	0,1890	0,1120	0,1220	0,0828	0,0569	0,0387
44	0,0863	0,2460	0,0940	0,2130	0,0884	0,1600	0,1100	0,1370	0,1690	0,1410	0,1930	0,1380	0,1140	0,0923	0,0422	0,0389
45	0,0821	0,2400	0,0882	0,2090	0,0852	0,1470	0,0862	0,1430	0,0952	0,2050	0,0944	0,2300	0,0720	0,1270	0,0314	0,0426

Eval. Run CFD	AvMag1b [m/s]	AvMag1t [m/s]	AvMag2b [m/s]	AvMag2t [m/s]	AvMag3b [m/s]	AvMag3t [m/s]	AvMag4b [m/s]	AvMag4t [m/s]	AvMag5b [m/s]	AvMag5t [m/s]	AvMag6b [m/s]	AvMag6t [m/s]	AvMag7b [m/s]	AvMag7t [m/s]	AvMag8b [m/s]	AvMag8t [m/s]
46	0,2900	0,0529	0,2200	0,0603	0,1440	0,0624	0,1150	0,0682	0,1330	0,0756	0,2070	0,0797	0,1690	0,0750	0,0892	0,0431
47	0,2720	0,0584	0,2130	0,0709	0,1460	0,0736	0,1190	0,0760	0,1400	0,0847	0,1960	0,0945	0,1440	0,0808	0,0572	0,0389
48	0,2800	0,0572	0,2160	0,0656	0,1450	0,0664	0,1190	0,0681	0,1160	0,0996	0,1220	0,1730	0,0933	0,1410	0,0429	0,0584
49	0,2050	0,0858	0,2040	0,0874	0,1500	0,0776	0,1180	0,0786	0,1380	0,0878	0,2140	0,0959	0,1740	0,0892	0,0949	0,0503
50	0,2080	0,0991	0,2050	0,1030	0,1550	0,0947	0,1280	0,0923	0,1570	0,1020	0,2140	0,1150	0,1570	0,0985	0,0634	0,0471
51	0,2240	0,0926	0,2070	0,0948	0,1500	0,0843	0,1250	0,0800	0,1240	0,1120	0,1290	0,1910	0,1000	0,1590	0,0477	0,0695
52	0,0697	0,1900	0,0794	0,1790	0,0765	0,1340	0,0739	0,1150	0,0955	0,1140	0,1720	0,1180	0,1530	0,0931	0,0867	0,0489
53	0,0828	0,2490	0,0903	0,2100	0,0879	0,1550	0,0855	0,1300	0,1130	0,1310	0,1750	0,1410	0,1400	0,1070	0,0600	0,0502
54	0,0795	0,2460	0,0856	0,2100	0,0839	0,1530	0,0841	0,1240	0,0894	0,1460	0,0981	0,2210	0,0876	0,1680	0,0437	0,0696
55	0,2710	0,0504	0,2100	0,0573	0,1390	0,0590	0,1150	0,0655	0,1130	0,0733	0,1650	0,0772	0,1670	0,0753	0,1080	0,0484
56	0,2840	0,0537	0,2150	0,0634	0,1450	0,0668	0,1220	0,0727	0,1200	0,0792	0,1680	0,0876	0,1530	0,0865	0,0776	0,0512
57	0,2280	0,0535	0,1930	0,0670	0,1350	0,0703	0,1120	0,0739	0,1090	0,0808	0,1140	0,1370	0,0928	0,1490	0,0493	0,0821
58	0,2030	0,0880	0,1980	0,0891	0,1460	0,0781	0,1210	0,0796	0,1230	0,0877	0,1730	0,0932	0,1700	0,0875	0,1110	0,0532
59	0,2220	0,0927	0,2090	0,0942	0,1540	0,0861	0,1290	0,0876	0,1310	0,0952	0,1780	0,1070	0,1640	0,1050	0,0887	0,0636
60	0,2360	0,0887	0,2160	0,0890	0,1530	0,0816	0,1270	0,0838	0,1270	0,0948	0,1280	0,1560	0,1030	0,1720	0,0569	0,0984
61	0,0719	0,2340	0,0770	0,1960	0,0760	0,1400	0,0770	0,1170	0,0825	0,1160	0,1360	0,1170	0,1530	0,0932	0,1050	0,0537
62	0,0802	0,2400	0,0885	0,2080	0,0875	0,1540	0,0879	0,1310	0,0949	0,1290	0,1470	0,1370	0,1500	0,1140	0,0823	0,0638
63	0,0729	0,2300	0,0799	0,1990	0,0793	0,1460	0,0814	0,1230	0,0852	0,1240	0,0901	0,1800	0,0851	0,1760	0,0505	0,0973
64	0,1680	0,0425	0,2470	0,0584	0,2230	0,0591	0,1640	0,0596	0,1420	0,0631	0,1370	0,0623	0,0877	0,0488	0,0331	0,0210
65	0,2600	0,0848	0,3270	0,0935	0,2680	0,0836	0,1880	0,0777	0,1610	0,0794	0,1490	0,0781	0,0940	0,0631	0,0362	0,0275
66	0,1630	0,1600	0,2240	0,1640	0,1930	0,1300	0,1420	0,1050	0,1190	0,0985	0,1080	0,0943	0,0714	0,0618	0,0268	0,0243
67	0,3130	0,0852	0,3000	0,0960	0,2310	0,0895	0,1790	0,0831	0,1530	0,0820	0,1410	0,0772	0,0860	0,0584	0,0319	0,0244
68	0,2020	0,0844	0,2650	0,1070	0,2390	0,1010	0,1800	0,0883	0,1530	0,0858	0,1410	0,0832	0,0841	0,0638	0,0313	0,0265
69	0,1630	0,1750	0,2090	0,1930	0,1930	0,1620	0,1530	0,1300	0,1300	0,1200	0,1160	0,1160	0,0748	0,0765	0,0291	0,0304
70	0,2870	0,1910	0,2390	0,2080	0,1650	0,1760	0,1290	0,1390	0,1130	0,1170	0,1030	0,1020	0,0666	0,0632	0,0256	0,0236
71	0,1590	0,1920	0,1860	0,2210	0,1600	0,1900	0,1270	0,1490	0,1150	0,1290	0,1090	0,1170	0,0711	0,0756	0,0280	0,0289

Eval. Run CFD	AvMag1b [m/s]	AvMag1t [m/s]	AvMag2b [m/s]	AvMag2t [m/s]	AvMag3b [m/s]	AvMag3t [m/s]	AvMag4b [m/s]	AvMag4t [m/s]	AvMag5b [m/s]	AvMag5t [m/s]	AvMag6b [m/s]	AvMag6t [m/s]	AvMag7b [m/s]	AvMag7t [m/s]	AvMag8b [m/s]	AvMag8t [m/s]
72	0,0964	0,2590	0,1090	0,2960	0,1010	0,2500	0,0918	0,1880	0,0887	0,1600	0,0834	0,1460	0,0627	0,0885	0,0263	0,0332
73	0,2980	0,0326	0,4100	0,0466	0,3380	0,0484	0,2290	0,0492	0,1720	0,0569	0,1500	0,0604	0,0976	0,0511	0,0368	0,0228
74	0,2840	0,0665	0,3870	0,0896	0,3330	0,0858	0,2310	0,0734	0,1720	0,0720	0,1480	0,0711	0,0918	0,0573	0,0344	0,0247
75	0,1720	0,1650	0,2550	0,2010	0,2220	0,1730	0,1560	0,1300	0,1200	0,1050	0,1070	0,0924	0,0715	0,0609	0,0271	0,0242
76	0,2840	0,0636	0,3850	0,0870	0,3300	0,0852	0,2310	0,0742	0,1730	0,0729	0,1480	0,0719	0,0917	0,0574	0,0342	0,0247
77	0,2280	0,0813	0,3330	0,1190	0,3140	0,1200	0,2320	0,0975	0,1690	0,0853	0,1400	0,0804	0,0809	0,0606	0,0292	0,0247
78	0,1360	0,1860	0,2030	0,2340	0,2080	0,2180	0,1680	0,1710	0,1290	0,1350	0,1100	0,1150	0,0697	0,0740	0,0268	0,0281
79	0,1770	0,1700	0,2620	0,2090	0,2350	0,1840	0,1680	0,1420	0,1270	0,1130	0,1110	0,0983	0,0748	0,0643	0,0285	0,0256
80	0,1390	0,1620	0,2120	0,2190	0,2130	0,2040	0,1650	0,1580	0,1230	0,1230	0,1030	0,1060	0,0643	0,0674	0,0243	0,0255
81	0,0717	0,3010	0,1010	0,3640	0,1060	0,3190	0,0922	0,2390	0,0808	0,1760	0,0728	0,1440	0,0535	0,0812	0,0219	0,0288
82	0,1620	0,0264	0,2880	0,0449	0,3410	0,0541	0,3030	0,0553	0,2200	0,0605	0,1690	0,0668	0,1110	0,0595	0,0438	0,0277
83	0,1790	0,0423	0,3130	0,0757	0,3410	0,0943	0,2960	0,0940	0,2250	0,0841	0,1620	0,0764	0,0963	0,0609	0,0360	0,0261
84	0,1530	0,0622	0,2550	0,1490	0,2500	0,2070	0,1910	0,2050	0,1420	0,1600	0,1170	0,1110	0,0804	0,0706	0,0318	0,0288
85	0,1430	0,0462	0,2580	0,0761	0,3310	0,0870	0,3120	0,0797	0,2250	0,0744	0,1650	0,0766	0,1050	0,0661	0,0422	0,0305
86	0,1270	0,0567	0,2480	0,1050	0,3130	0,1300	0,2910	0,1210	0,2150	0,0972	0,1500	0,0846	0,0865	0,0654	0,0326	0,0277
87	0,1100	0,0700	0,1900	0,1620	0,2230	0,2220	0,1980	0,2200	0,1470	0,1760	0,1120	0,1250	0,0723	0,0776	0,0287	0,0303
88	0,0648	0,1490	0,1370	0,1920	0,2070	0,1800	0,2250	0,1470	0,1720	0,1190	0,1270	0,1080	0,0867	0,0750	0,0346	0,0311
89	0,0650	0,1420	0,1480	0,2190	0,2120	0,2280	0,2190	0,1910	0,1660	0,1410	0,1120	0,1100	0,0679	0,0703	0,0261	0,0273
90	0,0523	0,1810	0,0936	0,2910	0,1170	0,3310	0,1140	0,2980	0,0938	0,2260	0,0759	0,1550	0,0566	0,0851	0,0237	0,0311
91	0,1290	0,0299	0,2110	0,0486	0,2380	0,0563	0,2520	0,0619	0,2640	0,0701	0,2120	0,0746	0,1260	0,0664	0,0520	0,0323
92	0,1390	0,0422	0,2410	0,0703	0,2660	0,0903	0,2610	0,1010	0,2440	0,0993	0,1880	0,0813	0,0958	0,0597	0,0362	0,0261
93	0,1480	0,0386	0,2430	0,0720	0,2400	0,1280	0,1960	0,1910	0,1600	0,2100	0,1320	0,1620	0,0881	0,0823	0,0352	0,0323
94	0,1230	0,0470	0,1920	0,0742	0,2250	0,0858	0,2590	0,0856	0,2710	0,0859	0,2160	0,0883	0,1280	0,0777	0,0557	0,0386
95	0,1220	0,0606	0,2070	0,0994	0,2560	0,1220	0,2730	0,1270	0,2620	0,1200	0,2010	0,1010	0,0976	0,0730	0,0368	0,0313
96	0,1220	0,0549	0,1970	0,0984	0,2200	0,1510	0,1960	0,2050	0,1600	0,2170	0,1260	0,1700	0,0781	0,0862	0,0307	0,0324
97	0,0403	0,1030	0,0665	0,1420	0,1010	0,1420	0,1610	0,1290	0,2030	0,1170	0,1640	0,1080	0,1010	0,0787	0,0439	0,0347

Eval. Run CFD	AvMag1b [m/s]	AvMag1t [m/s]	AvMag2b [m/s]	AvMag2t [m/s]	AvMag3b [m/s]	AvMag3t [m/s]	AvMag4b [m/s]	AvMag4t [m/s]	AvMag5b [m/s]	AvMag5t [m/s]	AvMag6b [m/s]	AvMag6t [m/s]	AvMag7b [m/s]	AvMag7t [m/s]	AvMag8b [m/s]	AvMag8t [m/s]
98	0,0509	0,1520	0,0923	0,2160	0,1390	0,2190	0,1900	0,2000	0,2110	0,1680	0,1620	0,1300	0,0809	0,0799	0,0307	0,0313
99	0,0553	0,1430	0,0923	0,2150	0,1120	0,2470	0,1190	0,2730	0,1110	0,2680	0,0918	0,2080	0,0640	0,0983	0,0268	0,0345
100	0,1260	0,0300	0,2120	0,0512	0,2040	0,0597	0,1760	0,0653	0,2190	0,0762	0,2520	0,0841	0,1620	0,0769	0,0715	0,0404
101	0,1480	0,0453	0,2410	0,0714	0,2340	0,0814	0,2150	0,0935	0,2440	0,1110	0,2530	0,1140	0,1510	0,0877	0,0533	0,0381
102	0,1450	0,0415	0,2390	0,0646	0,2260	0,0749	0,1830	0,1100	0,1620	0,1830	0,1510	0,2110	0,1050	0,1290	0,0422	0,0444
103	0,1040	0,0487	0,1680	0,0811	0,1820	0,0924	0,1790	0,0903	0,2130	0,0902	0,2400	0,0913	0,1480	0,0780	0,0644	0,0386
104	0,1200	0,0579	0,1930	0,0943	0,2060	0,1070	0,2030	0,1120	0,2310	0,1230	0,2440	0,1250	0,1420	0,0954	0,0511	0,0413
105	0,1180	0,0586	0,1860	0,0898	0,1970	0,1050	0,1730	0,1380	0,1500	0,1970	0,1340	0,2140	0,0872	0,1230	0,0345	0,0406
106	0,0487	0,1430	0,0784	0,1980	0,0924	0,1920	0,1100	0,1630	0,1730	0,1410	0,2170	0,1320	0,1490	0,1000	0,0737	0,0494
107	0,0615	0,1730	0,0905	0,2230	0,1040	0,2100	0,1320	0,1860	0,1890	0,1720	0,2110	0,1580	0,1280	0,1060	0,0471	0,0434
108	0,0534	0,1250	0,0906	0,1850	0,1060	0,1930	0,1110	0,2040	0,1120	0,2430	0,1050	0,2500	0,0785	0,1410	0,0331	0,0461
109	0,1220	0,0317	0,2110	0,0537	0,2060	0,0636	0,1560	0,0693	0,1600	0,0810	0,2300	0,0910	0,1890	0,0867	0,0979	0,0494
110	0,1480	0,0396	0,2430	0,0647	0,2240	0,0739	0,1750	0,0797	0,1810	0,0964	0,2350	0,1150	0,1770	0,1040	0,0719	0,0505
111	0,1440	0,0364	0,2350	0,0592	0,2220	0,0659	0,1710	0,0702	0,1490	0,1110	0,1510	0,1990	0,1200	0,1700	0,0556	0,0754
112	0,1110	0,0464	0,1700	0,0766	0,1800	0,0882	0,1550	0,0889	0,1550	0,0925	0,2230	0,0997	0,1800	0,0918	0,0968	0,0512
113	0,1250	0,0585	0,1970	0,0948	0,2070	0,1070	0,1790	0,1060	0,1820	0,1140	0,2350	0,1300	0,1790	0,1150	0,0770	0,0572
114	0,1170	0,0540	0,1800	0,0865	0,1870	0,1000	0,1580	0,1100	0,1330	0,1330	0,1190	0,1510	0,0772	0,1040	0,0298	0,0360
115	0,0438	0,1640	0,0709	0,2150	0,0823	0,2000	0,0892	0,1650	0,1230	0,1400	0,1860	0,1270	0,1520	0,0904	0,0728	0,0422
116	0,0524	0,1480	0,0866	0,2090	0,1010	0,2080	0,1040	0,1820	0,1340	0,1630	0,1960	0,1620	0,1600	0,1250	0,0716	0,0587
117	0,0533	0,1370	0,0889	0,1940	0,1040	0,1910	0,1070	0,1690	0,1080	0,1790	0,1130	0,2370	0,0996	0,1810	0,0496	0,0769
118	0,1390	0,0299	0,2220	0,0505	0,2040	0,0598	0,1550	0,0665	0,1360	0,0787	0,1880	0,0890	0,1870	0,0884	0,1170	0,0558
119	0,1390	0,0365	0,2310	0,0615	0,2180	0,0719	0,1670	0,0771	0,1470	0,0884	0,1940	0,1050	0,1780	0,1070	0,0916	0,0650
120	0,1370	0,0336	0,2240	0,0559	0,2160	0,0651	0,1660	0,0712	0,1430	0,0933	0,1410	0,1640	0,1120	0,1710	0,0544	0,0888
121	0,1210	0,0505	0,1830	0,0799	0,1870	0,0908	0,1560	0,0900	0,1380	0,0948	0,1860	0,1030	0,1840	0,0978	0,1190	0,0606
122	0,1130	0,0524	0,1830	0,0866	0,2010	0,0997	0,1730	0,0996	0,1520	0,1040	0,1930	0,1180	0,1730	0,1140	0,0903	0,0676
123	0,1220	0,0486	0,1920	0,0787	0,2040	0,0907	0,1760	0,0920	0,1480	0,1050	0,1420	0,1710	0,1140	0,1850	0,0620	0,1060

Eval. Run CFD	AvMag1b [m/s]	AvMag1t [m/s]	AvMag2b [m/s]	AvMag2t [m/s]	AvMag3b [m/s]	AvMag3t [m/s]	AvMag4b [m/s]	AvMag4t [m/s]	AvMag5b [m/s]	AvMag5t [m/s]	AvMag6b [m/s]	AvMag6t [m/s]	AvMag7b [m/s]	AvMag7t [m/s]	AvMag8b [m/s]	AvMag8t [m/s]
124	0,0440	0,1580	0,0712	0,2070	0,0823	0,1920	0,0834	0,1600	0,0908	0,1390	0,1480	0,1340	0,1700	0,1080	0,1200	0,0645
125	0,0522	0,1320	0,0872	0,1880	0,1020	0,1880	0,1030	0,1670	0,1060	0,1480	0,1570	0,1500	0,1630	0,1270	0,0927	0,0733
126	0,0474	0,1230	0,0802	0,1780	0,0948	0,1780	0,0962	0,1560	0,0946	0,1450	0,0984	0,1980	0,0902	0,1850	0,0498	0,0953
127	0,3250	0,0535	0,2760	0,0583	0,2600	0,0581	0,2480	0,0606	0,1930	0,0668	0,1590	0,0695	0,1040	0,0594	0,0411	0,0274
128	0,2030	0,0802	0,2350	0,0841	0,2440	0,0748	0,2350	0,0722	0,1910	0,0774	0,1580	0,0810	0,1000	0,0662	0,0391	0,0293
129	0,0754	0,2360	0,1220	0,2140	0,1740	0,1540	0,1930	0,1210	0,1560	0,1130	0,1220	0,1080	0,0811	0,0712	0,0316	0,0283
130	0,3000	0,0636	0,2620	0,0785	0,2350	0,0866	0,2150	0,0863	0,1770	0,0782	0,1380	0,0696	0,0826	0,0545	0,0311	0,0234
131	0,1310	0,0734	0,1900	0,0957	0,2130	0,0991	0,2070	0,0952	0,1790	0,0876	0,1440	0,0817	0,0864	0,0648	0,0338	0,0281
132	0,0916	0,2180	0,1380	0,2050	0,1760	0,1690	0,1870	0,1420	0,1560	0,1240	0,1160	0,1130	0,0756	0,0768	0,0308	0,0314
133	0,3190	0,0743	0,2300	0,1360	0,1620	0,1850	0,1300	0,1890	0,1090	0,1490	0,0991	0,1050	0,0665	0,0641	0,0263	0,0245
134	0,2090	0,1080	0,2130	0,1720	0,1720	0,2030	0,1380	0,1920	0,1190	0,1550	0,1060	0,1180	0,0702	0,0760	0,0283	0,0298
135	0,0732	0,1610	0,0913	0,2230	0,0985	0,2480	0,0956	0,2290	0,0832	0,1830	0,0734	0,1400	0,0569	0,0823	0,0245	0,0311
136	0,1690	0,0254	0,3030	0,0450	0,3360	0,0537	0,2890	0,0551	0,2090	0,0592	0,1580	0,0621	0,0997	0,0522	0,0377	0,0233
137	0,1530	0,0524	0,2710	0,0848	0,3310	0,0927	0,3050	0,0820	0,2200	0,0749	0,1620	0,0754	0,1000	0,0627	0,0379	0,0274
138	0,0596	0,1370	0,1310	0,1860	0,1990	0,1780	0,2170	0,1430	0,1700	0,1140	0,1240	0,1040	0,0832	0,0708	0,0325	0,0286
139	0,1810	0,0444	0,3260	0,0841	0,3470	0,1040	0,2940	0,0998	0,2150	0,0814	0,1510	0,0691	0,0904	0,0551	0,0342	0,0238
140	0,1420	0,0608	0,2650	0,1100	0,3210	0,1340	0,2930	0,1230	0,2170	0,0980	0,1490	0,0832	0,0847	0,0638	0,0316	0,0268
141	0,0760	0,1560	0,1470	0,2170	0,1990	0,2160	0,2060	0,1810	0,1660	0,1400	0,1160	0,1150	0,0725	0,0751	0,0290	0,0295
142	0,1530	0,0651	0,2600	0,1570	0,2580	0,2190	0,1980	0,2190	0,1500	0,1730	0,1250	0,1180	0,0888	0,0770	0,0368	0,0334
143	0,1260	0,0823	0,2130	0,1800	0,2340	0,2380	0,1940	0,2290	0,1420	0,1790	0,1110	0,1240	0,0703	0,0748	0,0275	0,0288
144	0,0542	0,1900	0,1000	0,3130	0,1250	0,3530	0,1180	0,3120	0,0941	0,2300	0,0746	0,1540	0,0548	0,0830	0,0228	0,0297
145	0,0537	0,0195	0,1740	0,0430	0,3190	0,0610	0,3690	0,0684	0,2780	0,0719	0,1910	0,0775	0,1220	0,0676	0,0477	0,0309
146	0,0620	0,0317	0,1790	0,0711	0,3070	0,1020	0,3550	0,1080	0,2750	0,0936	0,1790	0,0835	0,1080	0,0689	0,0412	0,0301
147	0,0446	0,0496	0,1160	0,1240	0,1940	0,1770	0,2260	0,1820	0,1780	0,1490	0,1260	0,1120	0,0835	0,0726	0,0328	0,0293
148	0,0762	0,0399	0,2030	0,0836	0,3340	0,1140	0,3680	0,1180	0,2780	0,1010	0,1840	0,0873	0,1150	0,0734	0,0459	0,0334
149	0,0750	0,0456	0,1990	0,1040	0,3130	0,1500	0,3460	0,1540	0,2720	0,1230	0,1690	0,0948	0,0954	0,0728	0,0368	0,0310

Eval. Run CFD	AvMag1b [m/s]	AvMag1t [m/s]	AvMag2b [m/s]	AvMag2t [m/s]	AvMag3b [m/s]	AvMag3t [m/s]	AvMag4b [m/s]	AvMag4t [m/s]	AvMag5b [m/s]	AvMag5t [m/s]	AvMag6b [m/s]	AvMag6t [m/s]	AvMag7b [m/s]	AvMag7t [m/s]	AvMag8b [m/s]	AvMag8t [m/s]
150	0,0504	0,0542	0,1140	0,1440	0,1720	0,2210	0,1960	0,2380	0,1710	0,1940	0,1230	0,1300	0,0793	0,0816	0,0322	0,0327
151	0,0497	0,0543	0,1410	0,1500	0,2480	0,2230	0,2720	0,2320	0,2060	0,1870	0,1490	0,1310	0,1040	0,0889	0,0458	0,0407
152	0,0530	0,0574	0,1400	0,1560	0,2250	0,2410	0,2470	0,2550	0,1930	0,2000	0,1270	0,1340	0,0778	0,0810	0,0302	0,0313
153	0,0368	0,0777	0,0831	0,2210	0,1230	0,3410	0,1350	0,3660	0,1160	0,2970	0,0881	0,1850	0,0638	0,0947	0,0266	0,0345
154	0,0367	0,0218	0,1030	0,0441	0,1940	0,0610	0,2860	0,0722	0,2970	0,0782	0,2170	0,0792	0,1240	0,0681	0,0493	0,0319
155	0,0440	0,0291	0,1160	0,0583	0,2210	0,0867	0,3080	0,1090	0,3000	0,1110	0,2080	0,0929	0,1070	0,0695	0,0414	0,0311
156	0,0449	0,0252	0,1140	0,0582	0,1920	0,1090	0,2360	0,1740	0,1990	0,2040	0,1380	0,1640	0,0884	0,0836	0,0358	0,0327
157	0,0438	0,0279	0,1020	0,0566	0,1780	0,0811	0,2660	0,0951	0,2950	0,0939	0,2170	0,0877	0,1260	0,0766	0,0537	0,0370
158	0,0413	0,0400	0,0736	0,0650	0,1210	0,0837	0,1860	0,1030	0,2290	0,1060	0,1910	0,0879	0,0901	0,0660	0,0354	0,0298
159	0,0521	0,0366	0,1270	0,0877	0,2010	0,1540	0,2390	0,2240	0,2110	0,2440	0,1460	0,1900	0,0893	0,0993	0,0360	0,0377
160	0,0302	0,0457	0,0719	0,1270	0,1250	0,1940	0,1980	0,2130	0,2380	0,1830	0,1880	0,1360	0,1180	0,0940	0,0531	0,0428
161	0,0360	0,0519	0,0870	0,1390	0,1550	0,2250	0,2250	0,2620	0,2450	0,2310	0,1830	0,1600	0,0962	0,0948	0,0368	0,0378
162	0,0350	0,0591	0,0759	0,1580	0,1160	0,2680	0,1410	0,3520	0,1360	0,3450	0,1100	0,2440	0,0793	0,1200	0,0333	0,0432
163	0,0308	0,0200	0,0904	0,0417	0,1730	0,0603	0,2350	0,0743	0,2660	0,0859	0,2680	0,0938	0,1750	0,0864	0,0795	0,0450
164	0,0406	0,0292	0,1040	0,0556	0,1960	0,0775	0,2660	0,0993	0,2860	0,1190	0,2690	0,1220	0,1610	0,0969	0,0595	0,0433
165	0,0473	0,0301	0,1050	0,0551	0,1590	0,0717	0,1930	0,1090	0,1830	0,1790	0,1430	0,2060	0,0973	0,1210	0,0403	0,0416
166	0,0417	0,0286	0,1150	0,0674	0,1880	0,1020	0,2400	0,1190	0,2780	0,1180	0,2730	0,1130	0,1760	0,1000	0,0833	0,0519
167	0,0487	0,0352	0,1220	0,0776	0,1990	0,1150	0,2560	0,1400	0,2870	0,1470	0,2650	0,1390	0,1540	0,1060	0,0566	0,0459
168	0,0488	0,0344	0,1090	0,0687	0,1630	0,0988	0,1950	0,1390	0,1870	0,2010	0,1480	0,2170	0,0975	0,1300	0,0401	0,0459
169	0,0251	0,0419	0,0585	0,1220	0,0926	0,1950	0,1270	0,2210	0,1940	0,1980	0,2340	0,1540	0,1610	0,1120	0,0782	0,0548
170	0,0311	0,0485	0,0661	0,1290	0,1050	0,2090	0,1500	0,2470	0,2060	0,2350	0,2210	0,1820	0,1360	0,1160	0,0502	0,0468
171	0,0315	0,0437	0,0684	0,1190	0,1040	0,2030	0,1300	0,2640	0,1380	0,3100	0,1280	0,2880	0,0989	0,1670	0,0428	0,0590
172	0,0356	0,0222	0,0972	0,0455	0,1690	0,0635	0,2070	0,0765	0,2020	0,0882	0,2440	0,0986	0,1970	0,0939	0,1040	0,0529
173	0,0406	0,0275	0,1090	0,0537	0,1910	0,0739	0,2350	0,0891	0,2310	0,1070	0,2510	0,1250	0,1880	0,1140	0,0780	0,0562
174	0,0462	0,0300	0,1110	0,0558	0,1840	0,0720	0,2240	0,0863	0,2000	0,1340	0,1700	0,2150	0,1300	0,1800	0,0598	0,0784
175	0,0393	0,0275	0,1070	0,0654	0,1780	0,1010	0,2140	0,1190	0,2150	0,1180	0,2490	0,1170	0,2000	0,1080	0,1070	0,0603

Eval. Run CFD	AvMag1b [m/s]	AvMag1t [m/s]	AvMag2b [m/s]	AvMag2t [m/s]	AvMag3b [m/s]	AvMag3t [m/s]	AvMag4b [m/s]	AvMag4t [m/s]	AvMag5b [m/s]	AvMag5t [m/s]	AvMag6b [m/s]	AvMag6t [m/s]	AvMag7b [m/s]	AvMag7t [m/s]	AvMag8b [m/s]	AvMag8t [m/s]
176	0,0457	0,0312	0,1150	0,0690	0,1840	0,1010	0,2240	0,1220	0,2340	0,1310	0,2490	0,1370	0,1810	0,1200	0,0779	0,0593
177	0,0458	0,0322	0,1190	0,0720	0,1960	0,1070	0,2340	0,1290	0,2120	0,1640	0,1730	0,2300	0,1290	0,1920	0,0598	0,0848
178	0,0270	0,0441	0,0607	0,1180	0,0907	0,1800	0,1090	0,1990	0,1330	0,1800	0,1970	0,1440	0,1690	0,1070	0,0940	0,0548
179	0,0303	0,0508	0,0656	0,1360	0,0975	0,2110	0,1200	0,2360	0,1510	0,2160	0,2050	0,1800	0,1650	0,1320	0,0710	0,0601
180	0,0307	0,0462	0,0682	0,1230	0,1030	0,1930	0,1230	0,2230	0,1280	0,2350	0,1260	0,2620	0,1090	0,1920	0,0536	0,0805
181	0,0318	0,0194	0,0975	0,0418	0,1830	0,0613	0,2180	0,0761	0,1870	0,0888	0,2110	0,1010	0,2070	0,1020	0,1280	0,0635
182	0,0400	0,0251	0,1100	0,0520	0,1910	0,0735	0,2320	0,0880	0,2030	0,0997	0,2120	0,1160	0,1870	0,1150	0,0978	0,0698
183	0,0413	0,0270	0,1040	0,0525	0,1770	0,0707	0,2170	0,0832	0,1910	0,1020	0,1610	0,1740	0,1310	0,1920	0,0692	0,1110
184	0,0378	0,0267	0,1010	0,0615	0,1650	0,0925	0,2010	0,1090	0,1880	0,1100	0,1990	0,1100	0,1920	0,1050	0,1260	0,0649
185	0,0451	0,0313	0,1170	0,0720	0,1840	0,1060	0,2160	0,1220	0,2010	0,1210	0,2080	0,1250	0,1830	0,1190	0,0955	0,0686
186	0,0424	0,0279	0,1060	0,0618	0,1650	0,0907	0,1920	0,1050	0,1710	0,1130	0,1350	0,1660	0,1010	0,1650	0,0498	0,0820
187	0,0242	0,0385	0,0566	0,1150	0,0876	0,1900	0,1070	0,2200	0,1160	0,2000	0,1660	0,1590	0,1840	0,1220	0,1250	0,0705
188	0,0300	0,0471	0,0666	0,1290	0,0987	0,2010	0,1160	0,2230	0,1240	0,1990	0,1690	0,1680	0,1710	0,1360	0,0946	0,0766
189	0,0288	0,0535	0,0636	0,1370	0,0921	0,1970	0,1060	0,2110	0,1060	0,1930	0,1060	0,2130	0,0980	0,1910	0,0543	0,0983
190	0,3180	0,0483	0,2320	0,0518	0,1650	0,0522	0,1990	0,0573	0,2350	0,0658	0,1940	0,0689	0,1130	0,0607	0,0462	0,0291
191	0,1870	0,0765	0,1890	0,0809	0,1630	0,0711	0,1930	0,0692	0,2330	0,0767	0,1940	0,0821	0,1160	0,0721	0,0493	0,0345
192	0,0821	0,2340	0,0827	0,2080	0,0950	0,1450	0,1560	0,1160	0,2050	0,1150	0,1680	0,1160	0,1090	0,0872	0,0500	0,0402
193	0,3090	0,0620	0,2310	0,0714	0,1840	0,0777	0,2050	0,0894	0,2200	0,0919	0,1750	0,0772	0,0886	0,0580	0,0342	0,0262
194	0,2160	0,0941	0,2150	0,1000	0,1980	0,0980	0,2150	0,1040	0,2290	0,1060	0,1810	0,0925	0,0917	0,0705	0,0363	0,0313
195	0,0858	0,2460	0,0919	0,2120	0,1180	0,1590	0,1690	0,1450	0,1950	0,1390	0,1520	0,1210	0,0817	0,0810	0,0336	0,0343
196	0,3330	0,0597	0,2390	0,0696	0,1620	0,1110	0,1410	0,1740	0,1290	0,1960	0,1120	0,1470	0,0736	0,0716	0,0295	0,0277
197	0,2290	0,1010	0,2100	0,0987	0,1540	0,1230	0,1340	0,1820	0,1300	0,2070	0,1160	0,1630	0,0772	0,0854	0,0326	0,0343
198	0,0850	0,1950	0,0938	0,1840	0,0909	0,1730	0,0965	0,2130	0,0967	0,2350	0,0857	0,1900	0,0659	0,0966	0,0291	0,0372
199	0,1500	0,0297	0,2330	0,0473	0,2420	0,0557	0,2570	0,0617	0,2670	0,0693	0,2140	0,0730	0,1280	0,0661	0,0537	0,0329
200	0,1270	0,0506	0,1930	0,0788	0,2190	0,0867	0,2490	0,0841	0,2650	0,0840	0,2110	0,0857	0,1250	0,0753	0,0544	0,0373
201	0,0489	0,1450	0,0832	0,1900	0,1220	0,1840	0,1860	0,1560	0,2210	0,1320	0,1760	0,1170	0,1090	0,0855	0,0476	0,0385

Eval. Run CFD	AvMag1b [m/s]	AvMag1t [m/s]	AvMag2b [m/s]	AvMag2t [m/s]	AvMag3b [m/s]	AvMag3t [m/s]	AvMag4b [m/s]	AvMag4t [m/s]	AvMag5b [m/s]	AvMag5t [m/s]	AvMag6b [m/s]	AvMag6t [m/s]	AvMag7b [m/s]	AvMag7t [m/s]	AvMag8b [m/s]	AvMag8t [m/s]
202	0,1480	0,0401	0,2490	0,0675	0,2680	0,0857	0,2630	0,0981	0,2480	0,0971	0,1890	0,0799	0,0968	0,0588	0,0359	0,0256
203	0,1220	0,0590	0,2040	0,0978	0,2470	0,1190	0,2650	0,1250	0,2550	0,1180	0,1940	0,0979	0,0946	0,0705	0,0351	0,0300
204	0,0528	0,1460	0,0956	0,2070	0,1440	0,2150	0,1930	0,1980	0,2080	0,1670	0,1580	0,1290	0,0799	0,0809	0,0318	0,0325
205	0,1520	0,0392	0,2480	0,0711	0,2360	0,1260	0,1910	0,1920	0,1580	0,2140	0,1300	0,1650	0,0875	0,0830	0,0348	0,0325
206	0,1240	0,0589	0,2040	0,1010	0,2230	0,1540	0,1990	0,2120	0,1640	0,2310	0,1310	0,1820	0,0829	0,0937	0,0327	0,0347
207	0,0507	0,1560	0,0863	0,2260	0,1090	0,2640	0,1190	0,2900	0,1130	0,2760	0,0922	0,2060	0,0635	0,0966	0,0267	0,0341
208	0,0336	0,0195	0,1070	0,0410	0,2200	0,0603	0,3250	0,0750	0,3270	0,0840	0,2480	0,0908	0,1580	0,0859	0,0706	0,0448
209	0,0423	0,0282	0,1170	0,0659	0,2090	0,0987	0,2990	0,1130	0,3150	0,1060	0,2300	0,0958	0,1320	0,0811	0,0552	0,0383
210	0,0294	0,0457	0,0703	0,1260	0,1250	0,1940	0,1980	0,2090	0,2350	0,1780	0,1850	0,1310	0,1140	0,0899	0,0488	0,0396
211	0,0467	0,0335	0,1320	0,0671	0,2630	0,1010	0,3550	0,1270	0,3310	0,1280	0,2390	0,1090	0,1310	0,0845	0,0529	0,0392
212	0,0500	0,0390	0,1360	0,0880	0,2470	0,1380	0,3320	0,1660	0,3240	0,1540	0,2250	0,1190	0,1120	0,0844	0,0415	0,0353
213	0,0365	0,0568	0,0881	0,1470	0,1560	0,2320	0,2210	0,2610	0,2360	0,2250	0,1770	0,1530	0,0911	0,0906	0,0352	0,0358
214	0,0445	0,0273	0,1160	0,0654	0,2110	0,1290	0,2580	0,2060	0,2180	0,2330	0,1610	0,1860	0,1100	0,1040	0,0458	0,0422
215	0,0450	0,0345	0,1200	0,0854	0,2040	0,1580	0,2520	0,2340	0,2230	0,2510	0,1540	0,1930	0,0944	0,1040	0,0371	0,0392
216	0,0356	0,0542	0,0771	0,1510	0,1200	0,2640	0,1470	0,3490	0,1440	0,3450	0,1140	0,2460	0,0792	0,1180	0,0326	0,0419
217	0,0174	0,0160	0,0472	0,0366	0,1130	0,0576	0,2550	0,0784	0,3610	0,0933	0,2880	0,0984	0,1730	0,0928	0,0796	0,0492
218	0,0265	0,0260	0,0654	0,0539	0,1400	0,0844	0,2630	0,1130	0,3420	0,1230	0,2670	0,1070	0,1360	0,0830	0,0534	0,0381
219	0,0269	0,0227	0,0605	0,0567	0,1130	0,1120	0,1980	0,1860	0,2510	0,2200	0,2020	0,1810	0,1210	0,0995	0,0514	0,0422
220	0,0256	0,0242	0,0660	0,0533	0,1420	0,0855	0,2710	0,1160	0,3580	0,1270	0,2810	0,1140	0,1500	0,0921	0,0642	0,0451
221	0,0324	0,0309	0,0837	0,0713	0,1720	0,1180	0,2920	0,1610	0,3540	0,1690	0,2710	0,1330	0,1250	0,0910	0,0467	0,0393
222	0,0291	0,0296	0,0711	0,0731	0,1350	0,1420	0,2180	0,2320	0,2590	0,2680	0,2040	0,2120	0,1080	0,1110	0,0418	0,0426
223	0,0261	0,0229	0,0600	0,0590	0,1140	0,1220	0,2070	0,2070	0,2640	0,2430	0,2150	0,2000	0,1330	0,1150	0,0585	0,0496
224	0,0302	0,0303	0,0736	0,0752	0,1370	0,1480	0,2180	0,2430	0,2560	0,2770	0,2010	0,2140	0,1060	0,1120	0,0412	0,0426
225	0,0276	0,0292	0,0611	0,0782	0,0973	0,1750	0,1320	0,3090	0,1430	0,3650	0,1180	0,2820	0,0812	0,1260	0,0341	0,0441
226	0,0163	0,0169	0,0394	0,0373	0,0827	0,0581	0,1810	0,0795	0,3070	0,0984	0,3220	0,1080	0,2050	0,1030	0,1000	0,0571
227	0,0237	0,0235	0,0519	0,0490	0,0998	0,0737	0,2070	0,1030	0,3240	0,1290	0,3160	0,1330	0,1820	0,1070	0,0714	0,0504

Eval. Run CFD	AvMag1b [m/s]	AvMag1t [m/s]	AvMag2b [m/s]	AvMag2t [m/s]	AvMag3b [m/s]	AvMag3t [m/s]	AvMag4b [m/s]	AvMag4t [m/s]	AvMag5b [m/s]	AvMag5t [m/s]	AvMag6b [m/s]	AvMag6t [m/s]	AvMag7b [m/s]	AvMag7t [m/s]	AvMag8b [m/s]	AvMag8t [m/s]
228	0,0262	0,0224	0,0568	0,0464	0,1030	0,0748	0,1910	0,1270	0,2570	0,2060	0,2210	0,2290	0,1410	0,1440	0,0602	0,0549
229	0,0239	0,0251	0,0586	0,0537	0,1160	0,0849	0,2000	0,1150	0,2950	0,1270	0,2960	0,1140	0,1660	0,0921	0,0721	0,0454
230	0,0267	0,0275	0,0665	0,0633	0,1290	0,1050	0,2290	0,1500	0,3310	0,1790	0,3220	0,1660	0,1740	0,1210	0,0639	0,0522
231	0,0272	0,0256	0,0673	0,0598	0,1290	0,1030	0,2110	0,1660	0,2620	0,2460	0,2240	0,2620	0,1320	0,1640	0,0539	0,0610
232	0,0205	0,0199	0,0454	0,0515	0,0742	0,1060	0,1180	0,1850	0,1960	0,2270	0,2340	0,1930	0,1580	0,1160	0,0776	0,0539
233	0,0262	0,0285	0,0588	0,0690	0,0987	0,1360	0,1560	0,2270	0,2260	0,2790	0,2420	0,2360	0,1500	0,1350	0,0567	0,0534
234	0,0266	0,0251	0,0586	0,0636	0,0927	0,1310	0,1280	0,2410	0,1510	0,3500	0,1420	0,3380	0,1060	0,1810	0,0460	0,0633
235	0,0172	0,0185	0,0410	0,0399	0,0822	0,0599	0,1640	0,0803	0,2510	0,0976	0,2950	0,1090	0,2260	0,1080	0,1230	0,0634
236	0,0241	0,0231	0,0529	0,0484	0,0957	0,0711	0,1800	0,0935	0,2690	0,1170	0,3010	0,1340	0,2120	0,1230	0,0931	0,0632
237	0,0273	0,0245	0,0584	0,0493	0,1020	0,0691	0,1780	0,0904	0,2370	0,1410	0,2140	0,2230	0,1490	0,1900	0,0691	0,0849
238	0,0221	0,0232	0,0560	0,0528	0,1110	0,0875	0,1870	0,1220	0,2530	0,1410	0,2940	0,1350	0,2120	0,1170	0,1140	0,0651
239	0,0260	0,0264	0,0631	0,0594	0,1200	0,0971	0,2030	0,1360	0,2810	0,1630	0,3090	0,1650	0,2070	0,1390	0,0890	0,0684
240	0,0267	0,0261	0,0645	0,0577	0,1190	0,0909	0,1920	0,1280	0,2440	0,1780	0,2240	0,2440	0,1450	0,1970	0,0671	0,0881
241	0,0246	0,0250	0,0521	0,0642	0,0798	0,1290	0,1080	0,2010	0,1480	0,2290	0,2120	0,1890	0,1780	0,1160	0,0972	0,0579
242	0,0273	0,0283	0,0581	0,0667	0,0892	0,1250	0,1240	0,2050	0,1730	0,2570	0,2230	0,2330	0,1740	0,1480	0,0757	0,0661
243	0,0224	0,0216	0,0504	0,0539	0,0822	0,1110	0,1170	0,2020	0,1420	0,2780	0,1470	0,3220	0,1250	0,2230	0,0633	0,0965
244	0,0177	0,0188	0,0431	0,0402	0,0849	0,0607	0,1610	0,0804	0,2270	0,0963	0,2510	0,1060	0,2200	0,1070	0,1390	0,0679
245	0,0237	0,0227	0,0526	0,0471	0,0950	0,0683	0,1660	0,0866	0,2270	0,1010	0,2480	0,1160	0,2010	0,1160	0,1020	0,0694
246	0,0205	0,0206	0,0481	0,0435	0,0914	0,0642	0,1670	0,0833	0,2230	0,1060	0,1930	0,1720	0,1350	0,1800	0,0664	0,0953
247	0,0237	0,0244	0,0586	0,0533	0,1110	0,0847	0,1760	0,1140	0,2180	0,1280	0,2390	0,1220	0,1990	0,1100	0,1280	0,0675
248	0,0279	0,0278	0,0664	0,0594	0,1190	0,0911	0,1790	0,1190	0,2180	0,1310	0,2340	0,1290	0,1790	0,1180	0,0917	0,0681
249	0,0246	0,0256	0,0594	0,0547	0,1130	0,0865	0,1840	0,1170	0,2250	0,1400	0,1930	0,1880	0,1240	0,1830	0,0619	0,0944
250	0,0236	0,0226	0,0509	0,0581	0,0794	0,1170	0,1070	0,1910	0,1270	0,2250	0,1740	0,1930	0,1840	0,1260	0,1260	0,0716
251	0,0256	0,0256	0,0559	0,0642	0,0873	0,1270	0,1170	0,2020	0,1390	0,2380	0,1810	0,2090	0,1750	0,1430	0,0975	0,0797
252	0,0252	0,0234	0,0540	0,0594	0,0850	0,1220	0,1150	0,2080	0,1330	0,2590	0,1320	0,2790	0,1170	0,2180	0,0650	0,1110
253	0,1890	0,0563	0,1800	0,0714	0,1250	0,0731	0,1150	0,0740	0,1820	0,0770	0,2290	0,0780	0,1450	0,0699	0,0676	0,0373

Eval. Run CFD	AvMag1b [m/s]	AvMag1t [m/s]	AvMag2b [m/s]	AvMag2t [m/s]	AvMag3b [m/s]	AvMag3t [m/s]	AvMag4b [m/s]	AvMag4t [m/s]	AvMag5b [m/s]	AvMag5t [m/s]	AvMag6b [m/s]	AvMag6t [m/s]	AvMag7b [m/s]	AvMag7t [m/s]	AvMag8b [m/s]	AvMag8t [m/s]
254	0,2120	0,0808	0,1960	0,0823	0,1360	0,0727	0,1170	0,0722	0,1790	0,0798	0,2230	0,0850	0,1380	0,0749	0,0627	0,0380
255	0,0771	0,2300	0,0799	0,1990	0,0715	0,1410	0,0810	0,1150	0,1440	0,1140	0,1900	0,1150	0,1240	0,0840	0,0582	0,0391
256	0,3240	0,0615	0,2300	0,0701	0,1520	0,0713	0,1400	0,0780	0,1910	0,0951	0,2200	0,0968	0,1270	0,0742	0,0463	0,0336
257	0,2150	0,0971	0,2050	0,1020	0,1480	0,0918	0,1440	0,0916	0,1990	0,1060	0,2220	0,1080	0,1250	0,0820	0,0459	0,0371
258	0,0838	0,2680	0,0886	0,2230	0,0829	0,1600	0,1010	0,1330	0,1590	0,1390	0,1900	0,1370	0,1130	0,0921	0,0432	0,0392
259	0,2730	0,0614	0,2210	0,0724	0,1530	0,0693	0,1270	0,0980	0,1270	0,1700	0,1240	0,1930	0,0844	0,1080	0,0340	0,0358
260	0,2440	0,1030	0,2190	0,0999	0,1570	0,0840	0,1310	0,1110	0,1360	0,1800	0,1300	0,2020	0,0857	0,1140	0,0348	0,0388
261	0,0818	0,1980	0,0915	0,1860	0,0892	0,1400	0,0894	0,1430	0,0976	0,2060	0,0971	0,2310	0,0741	0,1270	0,0322	0,0431
262	0,1420	0,0290	0,2260	0,0480	0,2130	0,0551	0,1850	0,0617	0,2210	0,0740	0,2470	0,0807	0,1560	0,0723	0,0643	0,0363
263	0,1200	0,0515	0,1830	0,0817	0,1860	0,0903	0,1720	0,0872	0,2120	0,0906	0,2470	0,0956	0,1560	0,0840	0,0707	0,0433
264	0,0499	0,1410	0,0770	0,1880	0,0881	0,1800	0,1060	0,1550	0,1680	0,1360	0,2140	0,1280	0,1450	0,0967	0,0702	0,0471
265	0,1480	0,0432	0,2410	0,0681	0,2260	0,0778	0,2030	0,0899	0,2340	0,1080	0,2470	0,1120	0,1460	0,0861	0,0519	0,0372
266	0,1250	0,0613	0,2000	0,0984	0,2090	0,1100	0,2030	0,1140	0,2330	0,1250	0,2480	0,1280	0,1460	0,0980	0,0535	0,0429
267	0,0597	0,1540	0,0933	0,2150	0,1070	0,2090	0,1320	0,1850	0,1860	0,1710	0,2100	0,1570	0,1280	0,1060	0,0467	0,0432
268	0,1500	0,0429	0,2480	0,0656	0,2320	0,0740	0,1860	0,1120	0,1670	0,1880	0,1560	0,2170	0,1100	0,1320	0,0440	0,0461
269	0,1230	0,0616	0,1960	0,0945	0,2080	0,1050	0,1800	0,1300	0,1600	0,1960	0,1460	0,2260	0,0993	0,1370	0,0399	0,0473
270	0,0555	0,1650	0,0896	0,2230	0,1040	0,2140	0,1090	0,2110	0,1160	0,2530	0,1150	0,2630	0,0884	0,1520	0,0380	0,0518
271	0,0336	0,0205	0,0970	0,0423	0,1820	0,0608	0,2420	0,0760	0,2730	0,0902	0,2830	0,1010	0,1920	0,0972	0,0914	0,0530
272	0,0408	0,0294	0,1100	0,0693	0,1820	0,1050	0,2280	0,1210	0,2640	0,1180	0,2710	0,1130	0,1760	0,0996	0,0837	0,0521
273	0,0243	0,0473	0,0556	0,1300	0,0869	0,1990	0,1210	0,2190	0,1880	0,1950	0,2290	0,1520	0,1590	0,1110	0,0792	0,0551
274	0,0461	0,0327	0,1140	0,0604	0,2050	0,0819	0,2700	0,1050	0,2930	0,1260	0,2820	0,1310	0,1750	0,1060	0,0673	0,0488
275	0,0499	0,0366	0,1260	0,0799	0,2050	0,1200	0,2600	0,1460	0,2920	0,1550	0,2730	0,1450	0,1630	0,1120	0,0616	0,0495
276	0,0342	0,0573	0,0698	0,1470	0,1080	0,2260	0,1520	0,2570	0,2100	0,2390	0,2260	0,1850	0,1410	0,1180	0,0518	0,0474
277	0,0437	0,0273	0,1120	0,0516	0,2010	0,0779	0,2480	0,1280	0,2190	0,2040	0,1770	0,2280	0,1240	0,1420	0,0517	0,0521
278	0,0506	0,0374	0,1240	0,0791	0,2010	0,1220	0,2390	0,1690	0,2220	0,2350	0,1790	0,2530	0,1230	0,1610	0,0519	0,0603
279	0,0345	0,0542	0,0715	0,1330	0,1040	0,2030	0,1270	0,2530	0,1350	0,2980	0,1250	0,2780	0,0946	0,1570	0,0404	0,0547

Eval. Run CFD	AvMag1b [m/s]	AvMag1t [m/s]	AvMag2b [m/s]	AvMag2t [m/s]	AvMag3b [m/s]	AvMag3t [m/s]	AvMag4b [m/s]	AvMag4t [m/s]	AvMag5b [m/s]	AvMag5t [m/s]	AvMag6b [m/s]	AvMag6t [m/s]	AvMag7b [m/s]	AvMag7t [m/s]	AvMag8b [m/s]	AvMag8t [m/s]
280	0,0164	0,0173	0,0395	0,0380	0,0835	0,0586	0,1840	0,0806	0,3090	0,0997	0,3260	0,1100	0,2090	0,1050	0,1030	0,0590
281	0,0229	0,0241	0,0563	0,0529	0,1110	0,0857	0,1990	0,1200	0,3070	0,1370	0,3210	0,1290	0,1880	0,1070	0,0872	0,0555
282	0,0211	0,0206	0,0474	0,0534	0,0783	0,1120	0,1270	0,1980	0,2070	0,2430	0,2470	0,2070	0,1690	0,1270	0,0820	0,0587
283	0,0247	0,0241	0,0528	0,0496	0,1010	0,0739	0,2100	0,1030	0,3290	0,1330	0,3230	0,1390	0,1930	0,1160	0,0791	0,0556
284	0,0316	0,0322	0,0713	0,0686	0,1300	0,1060	0,2220	0,1450	0,3160	0,1670	0,3060	0,1500	0,1610	0,1070	0,0595	0,0473
285	0,0286	0,0312	0,0609	0,0704	0,0991	0,1340	0,1530	0,2210	0,2120	0,2660	0,2190	0,2190	0,1270	0,1150	0,0451	0,0441
286	0,0267	0,0232	0,0568	0,0466	0,1010	0,0732	0,1870	0,1250	0,2570	0,2040	0,2220	0,2320	0,1440	0,1480	0,0631	0,0569
287	0,0285	0,0260	0,0676	0,0594	0,1250	0,1020	0,2010	0,1680	0,2510	0,2450	0,2140	0,2540	0,1210	0,1530	0,0481	0,0549
288	0,0287	0,0276	0,0615	0,0660	0,0952	0,1310	0,1290	0,2350	0,1490	0,3320	0,1360	0,3140	0,0949	0,1570	0,0392	0,0514
289	0,0158	0,0180	0,0334	0,0388	0,0566	0,0594	0,1120	0,0820	0,2610	0,1040	0,3580	0,1170	0,2370	0,1120	0,1180	0,0643
290	0,0227	0,0243	0,0464	0,0500	0,0753	0,0753	0,1390	0,1080	0,2770	0,1410	0,3580	0,1510	0,2250	0,1260	0,0985	0,0629
291	0,0221	0,0211	0,0467	0,0444	0,0727	0,0725	0,1160	0,1240	0,2070	0,2060	0,2620	0,2410	0,1830	0,1610	0,0881	0,0678
292	0,0219	0,0233	0,0450	0,0485	0,0733	0,0735	0,1360	0,1060	0,2770	0,1400	0,3600	0,1520	0,2270	0,1280	0,1000	0,0647
293	0,0241	0,0269	0,0527	0,0578	0,0906	0,0901	0,1670	0,1300	0,3000	0,1710	0,3560	0,1770	0,2100	0,1330	0,0756	0,0582
294	0,0257	0,0265	0,0547	0,0563	0,0889	0,0895	0,1450	0,1470	0,2270	0,2420	0,2590	0,2760	0,1660	0,1760	0,0638	0,0666
295	0,0255	0,0243	0,0519	0,0483	0,0773	0,0729	0,1210	0,1220	0,2040	0,2040	0,2470	0,2360	0,1670	0,1520	0,0753	0,0605
296	0,0255	0,0253	0,0550	0,0557	0,0889	0,0919	0,1420	0,1550	0,2240	0,2460	0,2560	0,2690	0,1610	0,1660	0,0606	0,0606
297	0,0259	0,0228	0,0559	0,0502	0,0874	0,0869	0,1240	0,1700	0,1620	0,3270	0,1710	0,3940	0,1350	0,2370	0,0599	0,0839
298	0,0199	0,0215	0,0400	0,0451	0,0585	0,0651	0,0931	0,0836	0,1940	0,1020	0,3240	0,1140	0,2530	0,1130	0,1410	0,0679
299	0,0219	0,0226	0,0458	0,0475	0,0686	0,0708	0,1070	0,0949	0,2140	0,1230	0,3380	0,1470	0,2540	0,1400	0,1200	0,0770
300	0,0216	0,0220	0,0448	0,0457	0,0675	0,0662	0,1040	0,0904	0,1840	0,1410	0,2450	0,2150	0,1770	0,1790	0,0867	0,0804
301	0,0235	0,0248	0,0479	0,0515	0,0732	0,0752	0,1160	0,1010	0,2030	0,1260	0,3050	0,1330	0,2200	0,1130	0,1090	0,0602
302	0,0250	0,0268	0,0522	0,0566	0,0830	0,0852	0,1370	0,1180	0,2390	0,1550	0,3310	0,1720	0,2290	0,1430	0,0927	0,0694
303	0,0241	0,0248	0,0509	0,0524	0,0806	0,0784	0,1270	0,1120	0,2010	0,1720	0,2460	0,2540	0,1710	0,2060	0,0734	0,0900
304	0,0233	0,0227	0,0479	0,0456	0,0711	0,0705	0,1010	0,1210	0,1540	0,2130	0,2410	0,2580	0,2120	0,1800	0,1170	0,0822
305	0,0235	0,0231	0,0506	0,0494	0,0769	0,0798	0,1110	0,1330	0,1700	0,2310	0,2440	0,2810	0,2000	0,1960	0,0895	0,0831

Eval. Run CFD	AvMag1b [m/s]	AvMag1t [m/s]	AvMag2b [m/s]	AvMag2t [m/s]	AvMag3b [m/s]	AvMag3t [m/s]	AvMag4b [m/s]	AvMag4t [m/s]	AvMag5b [m/s]	AvMag5t [m/s]	AvMag6b [m/s]	AvMag6t [m/s]	AvMag7b [m/s]	AvMag7t [m/s]	AvMag8b [m/s]	AvMag8t [m/s]
306	0,0233	0,0214	0,0499	0,0450	0,0770	0,0730	0,1080	0,1280	0,1430	0,2520	0,1630	0,3700	0,1430	0,2650	0,0709	0,1080
307	0,0191	0,0199	0,0391	0,0425	0,0589	0,0632	0,0940	0,0836	0,1800	0,1040	0,2900	0,1170	0,2540	0,1180	0,1570	0,0759
308	0,0222	0,0233	0,0455	0,0482	0,0672	0,0701	0,1030	0,0907	0,1890	0,1100	0,2930	0,1290	0,2410	0,1300	0,1270	0,0793
309	0,0213	0,0219	0,0433	0,0458	0,0644	0,0662	0,0994	0,0858	0,1770	0,1140	0,2330	0,1850	0,1720	0,1950	0,0882	0,1070
310	0,0246	0,0259	0,0486	0,0522	0,0719	0,0760	0,1160	0,1050	0,1980	0,1360	0,2920	0,1490	0,2430	0,1320	0,1380	0,0750
311	0,0278	0,0295	0,0559	0,0592	0,0829	0,0843	0,1270	0,1100	0,2010	0,1360	0,2820	0,1500	0,2240	0,1340	0,1100	0,0778
312	0,0260	0,0271	0,0528	0,0554	0,0798	0,0796	0,1230	0,1060	0,1890	0,1400	0,2230	0,2040	0,1540	0,1980	0,0709	0,1040
313	0,0245	0,0234	0,0507	0,0482	0,0726	0,0761	0,0954	0,1240	0,1210	0,1930	0,1780	0,2160	0,1830	0,1420	0,1190	0,0688
314	0,0246	0,0236	0,0518	0,0492	0,0777	0,0772	0,1070	0,1280	0,1440	0,2190	0,2070	0,2700	0,2060	0,2000	0,1140	0,1000
315	0,0268	0,0255	0,0538	0,0500	0,0772	0,0733	0,1020	0,1220	0,1290	0,2200	0,1410	0,3120	0,1230	0,2410	0,0638	0,1080
316	0,3140	0,0515	0,2250	0,0562	0,1480	0,0580	0,1170	0,0636	0,1310	0,0723	0,2090	0,0799	0,1740	0,0775	0,0938	0,0461
317	0,2040	0,0807	0,1960	0,0833	0,1410	0,0754	0,1130	0,0765	0,1320	0,0840	0,2040	0,0894	0,1660	0,0816	0,0865	0,0447
318	0,0794	0,1780	0,0881	0,1700	0,0828	0,1320	0,0780	0,1160	0,0952	0,1160	0,1750	0,1200	0,1610	0,0966	0,0956	0,0530
319	0,3130	0,0629	0,2300	0,0745	0,1580	0,0769	0,1280	0,0783	0,1480	0,0885	0,2080	0,1010	0,1540	0,0893	0,0627	0,0439
320	0,2010	0,0864	0,2080	0,0963	0,1620	0,0911	0,1320	0,0892	0,1570	0,1010	0,2140	0,1160	0,1560	0,1000	0,0639	0,0483
321	0,0793	0,1890	0,0917	0,1800	0,0892	0,1450	0,0866	0,1270	0,1170	0,1270	0,1740	0,1350	0,1350	0,1010	0,0552	0,0443
322	0,2800	0,0580	0,2250	0,0701	0,1540	0,0699	0,1260	0,0702	0,1230	0,1060	0,1300	0,1820	0,1000	0,1500	0,0461	0,0622
323	0,2300	0,1040	0,2120	0,1030	0,1550	0,0893	0,1300	0,0845	0,1310	0,1210	0,1360	0,1980	0,1030	0,1620	0,0477	0,0678
324	0,0840	0,2170	0,0898	0,1960	0,0872	0,1460	0,0866	0,1220	0,0913	0,1490	0,0991	0,2180	0,0857	0,1630	0,0412	0,0649
325	0,1430	0,0347	0,2270	0,0569	0,2090	0,0649	0,1570	0,0697	0,1630	0,0811	0,2340	0,0915	0,1950	0,0887	0,1020	0,0513
326	0,1320	0,0537	0,1890	0,0817	0,1890	0,0908	0,1560	0,0903	0,1620	0,0957	0,2290	0,1030	0,1870	0,0953	0,0987	0,0534
327	0,0487	0,1540	0,0790	0,2050	0,0879	0,1920	0,0875	0,1610	0,1130	0,1410	0,1940	0,1370	0,1770	0,1090	0,1010	0,0593
328	0,1500	0,0462	0,2470	0,0729	0,2310	0,0816	0,1780	0,0855	0,1820	0,1010	0,2390	0,1210	0,1870	0,1130	0,0807	0,0588
329	0,1190	0,0567	0,1900	0,0912	0,1980	0,1030	0,1680	0,1010	0,1690	0,1080	0,2230	0,1240	0,1700	0,1100	0,0731	0,0559
330	0,0511	0,1580	0,0843	0,2150	0,0977	0,2090	0,1010	0,1800	0,1300	0,1630	0,1960	0,1620	0,1630	0,1270	0,0749	0,0616
331	0,1430	0,0376	0,2350	0,0608	0,2230	0,0673	0,1720	0,0710	0,1500	0,1120	0,1520	0,1990	0,1220	0,1740	0,0573	0,0780

Eval. Run CFD	AvMag1b [m/s]	AvMag1t [m/s]	AvMag2b [m/s]	AvMag2t [m/s]	AvMag3b [m/s]	AvMag3t [m/s]	AvMag4b [m/s]	AvMag4t [m/s]	AvMag5b [m/s]	AvMag5t [m/s]	AvMag6b [m/s]	AvMag6t [m/s]	AvMag7b [m/s]	AvMag7t [m/s]	AvMag8b [m/s]	AvMag8t [m/s]
332	0,1180	0,0549	0,1920	0,0885	0,2040	0,0977	0,1730	0,0959	0,1480	0,1290	0,1440	0,2040	0,1100	0,1670	0,0505	0,0707
333	0,0493	0,1420	0,0845	0,2040	0,1010	0,2030	0,1040	0,1790	0,1070	0,1870	0,1130	0,2440	0,0983	0,1830	0,0476	0,0742
334	0,0352	0,0222	0,0999	0,0456	0,1810	0,0648	0,2240	0,0795	0,2190	0,0934	0,2600	0,1070	0,2150	0,1050	0,1110	0,0601
335	0,0409	0,0295	0,1100	0,0701	0,1810	0,1070	0,2180	0,1250	0,2210	0,1250	0,2540	0,1230	0,2070	0,1140	0,1130	0,0646
336	0,0286	0,0450	0,0629	0,1230	0,0934	0,1950	0,1130	0,2210	0,1400	0,2000	0,2100	0,1570	0,1880	0,1170	0,1060	0,0631
337	0,0437	0,0290	0,1120	0,0558	0,1940	0,0759	0,2370	0,0924	0,2350	0,1120	0,2660	0,1340	0,2110	0,1280	0,0962	0,0683
338	0,0465	0,0347	0,1200	0,0774	0,1990	0,1170	0,2410	0,1390	0,2470	0,1460	0,2670	0,1520	0,2030	0,1360	0,0908	0,0691
339	0,0324	0,0476	0,0702	0,1240	0,1060	0,1980	0,1300	0,2310	0,1600	0,2220	0,2170	0,1920	0,1810	0,1460	0,0846	0,0723
340	0,0408	0,0257	0,1120	0,0503	0,1980	0,0684	0,2320	0,0838	0,1990	0,1240	0,1730	0,2090	0,1370	0,1810	0,0650	0,0825
341	0,0471	0,0352	0,1210	0,0796	0,1950	0,1170	0,2280	0,1380	0,2080	0,1640	0,1750	0,2320	0,1370	0,1970	0,0670	0,0913
342	0,0308	0,0452	0,0668	0,1200	0,1010	0,1930	0,1230	0,2280	0,1290	0,2420	0,1300	0,2680	0,1140	0,1980	0,0568	0,0846
343	0,0213	0,0214	0,0477	0,0448	0,0880	0,0657	0,1650	0,0852	0,2510	0,1020	0,3010	0,1140	0,2370	0,1130	0,1340	0,0692
344	0,0224	0,0237	0,0551	0,0518	0,1040	0,0829	0,1740	0,1150	0,2430	0,1340	0,2920	0,1300	0,2100	0,1130	0,1140	0,0646
345	0,0222	0,0212	0,0487	0,0543	0,0785	0,1110	0,1120	0,1930	0,1570	0,2410	0,2270	0,2130	0,1980	0,1370	0,1110	0,0703
346	0,0263	0,0250	0,0556	0,0510	0,0973	0,0745	0,1810	0,0989	0,2790	0,1260	0,3150	0,1480	0,2320	0,1390	0,1090	0,0753
347	0,0272	0,0274	0,0642	0,0606	0,1170	0,0969	0,1920	0,1320	0,2640	0,1540	0,2880	0,1520	0,1880	0,1260	0,0792	0,0616
348	0,0256	0,0262	0,0568	0,0636	0,0903	0,1230	0,1300	0,2090	0,1810	0,2640	0,2390	0,2470	0,1930	0,1640	0,0882	0,0766
349	0,0242	0,0225	0,0532	0,0462	0,0957	0,0673	0,1780	0,0932	0,2440	0,1460	0,2200	0,2160	0,1530	0,1780	0,0707	0,0751
350	0,0250	0,0247	0,0621	0,0562	0,1200	0,0924	0,2010	0,1330	0,2530	0,1820	0,2260	0,2470	0,1500	0,2020	0,0708	0,0920
351	0,0247	0,0242	0,0552	0,0592	0,0891	0,1200	0,1260	0,2100	0,1500	0,2860	0,1540	0,3280	0,1320	0,2280	0,0677	0,1000
352	0,0183	0,0199	0,0379	0,0427	0,0582	0,0635	0,0975	0,0845	0,2010	0,1050	0,3290	0,1190	0,2580	0,1180	0,1420	0,0711
353	0,0211	0,0228	0,0442	0,0481	0,0709	0,0736	0,1190	0,1040	0,2160	0,1360	0,3240	0,1470	0,2430	0,1270	0,1210	0,0696
354	0,0297	0,0295	0,0575	0,0553	0,0796	0,0766	0,1060	0,1200	0,1570	0,1930	0,2130	0,2190	0,1590	0,1330	0,0636	0,0489
355	0,0213	0,0224	0,0447	0,0471	0,0680	0,0702	0,1090	0,0946	0,2200	0,1220	0,3350	0,1460	0,2510	0,1380	0,1190	0,0761
356	0,0245	0,0261	0,0515	0,0552	0,0806	0,0830	0,1310	0,1150	0,2330	0,1510	0,3270	0,1680	0,2270	0,1400	0,0925	0,0684
357	0,0235	0,0225	0,0508	0,0492	0,0783	0,0804	0,1140	0,1350	0,1740	0,2330	0,2560	0,2930	0,2180	0,2160	0,1020	0,0965

Eval. Run CFD	AvMag1b [m/s]	AvMag1t [m/s]	AvMag2b [m/s]	AvMag2t [m/s]	AvMag3b [m/s]	AvMag3t [m/s]	AvMag4b [m/s]	AvMag4t [m/s]	AvMag5b [m/s]	AvMag5t [m/s]	AvMag6b [m/s]	AvMag6t [m/s]	AvMag7b [m/s]	AvMag7t [m/s]	AvMag8b [m/s]	AvMag8t [m/s]
358	0,0212	0,0218	0,0449	0,0453	0,0689	0,0666	0,1070	0,0919	0,1940	0,1450	0,2540	0,2270	0,1860	0,1930	0,0932	0,0892
359	0,0233	0,0241	0,0502	0,0518	0,0820	0,0802	0,1340	0,1170	0,2180	0,1830	0,2630	0,2680	0,1870	0,2210	0,0826	0,0999
360	0,0247	0,0231	0,0524	0,0490	0,0793	0,0783	0,1090	0,1320	0,1390	0,2430	0,1540	0,3450	0,1310	0,2420	0,0644	0,0958
361	0,0205	0,0212	0,0423	0,0453	0,0603	0,0671	0,0815	0,0876	0,1490	0,1080	0,3070	0,1230	0,2810	0,1250	0,1640	0,0778
362	0,0226	0,0233	0,0465	0,0491	0,0680	0,0734	0,0955	0,0997	0,1680	0,1310	0,3240	0,1590	0,2900	0,1560	0,1550	0,0914
363	0,0227	0,0228	0,0473	0,0477	0,0696	0,0701	0,0940	0,0956	0,1410	0,1500	0,2350	0,2330	0,2180	0,2060	0,1240	0,1020
364	0,0233	0,0243	0,0477	0,0512	0,0690	0,0756	0,0975	0,1000	0,1740	0,1290	0,3200	0,1540	0,2760	0,1470	0,1420	0,0831
365	0,0254	0,0260	0,0525	0,0551	0,0770	0,0822	0,1090	0,1110	0,1880	0,1470	0,3190	0,1800	0,2630	0,1670	0,1170	0,0873
366	0,0239	0,0239	0,0504	0,0506	0,0743	0,0749	0,1020	0,1030	0,1540	0,1590	0,2360	0,2570	0,2080	0,2290	0,1010	0,1110
367	0,0249	0,0251	0,0504	0,0508	0,0716	0,0715	0,0928	0,0927	0,1350	0,1430	0,2210	0,2240	0,1970	0,1910	0,1070	0,0891
368	0,0238	0,0238	0,0504	0,0509	0,0761	0,0763	0,1070	0,1070	0,1630	0,1680	0,2460	0,2660	0,2150	0,2360	0,1040	0,1130
369	0,0257	0,0253	0,0543	0,0525	0,0800	0,0760	0,1050	0,1060	0,1330	0,1880	0,1580	0,3390	0,1460	0,2790	0,0762	0,1200
370	0,0203	0,0206	0,0424	0,0438	0,0612	0,0650	0,0808	0,0854	0,1270	0,1050	0,2670	0,1200	0,2790	0,1250	0,1810	0,0833
371	0,0237	0,0240	0,0487	0,0500	0,0693	0,0728	0,0892	0,0929	0,1370	0,1120	0,2690	0,1330	0,2640	0,1370	0,1500	0,0871
372	0,0226	0,0232	0,0468	0,0485	0,0666	0,0701	0,0862	0,0891	0,1280	0,1130	0,2110	0,1820	0,1980	0,1990	0,1130	0,1160
373	0,0289	0,0297	0,0559	0,0584	0,0770	0,0814	0,0960	0,1010	0,1450	0,1230	0,2710	0,1450	0,2680	0,1420	0,1590	0,0865
374	0,0242	0,0245	0,0508	0,0526	0,0745	0,0788	0,1020	0,1060	0,1600	0,1380	0,2900	0,1730	0,2800	0,1750	0,1490	0,1080
375	0,0259	0,0261	0,0530	0,0535	0,0752	0,0768	0,0960	0,0979	0,1380	0,1300	0,2100	0,2060	0,1820	0,2110	0,0884	0,1120
376	0,0240	0,0240	0,0501	0,0501	0,0729	0,0728	0,0943	0,0968	0,1210	0,1460	0,1950	0,2330	0,2190	0,2120	0,1500	0,1150
377	0,0263	0,0263	0,0550	0,0546	0,0797	0,0794	0,1030	0,1050	0,1320	0,1570	0,2020	0,2480	0,2100	0,2230	0,1200	0,1170
378	0,0252	0,0252	0,0520	0,0515	0,0748	0,0732	0,0943	0,0949	0,1130	0,1480	0,1310	0,2810	0,1260	0,2670	0,0713	0,1310
379	0,3110	0,0519	0,2210	0,0561	0,1440	0,0586	0,1200	0,0658	0,1160	0,0746	0,1670	0,0795	0,1700	0,0785	0,1120	0,0520
380	0,1860	0,0761	0,1920	0,0833	0,1480	0,0789	0,1210	0,0809	0,1230	0,0888	0,1730	0,0942	0,1720	0,0884	0,1110	0,0543
381	0,0677	0,1840	0,0780	0,1720	0,0774	0,1320	0,0777	0,1140	0,0820	0,1130	0,1330	0,1140	0,1490	0,0904	0,1010	0,0515
382	0,3060	0,0536	0,2190	0,0626	0,1480	0,0662	0,1240	0,0722	0,1210	0,0792	0,1700	0,0888	0,1590	0,0903	0,0849	0,0562
383	0,1900	0,0823	0,1890	0,0894	0,1440	0,0847	0,1210	0,0855	0,1230	0,0906	0,1730	0,1000	0,1600	0,0974	0,0851	0,0578

Eval. Run CFD	AvMag1b [m/s]	AvMag1t [m/s]	AvMag2b [m/s]	AvMag2t [m/s]	AvMag3b [m/s]	AvMag3t [m/s]	AvMag4b [m/s]	AvMag4t [m/s]	AvMag5b [m/s]	AvMag5t [m/s]	AvMag6b [m/s]	AvMag6t [m/s]	AvMag7b [m/s]	AvMag7t [m/s]	AvMag8b [m/s]	AvMag8t [m/s]
384	0,0762	0,2340	0,0850	0,2040	0,0856	0,1500	0,0864	0,1280	0,0930	0,1270	0,1420	0,1320	0,1440	0,1090	0,0772	0,0599
385	0,0516	0,0453	0,0827	0,0686	0,0989	0,0750	0,1050	0,0751	0,1040	0,0769	0,1100	0,1360	0,0925	0,1560	0,0498	0,0881
386	0,1440	0,0628	0,1590	0,0790	0,1320	0,0800	0,1130	0,0809	0,1110	0,0872	0,1170	0,1460	0,0947	0,1630	0,0516	0,0931
387	0,0756	0,2250	0,0816	0,2020	0,0808	0,1470	0,0830	0,1250	0,0878	0,1270	0,0932	0,1830	0,0888	0,1810	0,0524	0,0997
388	0,1410	0,0307	0,2250	0,0514	0,2050	0,0604	0,1550	0,0670	0,1370	0,0793	0,1890	0,0898	0,1890	0,0897	0,1190	0,0578
389	0,1110	0,0464	0,1750	0,0763	0,1830	0,0868	0,1530	0,0864	0,1360	0,0907	0,1800	0,0967	0,1750	0,0903	0,1090	0,0541
390	0,0438	0,1450	0,0740	0,2010	0,0878	0,1950	0,0892	0,1660	0,0966	0,1430	0,1530	0,1350	0,1670	0,1070	0,1100	0,0605
391	0,1450	0,0376	0,2360	0,0613	0,2200	0,0711	0,1680	0,0763	0,1480	0,0886	0,1970	0,1080	0,1870	0,1130	0,1000	0,0714
392	0,1250	0,0539	0,1930	0,0872	0,2000	0,0978	0,1680	0,0959	0,1480	0,1020	0,1900	0,1150	0,1730	0,1120	0,0921	0,0673
393	0,0523	0,1430	0,0819	0,1820	0,0944	0,1770	0,0957	0,1560	0,0995	0,1410	0,1510	0,1410	0,1580	0,1190	0,0911	0,0686
394	0,1460	0,0353	0,2360	0,0576	0,2180	0,0655	0,1680	0,0696	0,1450	0,0879	0,1460	0,1610	0,1220	0,1860	0,0639	0,1080
395	0,1190	0,0523	0,1890	0,0848	0,1970	0,0962	0,1670	0,0932	0,1420	0,1020	0,1390	0,1670	0,1150	0,1870	0,0646	0,1110
396	0,0493	0,1340	0,0804	0,1790	0,0941	0,1740	0,0958	0,1530	0,0956	0,1420	0,1000	0,1950	0,0954	0,1900	0,0568	0,1050
397	0,0321	0,0202	0,0973	0,0418	0,1820	0,0606	0,2180	0,0743	0,1880	0,0864	0,2120	0,0982	0,2020	0,0977	0,1190	0,0592
398	0,0384	0,0269	0,1030	0,0629	0,1690	0,0954	0,1980	0,1100	0,1810	0,1090	0,1960	0,1070	0,1850	0,1000	0,1150	0,0603
399	0,0241	0,0386	0,0553	0,1110	0,0838	0,1810	0,1010	0,2070	0,1090	0,1860	0,1580	0,1460	0,1710	0,1110	0,1110	0,0617
400	0,0395	0,0265	0,1070	0,0524	0,1900	0,0725	0,2290	0,0868	0,2020	0,1000	0,2230	0,1190	0,2040	0,1210	0,1070	0,0726
401	0,0466	0,0344	0,1180	0,0761	0,1920	0,1130	0,2240	0,1300	0,2060	0,1310	0,2170	0,1370	0,1970	0,1330	0,1090	0,0820
402	0,0299	0,0454	0,0642	0,1170	0,0943	0,1850	0,1110	0,2120	0,1200	0,1960	0,1670	0,1660	0,1750	0,1350	0,1020	0,0792
403	0,0367	0,0211	0,1090	0,0448	0,1960	0,0652	0,2340	0,0803	0,1970	0,1010	0,1640	0,1690	0,1310	0,1870	0,0675	0,1060
404	0,0400	0,0290	0,1100	0,0674	0,1870	0,1020	0,2220	0,1200	0,1990	0,1270	0,1610	0,1840	0,1280	0,2010	0,0702	0,1160
405	0,0289	0,0466	0,0651	0,1240	0,0982	0,1930	0,1170	0,2160	0,1190	0,2000	0,1170	0,2220	0,1100	0,2090	0,0639	0,1150
406	0,0181	0,0198	0,0443	0,0417	0,0907	0,0625	0,1710	0,0820	0,2330	0,0970	0,2540	0,1060	0,2140	0,1040	0,1270	0,0630
407	0,0237	0,0250	0,0593	0,0546	0,1150	0,0879	0,1860	0,1200	0,2320	0,1370	0,2510	0,1310	0,2100	0,1180	0,1350	0,0737
408	0,0233	0,0215	0,0496	0,0553	0,0769	0,1150	0,1050	0,1950	0,1280	0,2380	0,1770	0,2050	0,1870	0,1310	0,1230	0,0718
409	0,0223	0,0221	0,0510	0,0468	0,0951	0,0697	0,1740	0,0913	0,2440	0,1100	0,2680	0,1260	0,2190	0,1280	0,1130	0,0767

Eval. Run CFD	AvMag1b [m/s]	AvMag1t [m/s]	AvMag2b [m/s]	AvMag2t [m/s]	AvMag3b [m/s]	AvMag3t [m/s]	AvMag4b [m/s]	AvMag4t [m/s]	AvMag5b [m/s]	AvMag5t [m/s]	AvMag6b [m/s]	AvMag6t [m/s]	AvMag7b [m/s]	AvMag7t [m/s]	AvMag8b [m/s]	AvMag8t [m/s]
410	0,0278	0,0270	0,0652	0,0588	0,1180	0,0916	0,1870	0,1220	0,2340	0,1400	0,2550	0,1430	0,2020	0,1330	0,1090	0,0805
411	0,0246	0,0242	0,0544	0,0602	0,0859	0,1190	0,1190	0,2040	0,1450	0,2520	0,1940	0,2260	0,1920	0,1560	0,1080	0,0860
412	0,0197	0,0202	0,0466	0,0431	0,0899	0,0647	0,1730	0,0860	0,2370	0,1110	0,2130	0,1780	0,1560	0,1980	0,0838	0,1130
413	0,0232	0,0238	0,0566	0,0529	0,1080	0,0851	0,1810	0,1190	0,2290	0,1440	0,2020	0,1930	0,1340	0,1980	0,0698	0,1100
414	0,0296	0,0314	0,0557	0,0626	0,0748	0,0922	0,0886	0,1220	0,0958	0,1510	0,0952	0,2100	0,0870	0,1850	0,0511	0,1000
415	0,0203	0,0213	0,0411	0,0447	0,0603	0,0641	0,0952	0,0814	0,1750	0,0967	0,2750	0,1070	0,2390	0,1060	0,1450	0,0672
416	0,0241	0,0254	0,0490	0,0522	0,0753	0,0768	0,1210	0,1050	0,1980	0,1340	0,2830	0,1430	0,2370	0,1260	0,1370	0,0744
417	0,0263	0,0256	0,0528	0,0507	0,0744	0,0762	0,0975	0,1230	0,1260	0,1960	0,1830	0,2240	0,1860	0,1500	0,1140	0,0692
418	0,0249	0,0258	0,0504	0,0522	0,0740	0,0746	0,1110	0,0948	0,1920	0,1130	0,2920	0,1310	0,2410	0,1320	0,1250	0,0803
419	0,0262	0,0270	0,0525	0,0562	0,0789	0,0821	0,1240	0,1110	0,2070	0,1420	0,2940	0,1590	0,2290	0,1430	0,1080	0,0784
420	0,0268	0,0246	0,0564	0,0524	0,0842	0,0864	0,1150	0,1470	0,1520	0,2370	0,2120	0,2760	0,2080	0,2020	0,1140	0,0986
421	0,0208	0,0221	0,0433	0,0464	0,0651	0,0673	0,1020	0,0879	0,1830	0,1140	0,2410	0,1840	0,1840	0,2070	0,1040	0,1240
422	0,0243	0,0250	0,0498	0,0523	0,0781	0,0787	0,1280	0,1120	0,2080	0,1540	0,2480	0,2220	0,1780	0,2270	0,0876	0,1280
423	0,0241	0,0228	0,0511	0,0474	0,0769	0,0748	0,1060	0,1250	0,1360	0,2200	0,1520	0,3180	0,1380	0,2680	0,0778	0,1360
424	0,0217	0,0221	0,0446	0,0461	0,0628	0,0670	0,0800	0,0855	0,1230	0,1020	0,2610	0,1150	0,2700	0,1190	0,1770	0,0793
425	0,0253	0,0260	0,0511	0,0534	0,0717	0,0763	0,0941	0,0975	0,1470	0,1210	0,2690	0,1420	0,2640	0,1370	0,1540	0,0829
426	0,0227	0,0227	0,0472	0,0469	0,0688	0,0678	0,0890	0,0896	0,1150	0,1360	0,1840	0,2230	0,2070	0,2010	0,1380	0,1050
427	0,0277	0,0285	0,0549	0,0576	0,0750	0,0803	0,0908	0,0976	0,1380	0,1120	0,2700	0,1290	0,2580	0,1300	0,1420	0,0787
428	0,0271	0,0276	0,0559	0,0576	0,0805	0,0841	0,1060	0,1090	0,1620	0,1380	0,2850	0,1690	0,2690	0,1680	0,1390	0,1010
429	0,0278	0,0282	0,0565	0,0565	0,0806	0,0793	0,1020	0,1020	0,1310	0,1540	0,1920	0,2450	0,1860	0,2160	0,0961	0,1060
430	0,0215	0,0220	0,0453	0,0465	0,0663	0,0690	0,0885	0,0912	0,1310	0,1180	0,2250	0,1900	0,2160	0,2150	0,1340	0,1310
431	0,0260	0,0261	0,0535	0,0542	0,0765	0,0785	0,0997	0,1020	0,1460	0,1350	0,2230	0,2150	0,1980	0,2270	0,1010	0,1260
432	0,0252	0,0252	0,0527	0,0521	0,0768	0,0751	0,0992	0,0997	0,1230	0,1570	0,1440	0,2920	0,1420	0,2820	0,0821	0,1450
433	0,0219	0,0218	0,0457	0,0461	0,0658	0,0675	0,0840	0,0875	0,1100	0,1050	0,2270	0,1200	0,2780	0,1270	0,1990	0,0896
434	0,0249	0,0249	0,0511	0,0518	0,0730	0,0748	0,0915	0,0950	0,1190	0,1130	0,2330	0,1330	0,2670	0,1400	0,1720	0,0953
435	0,0228	0,0229	0,0477	0,0480	0,0690	0,0700	0,0877	0,0901	0,1090	0,1140	0,1770	0,1830	0,2050	0,2080	0,1440	0,1310

Eval. Run CFD	AvMag1b [m/s]	AvMag1t [m/s]	AvMag2b [m/s]	AvMag2t [m/s]	AvMag3b [m/s]	AvMag3t [m/s]	AvMag4b [m/s]	AvMag4t [m/s]	AvMag5b [m/s]	AvMag5t [m/s]	AvMag6b [m/s]	AvMag6t [m/s]	AvMag7b [m/s]	AvMag7t [m/s]	AvMag8b [m/s]	AvMag8t [m/s]
436	0,0260	0,0260	0,0530	0,0536	0,0756	0,0778	0,0957	0,1000	0,1270	0,1220	0,2430	0,1460	0,2750	0,1540	0,1780	0,1030
437	0,0250	0,0250	0,0526	0,0531	0,0765	0,0784	0,0991	0,1030	0,1310	0,1270	0,2480	0,1580	0,2800	0,1710	0,1690	0,1170
438	0,0239	0,0243	0,0505	0,0511	0,0741	0,0755	0,0967	0,0982	0,1240	0,1280	0,1940	0,2080	0,2110	0,2370	0,1260	0,1470
439	0,0226	0,0229	0,0475	0,0479	0,0687	0,0698	0,0883	0,0898	0,1100	0,1140	0,1760	0,1840	0,2060	0,2120	0,1460	0,1350
440	0,0260	0,0262	0,0541	0,0543	0,0774	0,0783	0,0972	0,0989	0,1190	0,1230	0,1830	0,1990	0,1960	0,2240	0,1180	0,1360
441	0,0254	0,0256	0,0527	0,0527	0,0754	0,0758	0,0949	0,0953	0,1110	0,1270	0,1280	0,2540	0,1310	0,2880	0,0810	0,1630

Appendix C

CFD calculated flow velocities digester overall, Thrust and Torque at mixer blades as well as Uniformity Index

The following Table gives the calculated flow velocity for the digester overall, the calculated thrust and torque at the mixer blades as well as the Uniformity Index of the flow velocity vector for the 441 CFD study runs.

Evaluation Run CFD	AvMagoa [m/s]	Avxoa [m/s]	Avyoa [m/s]	Avzoa [m/s]	Thrust RR1 [N]	Thrust RR2 [N]	Torque RR1 [Nm]	Torque RR2 [Nm]	Uniformity VelMag_oa [-]	Uniformity Velx_oa [-]	Uniformity Vely_oa [-]	Uniformity Velz_oa [-]
1	0,1060	0,0673	0,0556	0,0278	2,78E+03	2,89E+03	6,05E+02	6,19E+02	0,61	0,56	0,57	0,47
2	0,1100	0,0720	0,0597	0,0239	2,89E+03	2,81E+03	6,21E+02	6,04E+02	0,62	0,57	0,58	0,48
3	0,0910	0,0637	0,0456	0,0197	2,81E+03	2,96E+03	6,09E+02	6,28E+02	0,61	0,56	0,57	0,43
4	0,1090	0,0707	0,0595	0,0238	2,79E+03	2,79E+03	6,01E+02	6,04E+02	0,62	0,56	0,58	0,47
5	0,1170	0,0750	0,0652	0,0205	2,80E+03	2,76E+03	6,01E+02	5,95E+02	0,64	0,57	0,60	0,48
6	0,1050	0,0717	0,0561	0,0181	2,82E+03	2,78E+03	6,04E+02	6,01E+02	0,63	0,57	0,59	0,44
7	0,1020	0,0731	0,0499	0,0212	2,86E+03	2,83E+03	6,11E+02	6,10E+02	0,59	0,53	0,56	0,49
8	0,1070	0,0730	0,0575	0,0179	2,50E+03	2,83E+03	5,56E+02	6,09E+02	0,63	0,57	0,59	0,46
9	0,0958	0,0633	0,0513	0,0207	2,81E+03	2,77E+03	6,03E+02	5,99E+02	0,63	0,57	0,58	0,45
10	0,1090	0,0757	0,0542	0,0266	2,93E+03	2,89E+03	6,28E+02	6,21E+02	0,55	0,49	0,53	0,47
11	0,1020	0,0719	0,0515	0,0212	2,87E+03	2,87E+03	6,22E+02	6,13E+02	0,58	0,52	0,56	0,46
12	0,1010	0,0754	0,0455	0,0209	2,93E+03	2,88E+03	6,27E+02	6,14E+02	0,54	0,47	0,54	0,46
13	0,1080	0,0752	0,0555	0,0226	2,73E+03	2,87E+03	5,94E+02	6,16E+02	0,58	0,53	0,55	0,47
14	0,1130	0,0788	0,0608	0,0195	2,73E+03	2,84E+03	5,91E+02	6,09E+02	0,62	0,55	0,58	0,47
15	0,1060	0,0764	0,0536	0,0179	2,75E+03	2,92E+03	5,94E+02	6,21E+02	0,60	0,53	0,58	0,46
16	0,1050	0,0769	0,0495	0,0220	2,69E+03	2,90E+03	5,85E+02	6,20E+02	0,55	0,48	0,54	0,46

Evaluation Run CFD	AvMagoa [m/s]	Avxoa [m/s]	Avyoa [m/s]	Avzoa [m/s]	Thrust RR1 [N]	Thrust RR2 [N]	Torque RR1 [Nm]	Torque RR2 [Nm]	Uniformity VelMag_oa [-]	Uniformity Velx_oa [-]	Uniformity Vely_oa [-]	Uniformity Velz_oa [-]
17	0,1060	0,0764	0,0545	0,0182	2,73E+03	2,87E+03	5,91E+02	6,11E+02	0,59	0,52	0,57	0,47
18	0,1110	0,0780	0,0576	0,0220	2,80E+03	2,80E+03	6,02E+02	6,02E+02	0,58	0,52	0,57	0,46
19	0,0963	0,0682	0,0493	0,0231	2,77E+03	2,84E+03	6,05E+02	6,14E+02	0,57	0,51	0,53	0,48
20	0,1060	0,0767	0,0531	0,0203	2,98E+03	2,89E+03	6,39E+02	6,18E+02	0,55	0,48	0,53	0,46
21	0,0953	0,0704	0,0459	0,0202	2,86E+03	2,78E+03	6,18E+02	6,00E+02	0,56	0,50	0,54	0,47
22	0,1120	0,0801	0,0579	0,0202	2,88E+03	2,91E+03	6,16E+02	6,25E+02	0,56	0,50	0,53	0,48
23	0,1040	0,0747	0,0545	0,0177	2,72E+03	2,86E+03	5,91E+02	6,13E+02	0,61	0,55	0,57	0,46
24	0,1010	0,0736	0,0525	0,0188	2,70E+03	2,83E+03	5,89E+02	6,08E+02	0,60	0,55	0,55	0,47
25	0,1100	0,0792	0,0559	0,0221	2,81E+03	2,82E+03	6,03E+02	6,13E+02	0,56	0,50	0,53	0,49
26	0,1080	0,0788	0,0553	0,0189	2,79E+03	2,86E+03	6,00E+02	6,14E+02	0,57	0,51	0,55	0,49
27	0,1140	0,0817	0,0589	0,0222	2,69E+03	2,76E+03	5,85E+02	5,99E+02	0,57	0,51	0,55	0,46
28	0,1030	0,0706	0,0567	0,0231	2,85E+03	2,85E+03	6,17E+02	6,18E+02	0,55	0,49	0,52	0,47
29	0,1010	0,0723	0,0527	0,0197	2,96E+03	2,80E+03	6,33E+02	6,06E+02	0,57	0,51	0,53	0,47
30	0,1070	0,0766	0,0542	0,0226	2,97E+03	2,77E+03	6,37E+02	6,01E+02	0,55	0,49	0,52	0,49
31	0,1120	0,0771	0,0622	0,0218	2,86E+03	2,84E+03	6,11E+02	6,16E+02	0,59	0,54	0,55	0,48
32	0,1080	0,0769	0,0577	0,0181	2,85E+03	2,83E+03	6,09E+02	6,10E+02	0,60	0,54	0,55	0,48
33	0,1090	0,0788	0,0575	0,0191	2,87E+03	2,73E+03	6,13E+02	5,95E+02	0,58	0,53	0,55	0,50
34	0,1090	0,0751	0,0609	0,0224	2,77E+03	2,86E+03	5,96E+02	6,20E+02	0,57	0,52	0,53	0,47
35	0,1080	0,0771	0,0576	0,0196	2,78E+03	2,77E+03	5,99E+02	6,01E+02	0,60	0,54	0,55	0,47
36	0,1060	0,0749	0,0563	0,0210	2,74E+03	2,75E+03	5,93E+02	5,96E+02	0,59	0,54	0,55	0,47
37	0,1070	0,0716	0,0591	0,0236	2,88E+03	2,88E+03	6,20E+02	6,24E+02	0,55	0,51	0,52	0,45
38	0,1020	0,0708	0,0541	0,0198	2,93E+03	2,89E+03	6,28E+02	6,21E+02	0,58	0,53	0,54	0,46
39	0,0975	0,0685	0,0502	0,0208	2,92E+03	2,73E+03	6,27E+02	5,97E+02	0,58	0,53	0,54	0,47
40	0,1080	0,0739	0,0602	0,0200	2,88E+03	2,87E+03	6,14E+02	6,22E+02	0,59	0,55	0,55	0,44
41	0,1080	0,0742	0,0592	0,0191	2,81E+03	2,83E+03	6,03E+02	6,10E+02	0,62	0,58	0,56	0,46
42	0,1180	0,0828	0,0642	0,0202	2,90E+03	2,74E+03	6,18E+02	5,98E+02	0,60	0,55	0,55	0,48

Evaluation Run CFD	AvMagoa [m/s]	Avxoa [m/s]	Avyoa [m/s]	Avzoa [m/s]	Thrust RR1 [N]	Thrust RR2 [N]	Torque RR1 [Nm]	Torque RR2 [Nm]	Uniformity VelMag_oa [-]	Uniformity Velx_oa [-]	Uniformity Vely_oa [-]	Uniformity Velz_oa [-]
43	0,1050	0,0703	0,0586	0,0230	2,80E+03	2,89E+03	6,02E+02	6,25E+02	0,59	0,55	0,54	0,45
44	0,1170	0,0813	0,0641	0,0206	2,79E+03	2,91E+03	6,01E+02	6,26E+02	0,59	0,55	0,55	0,47
45	0,1120	0,0777	0,0610	0,0211	2,78E+03	2,76E+03	5,99E+02	6,01E+02	0,60	0,55	0,55	0,46
46	0,1090	0,0730	0,0581	0,0241	2,91E+03	2,78E+03	6,25E+02	6,08E+02	0,56	0,53	0,53	0,44
47	0,1060	0,0722	0,0566	0,0204	2,90E+03	2,74E+03	6,24E+02	5,96E+02	0,58	0,54	0,54	0,44
48	0,1060	0,0727	0,0561	0,0227	2,86E+03	2,79E+03	6,18E+02	6,04E+02	0,58	0,54	0,54	0,48
49	0,1160	0,0788	0,0633	0,0218	2,85E+03	2,82E+03	6,10E+02	6,16E+02	0,59	0,56	0,54	0,44
50	0,1190	0,0822	0,0645	0,0184	2,74E+03	2,77E+03	5,95E+02	6,02E+02	0,62	0,58	0,57	0,44
51	0,1160	0,0798	0,0632	0,0197	2,91E+03	2,74E+03	6,20E+02	5,96E+02	0,59	0,55	0,55	0,48
52	0,1080	0,0713	0,0593	0,0244	2,63E+03	2,79E+03	5,74E+02	6,11E+02	0,59	0,56	0,54	0,46
53	0,1160	0,0795	0,0625	0,0205	2,77E+03	2,74E+03	5,97E+02	5,97E+02	0,59	0,56	0,55	0,46
54	0,1160	0,0792	0,0632	0,0202	2,79E+03	2,76E+03	5,99E+02	6,00E+02	0,59	0,55	0,54	0,44
55	0,1050	0,0712	0,0543	0,0232	2,91E+03	2,82E+03	6,24E+02	6,15E+02	0,56	0,53	0,53	0,44
56	0,1060	0,0734	0,0544	0,0200	2,92E+03	2,79E+03	6,26E+02	6,03E+02	0,58	0,54	0,54	0,43
57	0,1030	0,0696	0,0544	0,0227	2,79E+03	2,75E+03	6,07E+02	5,97E+02	0,59	0,55	0,54	0,47
58	0,1130	0,0776	0,0595	0,0212	2,90E+03	2,83E+03	6,18E+02	6,15E+02	0,60	0,57	0,55	0,44
59	0,1180	0,0824	0,0625	0,0180	2,87E+03	2,80E+03	6,13E+02	6,08E+02	0,60	0,57	0,56	0,44
60	0,1180	0,0828	0,0622	0,0207	2,90E+03	2,76E+03	6,18E+02	5,99E+02	0,60	0,57	0,55	0,48
61	0,1090	0,0738	0,0569	0,0235	2,84E+03	2,83E+03	6,08E+02	6,17E+02	0,59	0,56	0,54	0,46
62	0,1170	0,0812	0,0612	0,0210	2,82E+03	2,77E+03	6,05E+02	6,04E+02	0,60	0,57	0,55	0,46
63	0,1120	0,0776	0,0597	0,0205	2,79E+03	2,76E+03	6,02E+02	5,99E+02	0,59	0,56	0,55	0,44
64	0,0873	0,0622	0,0421	0,0225	2,88E+03	2,66E+03	6,20E+02	5,86E+02	0,59	0,54	0,55	0,44
65	0,1060	0,0758	0,0539	0,0218	2,87E+03	2,80E+03	6,19E+02	6,03E+02	0,57	0,52	0,55	0,46
66	0,0955	0,0699	0,0456	0,0201	2,90E+03	2,85E+03	6,24E+02	6,08E+02	0,57	0,50	0,55	0,45
67	0,1020	0,0706	0,0529	0,0217	2,81E+03	2,92E+03	6,03E+02	6,25E+02	0,59	0,53	0,56	0,47
68	0,1020	0,0724	0,0533	0,0175	2,85E+03	2,72E+03	6,10E+02	5,91E+02	0,61	0,54	0,58	0,46

Evaluation Run CFD	AvMagoa [m/s]	Avxoa [m/s]	Avyoa [m/s]	Avzoa [m/s]	Thrust RR1 [N]	Thrust RR2 [N]	Torque RR1 [Nm]	Torque RR2 [Nm]	Uniformity VelMag_oa [-]	Uniformity Velx_oa [-]	Uniformity Vely_oa [-]	Uniformity Velz_oa [-]
69	0,1070	0,0756	0,0557	0,0192	2,85E+03	2,74E+03	6,11E+02	5,94E+02	0,61	0,54	0,58	0,46
70	0,1030	0,0762	0,0473	0,0215	2,79E+03	2,87E+03	6,01E+02	6,19E+02	0,55	0,48	0,55	0,46
71	0,1050	0,0766	0,0526	0,0183	2,79E+03	2,74E+03	6,02E+02	5,94E+02	0,60	0,53	0,57	0,46
72	0,1070	0,0739	0,0562	0,0223	2,84E+03	2,82E+03	6,10E+02	6,08E+02	0,60	0,54	0,57	0,45
73	0,1060	0,0815	0,0459	0,0213	2,89E+03	2,90E+03	6,25E+02	6,23E+02	0,49	0,42	0,49	0,47
74	0,1120	0,0866	0,0502	0,0191	2,95E+03	2,90E+03	6,34E+02	6,20E+02	0,52	0,45	0,52	0,47
75	0,1030	0,0805	0,0445	0,0206	2,94E+03	2,78E+03	6,32E+02	6,01E+02	0,51	0,44	0,52	0,47
76	0,1120	0,0859	0,0505	0,0198	2,88E+03	2,92E+03	6,18E+02	6,26E+02	0,52	0,45	0,52	0,47
77	0,1120	0,0871	0,0531	0,0155	2,84E+03	2,92E+03	6,10E+02	6,23E+02	0,55	0,49	0,55	0,48
78	0,1130	0,0867	0,0535	0,0197	2,80E+03	2,60E+03	6,04E+02	5,72E+02	0,56	0,50	0,55	0,47
79	0,1090	0,0847	0,0473	0,0221	2,73E+03	2,92E+03	5,91E+02	6,27E+02	0,51	0,44	0,52	0,46
80	0,1070	0,0829	0,0497	0,0180	2,74E+03	2,91E+03	5,94E+02	6,19E+02	0,55	0,48	0,55	0,47
81	0,1120	0,0864	0,0512	0,0204	2,76E+03	2,77E+03	5,95E+02	5,99E+02	0,53	0,47	0,54	0,45
82	0,1130	0,0832	0,0567	0,0216	2,85E+03	2,88E+03	6,19E+02	6,22E+02	0,52	0,44	0,51	0,49
83	0,1190	0,0899	0,0585	0,0202	2,88E+03	2,85E+03	6,22E+02	6,12E+02	0,54	0,48	0,53	0,50
84	0,1190	0,0905	0,0560	0,0218	2,93E+03	2,76E+03	6,31E+02	5,99E+02	0,52	0,45	0,51	0,51
85	0,1180	0,0874	0,0611	0,0191	2,86E+03	2,91E+03	6,13E+02	6,27E+02	0,54	0,47	0,53	0,48
86	0,1180	0,0903	0,0603	0,0159	2,85E+03	2,90E+03	6,12E+02	6,22E+02	0,57	0,51	0,55	0,49
87	0,1190	0,0906	0,0602	0,0192	2,85E+03	2,76E+03	6,12E+02	6,00E+02	0,56	0,51	0,54	0,52
88	0,1130	0,0835	0,0578	0,0224	2,72E+03	2,91E+03	5,91E+02	6,25E+02	0,55	0,49	0,53	0,48
89	0,1150	0,0877	0,0573	0,0189	2,74E+03	2,86E+03	5,92E+02	6,14E+02	0,55	0,49	0,53	0,49
90	0,1190	0,0910	0,0578	0,0192	2,62E+03	2,77E+03	5,75E+02	6,00E+02	0,54	0,49	0,53	0,48
91	0,1150	0,0796	0,0639	0,0226	2,87E+03	2,83E+03	6,20E+02	6,17E+02	0,54	0,48	0,53	0,48
92	0,1160	0,0846	0,0604	0,0194	2,93E+03	2,73E+03	6,30E+02	5,96E+02	0,55	0,49	0,53	0,50
93	0,1240	0,0892	0,0647	0,0227	2,94E+03	2,76E+03	6,33E+02	6,01E+02	0,54	0,48	0,52	0,51
94	0,1230	0,0863	0,0700	0,0202	2,87E+03	2,87E+03	6,15E+02	6,23E+02	0,56	0,50	0,54	0,48

Evaluation Run CFD	AvMagoa [m/s]	Avxoa [m/s]	Avyoa [m/s]	Avzoa [m/s]	Thrust RR1 [N]	Thrust RR2 [N]	Torque RR1 [Nm]	Torque RR2 [Nm]	Uniformity VelMag_oa [-]	Uniformity Velx_oa [-]	Uniformity Vely_oa [-]	Uniformity Velz_oa [-]
95	0,1260	0,0928	0,0681	0,0176	2,86E+03	2,76E+03	6,13E+02	6,01E+02	0,58	0,53	0,55	0,49
96	0,1230	0,0905	0,0664	0,0194	2,89E+03	2,73E+03	6,19E+02	5,96E+02	0,57	0,52	0,54	0,51
97	0,1050	0,0727	0,0599	0,0217	2,70E+03	2,86E+03	5,88E+02	6,19E+02	0,58	0,53	0,54	0,46
98	0,1230	0,0892	0,0656	0,0200	2,71E+03	2,81E+03	5,89E+02	6,09E+02	0,56	0,51	0,54	0,49
99	0,1230	0,0898	0,0659	0,0186	2,77E+03	2,73E+03	5,99E+02	5,95E+02	0,56	0,51	0,54	0,49
100	0,1180	0,0790	0,0678	0,0226	2,96E+03	2,81E+03	6,36E+02	6,15E+02	0,54	0,48	0,52	0,49
101	0,1310	0,0908	0,0731	0,0212	2,94E+03	2,86E+03	6,33E+02	6,18E+02	0,57	0,50	0,54	0,50
102	0,1270	0,0875	0,0714	0,0218	2,99E+03	2,81E+03	6,40E+02	6,11E+02	0,56	0,50	0,53	0,50
103	0,1180	0,0805	0,0680	0,0208	2,81E+03	2,84E+03	6,04E+02	6,16E+02	0,59	0,55	0,56	0,45
104	0,1300	0,0915	0,0747	0,0172	2,96E+03	2,84E+03	6,30E+02	6,15E+02	0,59	0,54	0,55	0,49
105	0,1220	0,0867	0,0686	0,0199	2,89E+03	2,73E+03	6,17E+02	5,96E+02	0,59	0,55	0,56	0,49
106	0,1260	0,0859	0,0725	0,0238	2,80E+03	2,85E+03	6,03E+02	6,21E+02	0,56	0,52	0,53	0,46
107	0,1320	0,0933	0,0734	0,0212	2,84E+03	2,92E+03	6,11E+02	6,28E+02	0,58	0,54	0,55	0,48
108	0,1250	0,0877	0,0703	0,0206	2,80E+03	2,72E+03	6,06E+02	5,95E+02	0,59	0,54	0,55	0,47
109	0,1200	0,0793	0,0678	0,0242	2,98E+03	2,75E+03	6,38E+02	6,06E+02	0,56	0,51	0,53	0,48
110	0,1270	0,0869	0,0708	0,0205	2,99E+03	2,78E+03	6,40E+02	6,04E+02	0,57	0,51	0,54	0,49
111	0,1260	0,0854	0,0704	0,0224	2,97E+03	2,69E+03	6,39E+02	5,91E+02	0,56	0,51	0,54	0,49
112	0,1200	0,0814	0,0689	0,0216	2,87E+03	2,79E+03	6,14E+02	6,12E+02	0,58	0,55	0,55	0,46
113	0,1340	0,0927	0,0766	0,0188	3,02E+03	2,75E+03	6,40E+02	6,01E+02	0,59	0,56	0,56	0,48
114	0,1030	0,0762	0,0513	0,0176	2,80E+03	2,63E+03	6,04E+02	5,86E+02	0,62	0,59	0,53	0,46
115	0,1180	0,0799	0,0625	0,0257	2,86E+03	2,74E+03	6,13E+02	6,03E+02	0,59	0,56	0,55	0,44
116	0,1330	0,0911	0,0746	0,0212	2,73E+03	2,79E+03	5,92E+02	6,04E+02	0,59	0,55	0,55	0,47
117	0,1290	0,0883	0,0726	0,0210	2,84E+03	2,85E+03	6,09E+02	6,16E+02	0,59	0,55	0,55	0,46
118	0,1170	0,0789	0,0636	0,0232	2,94E+03	2,75E+03	6,31E+02	6,04E+02	0,55	0,51	0,53	0,48
119	0,1230	0,0843	0,0670	0,0203	2,97E+03	2,69E+03	6,36E+02	5,91E+02	0,57	0,52	0,54	0,48
120	0,1200	0,0835	0,0647	0,0234	2,95E+03	2,61E+03	6,34E+02	5,76E+02	0,58	0,54	0,55	0,48

Evaluation Run CFD	AvMagoa [m/s]	Avxoa [m/s]	Avyoa [m/s]	Avzoa [m/s]	Thrust RR1 [N]	Thrust RR2 [N]	Torque RR1 [Nm]	Torque RR2 [Nm]	Uniformity VelMag_oa [-]	Uniformity Velx_oa [-]	Uniformity Vely_oa [-]	Uniformity Velz_oa [-]
121	0,1220	0,0843	0,0677	0,0211	2,88E+03	2,76E+03	6,17E+02	6,08E+02	0,58	0,54	0,55	0,46
122	0,1260	0,0881	0,0705	0,0185	2,87E+03	2,73E+03	6,14E+02	5,96E+02	0,60	0,57	0,56	0,46
123	0,1280	0,0892	0,0714	0,0208	2,94E+03	2,68E+03	6,27E+02	5,91E+02	0,59	0,56	0,56	0,48
124	0,1230	0,0833	0,0667	0,0249	2,83E+03	2,76E+03	6,07E+02	6,07E+02	0,57	0,53	0,54	0,47
125	0,1270	0,0879	0,0703	0,0209	2,74E+03	2,76E+03	5,93E+02	6,02E+02	0,59	0,56	0,56	0,45
126	0,1190	0,0831	0,0653	0,0205	2,71E+03	2,60E+03	5,88E+02	5,78E+02	0,59	0,56	0,55	0,45
127	0,1080	0,0765	0,0544	0,0235	2,91E+03	2,95E+03	6,30E+02	6,31E+02	0,53	0,47	0,51	0,47
128	0,1070	0,0761	0,0566	0,0210	2,87E+03	2,78E+03	6,22E+02	5,99E+02	0,58	0,53	0,54	0,48
129	0,1060	0,0768	0,0543	0,0224	2,85E+03	2,78E+03	6,18E+02	5,99E+02	0,57	0,52	0,54	0,49
130	0,1020	0,0741	0,0504	0,0199	2,76E+03	2,93E+03	5,99E+02	6,28E+02	0,55	0,48	0,53	0,46
131	0,1010	0,0718	0,0537	0,0182	2,83E+03	2,70E+03	6,10E+02	5,87E+02	0,62	0,56	0,56	0,46
132	0,1090	0,0786	0,0572	0,0194	2,98E+03	2,79E+03	6,35E+02	6,00E+02	0,59	0,53	0,56	0,48
133	0,1040	0,0779	0,0485	0,0211	3,08E+03	2,98E+03	6,52E+02	6,37E+02	0,53	0,46	0,51	0,49
134	0,1100	0,0829	0,0539	0,0180	2,81E+03	2,86E+03	6,06E+02	6,14E+02	0,56	0,50	0,55	0,49
135	0,1020	0,0742	0,0525	0,0200	2,81E+03	2,62E+03	6,04E+02	5,75E+02	0,58	0,52	0,54	0,45
136	0,1080	0,0809	0,0515	0,0205	2,90E+03	2,92E+03	6,29E+02	6,26E+02	0,51	0,44	0,51	0,49
137	0,1170	0,0879	0,0585	0,0180	2,92E+03	2,95E+03	6,31E+02	6,26E+02	0,53	0,47	0,53	0,48
138	0,1090	0,0810	0,0556	0,0212	2,85E+03	2,82E+03	6,18E+02	6,07E+02	0,55	0,49	0,53	0,49
139	0,1170	0,0896	0,0550	0,0188	2,90E+03	2,95E+03	6,23E+02	6,33E+02	0,52	0,45	0,51	0,49
140	0,1190	0,0917	0,0600	0,0155	2,95E+03	2,88E+03	6,31E+02	6,16E+02	0,56	0,50	0,54	0,49
141	0,1150	0,0876	0,0571	0,0195	2,95E+03	2,71E+03	6,31E+02	5,90E+02	0,57	0,52	0,54	0,48
142	0,1260	0,0948	0,0608	0,0234	3,19E+03	2,91E+03	6,71E+02	6,26E+02	0,53	0,45	0,52	0,51
143	0,1210	0,0934	0,0595	0,0184	2,91E+03	2,93E+03	6,24E+02	6,23E+02	0,54	0,49	0,53	0,51
144	0,1220	0,0938	0,0581	0,0188	2,99E+03	2,81E+03	6,38E+02	6,04E+02	0,53	0,47	0,52	0,49
145	0,1210	0,0848	0,0689	0,0227	2,88E+03	2,89E+03	6,26E+02	6,22E+02	0,56	0,48	0,54	0,48
146	0,1240	0,0889	0,0699	0,0195	2,86E+03	2,86E+03	6,20E+02	6,13E+02	0,57	0,51	0,55	0,50

Evaluation Run CFD	AvMagoa [m/s]	Avxoa [m/s]	Avyoa [m/s]	Avzoa [m/s]	Thrust RR1 [N]	Thrust RR2 [N]	Torque RR1 [Nm]	Torque RR2 [Nm]	Uniformity VelMag_oa [-]	Uniformity Velx_oa [-]	Uniformity Vely_oa [-]	Uniformity Velz_oa [-]
147	0,1110	0,0807	0,0611	0,0211	2,84E+03	2,72E+03	6,18E+02	5,92E+02	0,57	0,51	0,54	0,51
148	0,1320	0,0955	0,0728	0,0199	3,15E+03	2,93E+03	6,67E+02	6,31E+02	0,57	0,50	0,54	0,50
149	0,1320	0,0982	0,0721	0,0165	3,00E+03	2,95E+03	6,38E+02	6,30E+02	0,59	0,54	0,56	0,50
150	0,1190	0,0888	0,0642	0,0187	3,24E+03	2,88E+03	6,86E+02	6,16E+02	0,59	0,55	0,55	0,52
151	0,1370	0,0975	0,0752	0,0232	2,95E+03	2,94E+03	6,32E+02	6,35E+02	0,56	0,48	0,53	0,51
152	0,1290	0,0951	0,0708	0,0190	2,78E+03	2,97E+03	6,03E+02	6,35E+02	0,57	0,51	0,54	0,53
153	0,1320	0,0966	0,0715	0,0200	2,74E+03	2,83E+03	5,96E+02	6,10E+02	0,57	0,51	0,54	0,52
154	0,1140	0,0765	0,0683	0,0248	2,82E+03	2,85E+03	6,16E+02	6,18E+02	0,59	0,55	0,56	0,47
155	0,1210	0,0841	0,0720	0,0201	2,90E+03	2,88E+03	6,28E+02	6,21E+02	0,60	0,56	0,57	0,48
156	0,1190	0,0824	0,0704	0,0219	2,87E+03	2,75E+03	6,23E+02	5,98E+02	0,60	0,55	0,56	0,51
157	0,1180	0,0808	0,0711	0,0210	2,88E+03	2,87E+03	6,21E+02	6,21E+02	0,60	0,56	0,55	0,48
158	0,0983	0,0691	0,0562	0,0162	2,87E+03	2,79E+03	6,23E+02	6,04E+02	0,63	0,61	0,56	0,44
159	0,1340	0,0947	0,0792	0,0190	2,98E+03	2,86E+03	6,36E+02	6,17E+02	0,60	0,56	0,57	0,52
160	0,1300	0,0883	0,0786	0,0224	3,02E+03	2,87E+03	6,42E+02	6,22E+02	0,59	0,54	0,55	0,50
161	0,1390	0,0976	0,0822	0,0194	2,96E+03	2,85E+03	6,32E+02	6,16E+02	0,60	0,55	0,56	0,53
162	0,1420	0,0989	0,0832	0,0215	2,91E+03	2,87E+03	6,24E+02	6,19E+02	0,59	0,53	0,56	0,53
163	0,1240	0,0793	0,0782	0,0244	2,97E+03	2,83E+03	6,41E+02	6,17E+02	0,59	0,54	0,56	0,49
164	0,1340	0,0876	0,0833	0,0207	2,94E+03	2,82E+03	6,34E+02	6,13E+02	0,60	0,54	0,56	0,50
165	0,1160	0,0779	0,0692	0,0230	2,83E+03	2,76E+03	6,20E+02	5,99E+02	0,61	0,58	0,56	0,49
166	0,1390	0,0917	0,0868	0,0225	3,14E+03	2,83E+03	6,62E+02	6,17E+02	0,61	0,56	0,57	0,50
167	0,1420	0,0963	0,0873	0,0181	3,00E+03	2,84E+03	6,39E+02	6,15E+02	0,61	0,57	0,57	0,51
168	0,1240	0,0852	0,0749	0,0191	2,87E+03	2,83E+03	6,18E+02	6,11E+02	0,62	0,59	0,57	0,50
169	0,1370	0,0898	0,0857	0,0234	2,79E+03	2,85E+03	6,05E+02	6,22E+02	0,59	0,54	0,56	0,50
170	0,1410	0,0945	0,0866	0,0202	2,82E+03	2,80E+03	6,09E+02	6,08E+02	0,61	0,56	0,57	0,51
171	0,1430	0,0952	0,0887	0,0216	3,05E+03	2,74E+03	6,46E+02	5,99E+02	0,61	0,56	0,57	0,52
172	0,1230	0,0783	0,0763	0,0254	2,92E+03	2,73E+03	6,30E+02	6,00E+02	0,59	0,55	0,56	0,49

Evaluation Run CFD	AvMagoa [m/s]	Avxoa [m/s]	Avyoa [m/s]	Avzoa [m/s]	Thrust RR1 [N]	Thrust RR2 [N]	Torque RR1 [Nm]	Torque RR2 [Nm]	Uniformity VelMag_oa [-]	Uniformity Velx_oa [-]	Uniformity Vely_oa [-]	Uniformity Velz_oa [-]
173	0,1320	0,0861	0,0818	0,0217	2,96E+03	2,71E+03	6,38E+02	5,94E+02	0,61	0,56	0,57	0,48
174	0,1330	0,0860	0,0828	0,0234	2,90E+03	2,71E+03	6,27E+02	5,94E+02	0,61	0,56	0,57	0,50
175	0,1370	0,0894	0,0849	0,0227	3,04E+03	2,78E+03	6,45E+02	6,11E+02	0,60	0,57	0,57	0,49
176	0,1380	0,0925	0,0850	0,0191	2,91E+03	2,80E+03	6,23E+02	6,08E+02	0,62	0,58	0,58	0,49
177	0,1450	0,0961	0,0898	0,0209	3,03E+03	2,68E+03	6,43E+02	5,90E+02	0,62	0,57	0,58	0,50
178	0,1270	0,0840	0,0764	0,0237	2,82E+03	2,79E+03	6,06E+02	6,11E+02	0,60	0,57	0,56	0,47
179	0,1400	0,0931	0,0846	0,0205	2,91E+03	2,73E+03	6,22E+02	5,98E+02	0,61	0,57	0,57	0,49
180	0,1390	0,0921	0,0847	0,0210	2,90E+03	2,70E+03	6,20E+02	5,92E+02	0,61	0,57	0,57	0,51
181	0,1260	0,0808	0,0767	0,0248	2,95E+03	2,75E+03	6,36E+02	6,05E+02	0,58	0,54	0,56	0,48
182	0,1290	0,0859	0,0777	0,0228	2,88E+03	2,77E+03	6,26E+02	6,01E+02	0,61	0,58	0,57	0,46
183	0,1300	0,0852	0,0791	0,0240	2,87E+03	2,66E+03	6,22E+02	5,87E+02	0,60	0,57	0,56	0,49
184	0,1290	0,0853	0,0774	0,0225	2,79E+03	2,78E+03	6,03E+02	6,09E+02	0,61	0,58	0,57	0,48
185	0,1340	0,0914	0,0797	0,0187	3,10E+03	2,77E+03	6,56E+02	6,02E+02	0,62	0,60	0,58	0,48
186	0,1170	0,0812	0,0679	0,0195	2,87E+03	2,56E+03	6,14E+02	5,70E+02	0,62	0,60	0,57	0,47
187	0,1350	0,0881	0,0814	0,0242	2,75E+03	2,73E+03	5,98E+02	6,04E+02	0,60	0,56	0,57	0,48
188	0,1360	0,0918	0,0811	0,0202	2,78E+03	2,72E+03	6,01E+02	5,96E+02	0,61	0,57	0,57	0,48
189	0,1280	0,0881	0,0740	0,0218	2,93E+03	2,72E+03	6,26E+02	5,96E+02	0,61	0,58	0,57	0,48
190	0,1060	0,0737	0,0566	0,0226	2,87E+03	2,92E+03	6,24E+02	6,26E+02	0,54	0,48	0,52	0,47
191	0,1090	0,0753	0,0605	0,0208	2,89E+03	2,81E+03	6,27E+02	6,05E+02	0,58	0,54	0,55	0,47
192	0,1140	0,0784	0,0633	0,0233	2,93E+03	2,65E+03	6,34E+02	5,80E+02	0,58	0,53	0,54	0,47
193	0,1070	0,0765	0,0548	0,0202	2,87E+03	2,91E+03	6,19E+02	6,25E+02	0,56	0,49	0,53	0,47
194	0,1140	0,0832	0,0603	0,0172	2,90E+03	2,88E+03	6,23E+02	6,16E+02	0,59	0,53	0,55	0,48
195	0,1130	0,0807	0,0609	0,0203	2,92E+03	2,76E+03	6,26E+02	5,95E+02	0,59	0,54	0,55	0,48
196	0,1100	0,0798	0,0543	0,0226	2,91E+03	2,96E+03	6,26E+02	6,34E+02	0,54	0,48	0,51	0,49
197	0,1140	0,0827	0,0600	0,0189	2,95E+03	2,92E+03	6,31E+02	6,22E+02	0,58	0,53	0,55	0,50
198	0,1100	0,0778	0,0598	0,0215	2,84E+03	2,56E+03	6,11E+02	5,67E+02	0,59	0,54	0,55	0,47

Evaluation Run CFD	AvMagoa [m/s]	Avxoa [m/s]	Avyoa [m/s]	Avzoa [m/s]	Thrust RR1 [N]	Thrust RR2 [N]	Torque RR1 [Nm]	Torque RR2 [Nm]	Uniformity VelMag_oa [-]	Uniformity Velx_oa [-]	Uniformity Vely_oa [-]	Uniformity Velz_oa [-]
199	0,1170	0,0816	0,0634	0,0218	2,90E+03	2,93E+03	6,31E+02	6,28E+02	0,53	0,45	0,51	0,49
200	0,1210	0,0847	0,0681	0,0192	2,89E+03	2,92E+03	6,29E+02	6,22E+02	0,55	0,49	0,53	0,47
201	0,1200	0,0843	0,0670	0,0228	2,89E+03	2,70E+03	6,29E+02	5,86E+02	0,55	0,50	0,53	0,48
202	0,1160	0,0848	0,0600	0,0194	2,84E+03	2,95E+03	6,13E+02	6,31E+02	0,55	0,48	0,52	0,50
203	0,1230	0,0902	0,0667	0,0161	2,92E+03	2,93E+03	6,28E+02	6,23E+02	0,57	0,52	0,55	0,49
204	0,1220	0,0893	0,0651	0,0198	2,98E+03	2,69E+03	6,38E+02	5,85E+02	0,58	0,53	0,55	0,48
205	0,1240	0,0889	0,0650	0,0223	2,91E+03	2,95E+03	6,27E+02	6,33E+02	0,54	0,47	0,52	0,51
206	0,1290	0,0939	0,0702	0,0195	2,81E+03	2,92E+03	6,10E+02	6,22E+02	0,56	0,51	0,54	0,52
207	0,1250	0,0914	0,0666	0,0202	2,86E+03	2,78E+03	6,17E+02	6,00E+02	0,56	0,51	0,53	0,49
208	0,1310	0,0848	0,0815	0,0250	2,92E+03	2,88E+03	6,34E+02	6,22E+02	0,57	0,49	0,55	0,49
209	0,1290	0,0880	0,0787	0,0206	2,86E+03	2,86E+03	6,23E+02	6,14E+02	0,60	0,55	0,56	0,49
210	0,1270	0,0868	0,0763	0,0218	2,92E+03	2,77E+03	6,34E+02	5,98E+02	0,59	0,53	0,55	0,50
211	0,1410	0,0959	0,0838	0,0215	2,96E+03	2,91E+03	6,38E+02	6,28E+02	0,59	0,52	0,55	0,51
212	0,1410	0,0994	0,0838	0,0172	2,96E+03	2,90E+03	6,35E+02	6,22E+02	0,60	0,55	0,56	0,52
213	0,1360	0,0965	0,0795	0,0197	3,02E+03	2,74E+03	6,45E+02	5,95E+02	0,60	0,55	0,56	0,53
214	0,1370	0,0921	0,0823	0,0230	3,03E+03	2,91E+03	6,47E+02	6,27E+02	0,59	0,51	0,55	0,52
215	0,1390	0,0960	0,0829	0,0201	2,76E+03	2,84E+03	6,01E+02	6,11E+02	0,60	0,54	0,56	0,53
216	0,1430	0,0992	0,0838	0,0209	2,89E+03	2,75E+03	6,24E+02	5,96E+02	0,59	0,53	0,56	0,53
217	0,1310	0,0807	0,0870	0,0255	2,90E+03	2,85E+03	6,30E+02	6,20E+02	0,59	0,54	0,56	0,49
218	0,1280	0,0842	0,0823	0,0208	2,89E+03	2,87E+03	6,27E+02	6,17E+02	0,62	0,58	0,58	0,50
219	0,1300	0,0850	0,0833	0,0228	2,96E+03	2,79E+03	6,40E+02	6,03E+02	0,61	0,57	0,57	0,50
220	0,1360	0,0881	0,0880	0,0226	2,88E+03	2,85E+03	6,19E+02	6,19E+02	0,62	0,57	0,57	0,50
221	0,1420	0,0968	0,0890	0,0184	3,06E+03	2,81E+03	6,54E+02	6,08E+02	0,63	0,59	0,58	0,52
222	0,1430	0,0953	0,0899	0,0200	2,92E+03	2,74E+03	6,29E+02	5,97E+02	0,63	0,58	0,58	0,53
223	0,1410	0,0908	0,0913	0,0238	2,73E+03	2,88E+03	5,96E+02	6,26E+02	0,61	0,55	0,57	0,52
224	0,1440	0,0967	0,0901	0,0199	2,81E+03	2,78E+03	6,09E+02	6,04E+02	0,62	0,58	0,57	0,53

Evaluation Run CFD	AvMagoa [m/s]	Avxoa [m/s]	Avyoa [m/s]	Avzoa [m/s]	Thrust RR1 [N]	Thrust RR2 [N]	Torque RR1 [Nm]	Torque RR2 [Nm]	Uniformity VelMag_oa [-]	Uniformity Velx_oa [-]	Uniformity Vely_oa [-]	Uniformity Velz_oa [-]
225	0,1370	0,0919	0,0851	0,0212	2,74E+03	2,77E+03	5,97E+02	6,02E+02	0,62	0,56	0,57	0,53
226	0,1320	0,0795	0,0894	0,0265	2,93E+03	2,85E+03	6,35E+02	6,20E+02	0,60	0,55	0,57	0,49
227	0,1370	0,0859	0,0907	0,0220	2,89E+03	2,78E+03	6,28E+02	6,05E+02	0,62	0,58	0,58	0,50
228	0,1370	0,0863	0,0905	0,0226	2,94E+03	2,73E+03	6,37E+02	5,97E+02	0,62	0,58	0,58	0,49
229	0,1300	0,0838	0,0842	0,0213	2,96E+03	2,82E+03	6,35E+02	6,14E+02	0,63	0,60	0,58	0,49
230	0,1510	0,0984	0,0984	0,0192	3,02E+03	2,86E+03	6,47E+02	6,19E+02	0,64	0,60	0,59	0,52
231	0,1510	0,0977	0,0979	0,0202	3,06E+03	2,70E+03	6,52E+02	5,92E+02	0,64	0,60	0,59	0,51
232	0,1320	0,0830	0,0867	0,0232	2,80E+03	2,82E+03	6,06E+02	6,16E+02	0,61	0,57	0,57	0,49
233	0,1490	0,0967	0,0960	0,0209	2,91E+03	2,83E+03	6,24E+02	6,13E+02	0,64	0,60	0,58	0,51
234	0,1470	0,0951	0,0951	0,0230	3,00E+03	2,74E+03	6,41E+02	5,98E+02	0,63	0,59	0,58	0,53
235	0,1310	0,0782	0,0871	0,0273	2,86E+03	2,82E+03	6,23E+02	6,16E+02	0,60	0,57	0,57	0,49
236	0,1370	0,0846	0,0900	0,0230	2,90E+03	2,75E+03	6,30E+02	5,99E+02	0,62	0,59	0,58	0,49
237	0,1370	0,0846	0,0895	0,0237	2,92E+03	2,70E+03	6,32E+02	5,92E+02	0,62	0,59	0,58	0,48
238	0,1420	0,0891	0,0924	0,0236	2,93E+03	2,79E+03	6,30E+02	6,11E+02	0,62	0,59	0,58	0,50
239	0,1510	0,0968	0,0983	0,0207	2,94E+03	2,71E+03	6,31E+02	5,94E+02	0,64	0,61	0,59	0,50
240	0,1480	0,0943	0,0955	0,0214	2,81E+03	2,66E+03	6,09E+02	5,85E+02	0,64	0,61	0,59	0,50
241	0,1340	0,0851	0,0846	0,0254	2,78E+03	2,73E+03	6,03E+02	6,01E+02	0,62	0,59	0,57	0,49
242	0,1450	0,0928	0,0925	0,0208	2,83E+03	2,72E+03	6,11E+02	5,97E+02	0,64	0,61	0,58	0,49
243	0,1470	0,0917	0,0960	0,0228	2,73E+03	2,68E+03	5,97E+02	5,91E+02	0,63	0,58	0,58	0,52
244	0,1270	0,0778	0,0819	0,0264	2,90E+03	2,78E+03	6,30E+02	6,10E+02	0,60	0,58	0,57	0,48
245	0,1250	0,0792	0,0797	0,0219	2,88E+03	2,74E+03	6,25E+02	5,98E+02	0,62	0,60	0,57	0,46
246	0,1230	0,0785	0,0785	0,0224	2,89E+03	2,67E+03	6,27E+02	5,88E+02	0,62	0,59	0,57	0,46
247	0,1320	0,0852	0,0827	0,0231	2,81E+03	2,76E+03	6,08E+02	6,07E+02	0,62	0,60	0,58	0,48
248	0,1290	0,0860	0,0791	0,0187	2,89E+03	2,72E+03	6,23E+02	5,95E+02	0,64	0,62	0,58	0,47
249	0,1320	0,0865	0,0824	0,0202	2,89E+03	2,61E+03	6,21E+02	5,78E+02	0,64	0,61	0,58	0,48
250	0,1340	0,0856	0,0836	0,0241	2,74E+03	2,74E+03	5,97E+02	6,05E+02	0,62	0,59	0,58	0,48

Evaluation Run CFD	AvMagoa [m/s]	Avxoa [m/s]	Avyoa [m/s]	Avzoa [m/s]	Thrust RR1 [N]	Thrust RR2 [N]	Torque RR1 [Nm]	Torque RR2 [Nm]	Uniformity VelMag_oa [-]	Uniformity Velx_oa [-]	Uniformity Vely_oa [-]	Uniformity Velz_oa [-]
251	0,1380	0,0903	0,0862	0,0203	2,74E+03	2,70E+03	5,96E+02	5,93E+02	0,63	0,60	0,58	0,48
252	0,1420	0,0919	0,0897	0,0229	2,86E+03	2,64E+03	6,18E+02	5,83E+02	0,63	0,60	0,58	0,51
253	0,1060	0,0673	0,0604	0,0264	2,83E+03	2,69E+03	6,17E+02	5,92E+02	0,60	0,56	0,54	0,44
254	0,1070	0,0732	0,0595	0,0198	2,88E+03	2,92E+03	6,24E+02	6,21E+02	0,59	0,55	0,55	0,44
255	0,1070	0,0727	0,0588	0,0225	2,88E+03	2,80E+03	6,25E+02	6,02E+02	0,59	0,55	0,54	0,46
256	0,1120	0,0778	0,0593	0,0191	2,96E+03	2,97E+03	6,33E+02	6,36E+02	0,56	0,51	0,52	0,45
257	0,1150	0,0802	0,0636	0,0182	2,96E+03	2,85E+03	6,33E+02	6,12E+02	0,61	0,56	0,56	0,46
258	0,1150	0,0806	0,0619	0,0207	2,82E+03	2,80E+03	6,09E+02	6,02E+02	0,59	0,55	0,55	0,47
259	0,1100	0,0755	0,0591	0,0227	2,86E+03	2,91E+03	6,17E+02	6,26E+02	0,57	0,52	0,53	0,48
260	0,1160	0,0823	0,0616	0,0194	2,84E+03	2,90E+03	6,14E+02	6,18E+02	0,60	0,55	0,55	0,48
261	0,1110	0,0768	0,0618	0,0206	2,86E+03	2,71E+03	6,16E+02	5,87E+02	0,60	0,55	0,55	0,45
262	0,1160	0,0794	0,0646	0,0226	2,88E+03	2,92E+03	6,26E+02	6,27E+02	0,55	0,49	0,53	0,48
263	0,1210	0,0833	0,0703	0,0200	2,88E+03	2,91E+03	6,27E+02	6,22E+02	0,57	0,52	0,54	0,47
264	0,1220	0,0829	0,0699	0,0233	2,90E+03	2,80E+03	6,30E+02	6,03E+02	0,57	0,52	0,54	0,46
265	0,1270	0,0876	0,0710	0,0204	2,88E+03	2,96E+03	6,23E+02	6,34E+02	0,56	0,49	0,53	0,50
266	0,1330	0,0928	0,0769	0,0175	2,92E+03	2,96E+03	6,30E+02	6,29E+02	0,58	0,53	0,55	0,49
267	0,1310	0,0922	0,0739	0,0199	2,92E+03	2,89E+03	6,28E+02	6,18E+02	0,58	0,53	0,55	0,48
268	0,1300	0,0895	0,0730	0,0226	2,86E+03	2,95E+03	6,21E+02	6,33E+02	0,56	0,49	0,53	0,50
269	0,1300	0,0911	0,0739	0,0197	2,77E+03	2,92E+03	6,04E+02	6,23E+02	0,58	0,54	0,56	0,50
270	0,1340	0,0937	0,0752	0,0205	2,91E+03	2,90E+03	6,28E+02	6,18E+02	0,57	0,52	0,54	0,49
271	0,1320	0,0834	0,0842	0,0259	2,85E+03	2,89E+03	6,24E+02	6,23E+02	0,58	0,52	0,55	0,49
272	0,1370	0,0902	0,0856	0,0219	2,87E+03	2,92E+03	6,26E+02	6,24E+02	0,60	0,55	0,57	0,50
273	0,1360	0,0887	0,0838	0,0245	2,86E+03	2,80E+03	6,24E+02	6,06E+02	0,59	0,54	0,56	0,49
274	0,1420	0,0920	0,0884	0,0223	2,91E+03	2,94E+03	6,31E+02	6,32E+02	0,60	0,53	0,56	0,51
275	0,1470	0,0997	0,0912	0,0187	2,88E+03	3,06E+03	6,23E+02	6,49E+02	0,61	0,57	0,57	0,51
276	0,1450	0,0977	0,0886	0,0221	2,78E+03	2,85E+03	6,05E+02	6,13E+02	0,61	0,56	0,57	0,51

Evaluation Run CFD	AvMagoa [m/s]	Avxoa [m/s]	Avyoa [m/s]	Avzoa [m/s]	Thrust RR1 [N]	Thrust RR2 [N]	Torque RR1 [Nm]	Torque RR2 [Nm]	Uniformity VelMag_oa [-]	Uniformity Velx_oa [-]	Uniformity Vely_oa [-]	Uniformity Velz_oa [-]
277	0,1380	0,0898	0,0858	0,0234	2,77E+03	2,91E+03	6,05E+02	6,28E+02	0,60	0,54	0,56	0,50
278	0,1500	0,1010	0,0932	0,0197	2,90E+03	2,96E+03	6,27E+02	6,32E+02	0,61	0,56	0,57	0,52
279	0,1390	0,0938	0,0847	0,0210	2,96E+03	2,76E+03	6,35E+02	5,98E+02	0,61	0,56	0,57	0,52
280	0,1340	0,0804	0,0908	0,0271	2,85E+03	2,87E+03	6,22E+02	6,23E+02	0,60	0,55	0,57	0,50
281	0,1410	0,0889	0,0928	0,0232	2,90E+03	3,02E+03	6,30E+02	6,44E+02	0,63	0,59	0,58	0,51
282	0,1410	0,0880	0,0930	0,0243	2,86E+03	2,77E+03	6,26E+02	6,01E+02	0,62	0,57	0,58	0,49
283	0,1420	0,0882	0,0947	0,0228	2,90E+03	2,89E+03	6,27E+02	6,26E+02	0,62	0,57	0,58	0,51
284	0,1430	0,0947	0,0918	0,0198	2,94E+03	2,79E+03	6,30E+02	6,05E+02	0,65	0,62	0,59	0,50
285	0,1370	0,0908	0,0861	0,0216	2,80E+03	2,77E+03	6,07E+02	6,00E+02	0,64	0,60	0,58	0,50
286	0,1380	0,0863	0,0914	0,0228	2,77E+03	2,87E+03	6,02E+02	6,23E+02	0,62	0,58	0,58	0,49
287	0,1440	0,0945	0,0930	0,0204	2,80E+03	2,78E+03	6,08E+02	6,04E+02	0,64	0,60	0,58	0,51
288	0,1380	0,0907	0,0879	0,0213	2,76E+03	2,70E+03	6,00E+02	5,90E+02	0,63	0,60	0,58	0,52
289	0,1350	0,0791	0,0919	0,0276	2,88E+03	2,88E+03	6,26E+02	6,26E+02	0,61	0,57	0,57	0,49
290	0,1440	0,0883	0,0975	0,0234	2,90E+03	2,92E+03	6,31E+02	6,28E+02	0,63	0,60	0,59	0,50
291	0,1420	0,0866	0,0952	0,0232	2,93E+03	2,70E+03	6,36E+02	5,91E+02	0,62	0,59	0,58	0,48
292	0,1450	0,0880	0,0980	0,0236	2,90E+03	2,84E+03	6,25E+02	6,19E+02	0,63	0,60	0,59	0,50
293	0,1510	0,0952	0,1000	0,0205	2,83E+03	2,92E+03	6,13E+02	6,28E+02	0,65	0,62	0,59	0,51
294	0,1500	0,0944	0,0996	0,0215	2,95E+03	2,80E+03	6,34E+02	6,07E+02	0,65	0,62	0,59	0,49
295	0,1360	0,0841	0,0902	0,0231	2,94E+03	2,84E+03	6,31E+02	6,18E+02	0,63	0,61	0,58	0,47
296	0,1470	0,0937	0,0971	0,0203	2,75E+03	2,84E+03	5,99E+02	6,14E+02	0,65	0,62	0,59	0,49
297	0,1580	0,0980	0,1060	0,0242	2,85E+03	2,94E+03	6,18E+02	6,31E+02	0,65	0,60	0,60	0,53
298	0,1310	0,0765	0,0872	0,0283	2,83E+03	2,80E+03	6,19E+02	6,12E+02	0,61	0,59	0,57	0,48
299	0,1420	0,0849	0,0948	0,0240	2,86E+03	2,74E+03	6,23E+02	6,00E+02	0,63	0,60	0,58	0,49
300	0,1310	0,0795	0,0872	0,0227	2,86E+03	2,69E+03	6,24E+02	5,90E+02	0,63	0,61	0,58	0,45
301	0,1300	0,0804	0,0841	0,0235	2,80E+03	2,78E+03	6,06E+02	6,10E+02	0,63	0,62	0,58	0,48
302	0,1460	0,0915	0,0961	0,0201	2,86E+03	2,74E+03	6,19E+02	6,00E+02	0,65	0,63	0,59	0,50

Evaluation Run CFD	AvMagoa [m/s]	Avxoa [m/s]	Avyoa [m/s]	Avzoa [m/s]	Thrust RR1 [N]	Thrust RR2 [N]	Torque RR1 [Nm]	Torque RR2 [Nm]	Uniformity VelMag_oa [-]	Uniformity Velx_oa [-]	Uniformity Vely_oa [-]	Uniformity Velz_oa [-]
303	0,1430	0,0893	0,0945	0,0201	2,82E+03	2,66E+03	6,10E+02	5,87E+02	0,65	0,62	0,59	0,47
304	0,1460	0,0877	0,0977	0,0249	2,82E+03	2,79E+03	6,12E+02	6,12E+02	0,63	0,60	0,59	0,47
305	0,1500	0,0927	0,0995	0,0216	2,72E+03	2,72E+03	5,95E+02	5,96E+02	0,64	0,61	0,59	0,47
306	0,1510	0,0922	0,1010	0,0239	2,84E+03	2,68E+03	6,15E+02	5,89E+02	0,64	0,60	0,59	0,52
307	0,1310	0,0780	0,0855	0,0275	2,87E+03	2,77E+03	6,24E+02	6,08E+02	0,61	0,59	0,57	0,48
308	0,1320	0,0810	0,0855	0,0238	2,88E+03	2,72E+03	6,25E+02	5,95E+02	0,63	0,61	0,58	0,47
309	0,1290	0,0794	0,0832	0,0240	2,89E+03	2,68E+03	6,29E+02	5,89E+02	0,62	0,61	0,57	0,45
310	0,1390	0,0861	0,0906	0,0238	2,91E+03	2,74E+03	6,27E+02	6,04E+02	0,64	0,61	0,59	0,48
311	0,1370	0,0868	0,0874	0,0206	2,77E+03	2,76E+03	6,02E+02	6,02E+02	0,65	0,63	0,59	0,46
312	0,1330	0,0851	0,0846	0,0202	2,84E+03	2,66E+03	6,14E+02	5,84E+02	0,64	0,63	0,58	0,46
313	0,1270	0,0797	0,0800	0,0233	2,73E+03	2,78E+03	5,95E+02	6,09E+02	0,63	0,61	0,57	0,46
314	0,1480	0,0923	0,0968	0,0210	2,83E+03	2,73E+03	6,13E+02	5,99E+02	0,64	0,61	0,59	0,46
315	0,1370	0,0861	0,0879	0,0222	2,81E+03	2,65E+03	6,10E+02	5,85E+02	0,64	0,62	0,58	0,49
316	0,1110	0,0748	0,0582	0,0226	2,82E+03	2,92E+03	6,16E+02	6,27E+02	0,54	0,50	0,51	0,44
317	0,1100	0,0742	0,0599	0,0206	2,87E+03	2,89E+03	6,23E+02	6,16E+02	0,59	0,56	0,55	0,44
318	0,1120	0,0730	0,0618	0,0247	2,84E+03	2,72E+03	6,19E+02	5,90E+02	0,59	0,56	0,54	0,45
319	0,1140	0,0781	0,0607	0,0201	2,82E+03	2,92E+03	6,09E+02	6,27E+02	0,57	0,52	0,53	0,44
320	0,1190	0,0824	0,0648	0,0180	2,75E+03	2,67E+03	5,99E+02	5,83E+02	0,61	0,57	0,56	0,45
321	0,1100	0,0748	0,0606	0,0203	2,94E+03	2,69E+03	6,27E+02	5,85E+02	0,61	0,58	0,56	0,45
322	0,1130	0,0765	0,0602	0,0235	2,78E+03	2,88E+03	6,03E+02	6,20E+02	0,57	0,53	0,53	0,48
323	0,1200	0,0835	0,0651	0,0202	2,75E+03	2,94E+03	5,97E+02	6,25E+02	0,60	0,56	0,56	0,48
324	0,1130	0,0779	0,0614	0,0202	2,75E+03	2,72E+03	5,97E+02	5,92E+02	0,60	0,57	0,56	0,45
325	0,1230	0,0813	0,0692	0,0247	2,80E+03	2,93E+03	6,13E+02	6,27E+02	0,55	0,50	0,53	0,48
326	0,1250	0,0848	0,0710	0,0225	2,77E+03	2,84E+03	6,09E+02	6,08E+02	0,58	0,55	0,55	0,47
327	0,1270	0,0855	0,0715	0,0243	2,82E+03	2,87E+03	6,17E+02	6,13E+02	0,56	0,52	0,54	0,47
328	0,1340	0,0897	0,0758	0,0222	2,71E+03	2,95E+03	5,95E+02	6,30E+02	0,57	0,51	0,54	0,49

Evaluation Run CFD	AvMagoa [m/s]	Avxoa [m/s]	Avyoa [m/s]	Avzoa [m/s]	Thrust RR1 [N]	Thrust RR2 [N]	Torque RR1 [Nm]	Torque RR2 [Nm]	Uniformity VelMag_oa [-]	Uniformity Velx_oa [-]	Uniformity Vely_oa [-]	Uniformity Velz_oa [-]
329	0,1280	0,0878	0,0732	0,0174	2,81E+03	2,93E+03	6,10E+02	6,23E+02	0,59	0,55	0,56	0,47
330	0,1330	0,0911	0,0753	0,0215	2,81E+03	2,73E+03	6,08E+02	5,91E+02	0,58	0,54	0,55	0,47
331	0,1280	0,0856	0,0717	0,0227	2,69E+03	2,96E+03	5,91E+02	6,32E+02	0,56	0,50	0,53	0,48
332	0,1270	0,0873	0,0723	0,0190	2,83E+03	2,92E+03	6,12E+02	6,21E+02	0,59	0,55	0,56	0,49
333	0,1300	0,0897	0,0737	0,0211	2,78E+03	2,76E+03	6,02E+02	5,97E+02	0,59	0,55	0,55	0,47
334	0,1330	0,0834	0,0830	0,0267	2,77E+03	2,89E+03	6,09E+02	6,23E+02	0,59	0,54	0,56	0,49
335	0,1420	0,0927	0,0881	0,0234	2,80E+03	2,99E+03	6,14E+02	6,36E+02	0,61	0,57	0,57	0,50
336	0,1380	0,0896	0,0854	0,0258	2,77E+03	2,73E+03	6,11E+02	5,93E+02	0,60	0,57	0,57	0,49
337	0,1430	0,0906	0,0894	0,0231	2,89E+03	2,89E+03	6,25E+02	6,24E+02	0,60	0,55	0,57	0,50
338	0,1530	0,1010	0,0949	0,0202	2,83E+03	3,06E+03	6,15E+02	6,48E+02	0,62	0,57	0,58	0,51
339	0,1480	0,0978	0,0914	0,0201	2,82E+03	2,75E+03	6,14E+02	5,98E+02	0,61	0,57	0,57	0,50
340	0,1340	0,0863	0,0835	0,0221	2,70E+03	2,95E+03	5,94E+02	6,34E+02	0,59	0,54	0,56	0,49
341	0,1490	0,0988	0,0920	0,0201	2,72E+03	3,04E+03	5,97E+02	6,45E+02	0,61	0,57	0,58	0,50
342	0,1420	0,0939	0,0874	0,0215	2,79E+03	2,82E+03	6,07E+02	6,08E+02	0,61	0,57	0,57	0,51
343	0,1370	0,0812	0,0909	0,0285	2,84E+03	2,85E+03	6,20E+02	6,19E+02	0,60	0,57	0,57	0,49
344	0,1380	0,0867	0,0893	0,0239	2,82E+03	2,81E+03	6,17E+02	6,08E+02	0,62	0,60	0,58	0,50
345	0,1430	0,0890	0,0932	0,0245	2,80E+03	2,79E+03	6,14E+02	6,05E+02	0,62	0,58	0,58	0,49
346	0,1470	0,0898	0,0980	0,0241	2,83E+03	2,88E+03	6,15E+02	6,25E+02	0,62	0,58	0,58	0,50
347	0,1410	0,0917	0,0903	0,0196	2,83E+03	2,78E+03	6,13E+02	6,04E+02	0,64	0,62	0,59	0,49
348	0,1540	0,0978	0,1000	0,0205	2,88E+03	2,74E+03	6,22E+02	5,97E+02	0,64	0,60	0,59	0,50
349	0,1350	0,0837	0,0891	0,0226	2,72E+03	2,89E+03	5,94E+02	6,25E+02	0,62	0,59	0,58	0,48
350	0,1510	0,0960	0,0987	0,0205	2,74E+03	2,95E+03	5,99E+02	6,31E+02	0,64	0,60	0,59	0,50
351	0,1530	0,0960	0,1000	0,0232	2,83E+03	2,82E+03	6,15E+02	6,11E+02	0,63	0,58	0,59	0,53
352	0,1340	0,0785	0,0894	0,0284	2,85E+03	2,82E+03	6,21E+02	6,15E+02	0,61	0,59	0,57	0,49
353	0,1400	0,0852	0,0926	0,0239	2,79E+03	2,82E+03	6,12E+02	6,12E+02	0,63	0,61	0,58	0,49
354	0,1230	0,0773	0,0759	0,0240	2,74E+03	2,75E+03	6,05E+02	5,97E+02	0,64	0,64	0,57	0,45

Evaluation Run CFD	AvMagoa [m/s]	Avxoa [m/s]	Avyoa [m/s]	Avzoa [m/s]	Thrust RR1 [N]	Thrust RR2 [N]	Torque RR1 [Nm]	Torque RR2 [Nm]	Uniformity VelMag_oa [-]	Uniformity Velx_oa [-]	Uniformity Vely_oa [-]	Uniformity Velz_oa [-]
355	0,1410	0,0847	0,0942	0,0244	2,74E+03	2,85E+03	5,98E+02	6,21E+02	0,63	0,60	0,58	0,49
356	0,1430	0,0898	0,0942	0,0201	2,80E+03	2,82E+03	6,08E+02	6,10E+02	0,65	0,63	0,59	0,49
357	0,1590	0,0970	0,1070	0,0216	2,83E+03	2,73E+03	6,14E+02	5,97E+02	0,64	0,61	0,59	0,48
358	0,1380	0,0833	0,0921	0,0238	2,70E+03	2,84E+03	5,91E+02	6,19E+02	0,62	0,60	0,58	0,46
359	0,1540	0,0947	0,1020	0,0208	2,74E+03	2,92E+03	5,98E+02	6,28E+02	0,64	0,61	0,59	0,48
360	0,1430	0,0890	0,0943	0,0221	2,74E+03	2,69E+03	5,97E+02	5,91E+02	0,64	0,62	0,59	0,51
361	0,1350	0,0787	0,0882	0,0290	2,82E+03	2,80E+03	6,15E+02	6,11E+02	0,61	0,60	0,57	0,48
362	0,1490	0,0883	0,0986	0,0254	2,81E+03	2,77E+03	6,15E+02	6,04E+02	0,63	0,61	0,59	0,49
363	0,1420	0,0852	0,0937	0,0245	2,82E+03	2,63E+03	6,16E+02	5,81E+02	0,63	0,61	0,58	0,46
364	0,1440	0,0867	0,0948	0,0254	2,83E+03	2,79E+03	6,12E+02	6,12E+02	0,63	0,62	0,59	0,49
365	0,1490	0,0918	0,0977	0,0206	2,76E+03	2,70E+03	6,02E+02	5,94E+02	0,65	0,63	0,59	0,49
366	0,1470	0,0895	0,0969	0,0211	2,74E+03	2,70E+03	5,98E+02	5,92E+02	0,64	0,62	0,59	0,46
367	0,1330	0,0808	0,0863	0,0242	2,70E+03	2,80E+03	5,90E+02	6,11E+02	0,63	0,62	0,58	0,45
368	0,1520	0,0928	0,1000	0,0211	2,68E+03	2,73E+03	5,90E+02	5,98E+02	0,64	0,62	0,59	0,47
369	0,1460	0,0894	0,0955	0,0232	2,74E+03	2,65E+03	5,97E+02	5,83E+02	0,64	0,62	0,59	0,51
370	0,1320	0,0778	0,0846	0,0279	2,83E+03	2,80E+03	6,17E+02	6,12E+02	0,61	0,60	0,57	0,48
371	0,1330	0,0808	0,0845	0,0243	2,82E+03	2,75E+03	6,17E+02	6,01E+02	0,63	0,62	0,57	0,46
372	0,1300	0,0791	0,0825	0,0245	2,82E+03	2,66E+03	6,15E+02	5,85E+02	0,62	0,62	0,57	0,45
373	0,1390	0,0848	0,0892	0,0254	2,78E+03	2,80E+03	6,03E+02	6,12E+02	0,63	0,62	0,58	0,47
374	0,1510	0,0926	0,0974	0,0211	2,75E+03	2,72E+03	6,00E+02	5,98E+02	0,64	0,62	0,59	0,48
375	0,1320	0,0831	0,0835	0,0205	2,78E+03	2,61E+03	6,04E+02	5,77E+02	0,64	0,64	0,58	0,44
376	0,1430	0,0862	0,0921	0,0256	2,74E+03	2,75E+03	5,96E+02	6,06E+02	0,63	0,61	0,58	0,46
377	0,1450	0,0899	0,0933	0,0210	2,76E+03	2,73E+03	6,01E+02	5,98E+02	0,64	0,63	0,59	0,46
378	0,1310	0,0816	0,0834	0,0217	2,75E+03	2,64E+03	5,98E+02	5,83E+02	0,64	0,63	0,58	0,49
379	0,1090	0,0748	0,0549	0,0231	2,80E+03	2,93E+03	6,11E+02	6,28E+02	0,55	0,52	0,52	0,43
380	0,1130	0,0769	0,0600	0,0220	2,84E+03	2,81E+03	6,18E+02	6,04E+02	0,60	0,57	0,55	0,44

Evaluation Run CFD	AvMagoa [m/s]	Avxoa [m/s]	Avyoa [m/s]	Avzoa [m/s]	Thrust RR1 [N]	Thrust RR2 [N]	Torque RR1 [Nm]	Torque RR2 [Nm]	Uniformity VelMag_oa [-]	Uniformity Velx_oa [-]	Uniformity Vely_oa [-]	Uniformity Velz_oa [-]
381	0,1050	0,0698	0,0557	0,0236	2,80E+03	2,80E+03	6,12E+02	6,03E+02	0,59	0,57	0,54	0,45
382	0,1090	0,0759	0,0560	0,0197	2,82E+03	2,94E+03	6,09E+02	6,29E+02	0,56	0,53	0,53	0,43
383	0,1120	0,0767	0,0601	0,0174	2,84E+03	2,88E+03	6,10E+02	6,14E+02	0,61	0,57	0,56	0,43
384	0,1130	0,0779	0,0595	0,0205	2,75E+03	2,81E+03	5,99E+02	6,04E+02	0,60	0,57	0,55	0,46
385	0,0946	0,0595	0,0551	0,0206	2,73E+03	2,51E+03	5,93E+02	5,68E+02	0,60	0,59	0,54	0,43
386	0,1060	0,0718	0,0577	0,0200	2,75E+03	2,76E+03	5,97E+02	5,98E+02	0,61	0,58	0,55	0,46
387	0,1150	0,0795	0,0609	0,0212	2,77E+03	2,66E+03	6,00E+02	5,80E+02	0,60	0,56	0,55	0,44
388	0,1180	0,0797	0,0643	0,0235	2,76E+03	2,94E+03	6,08E+02	6,29E+02	0,55	0,51	0,53	0,48
389	0,1160	0,0800	0,0642	0,0207	2,77E+03	2,91E+03	6,07E+02	6,19E+02	0,58	0,55	0,55	0,45
390	0,1230	0,0842	0,0665	0,0247	2,76E+03	2,80E+03	6,08E+02	6,02E+02	0,58	0,54	0,55	0,46
391	0,1260	0,0859	0,0693	0,0211	2,68E+03	2,96E+03	5,91E+02	6,33E+02	0,56	0,51	0,54	0,48
392	0,1250	0,0878	0,0692	0,0177	2,76E+03	2,90E+03	6,01E+02	6,17E+02	0,59	0,56	0,56	0,46
393	0,1210	0,0832	0,0664	0,0209	2,80E+03	2,70E+03	6,06E+02	5,89E+02	0,59	0,56	0,55	0,45
394	0,1260	0,0860	0,0688	0,0232	2,66E+03	2,94E+03	5,86E+02	6,31E+02	0,56	0,51	0,54	0,48
395	0,1280	0,0884	0,0716	0,0197	2,67E+03	2,97E+03	5,89E+02	6,30E+02	0,58	0,55	0,55	0,48
396	0,1210	0,0837	0,0670	0,0210	2,70E+03	2,71E+03	5,91E+02	5,88E+02	0,59	0,55	0,55	0,45
397	0,1230	0,0795	0,0744	0,0254	2,75E+03	2,93E+03	6,05E+02	6,29E+02	0,59	0,55	0,55	0,47
398	0,1250	0,0838	0,0747	0,0215	2,74E+03	2,97E+03	6,04E+02	6,31E+02	0,61	0,58	0,57	0,47
399	0,1250	0,0832	0,0742	0,0234	2,76E+03	2,77E+03	6,06E+02	5,98E+02	0,60	0,57	0,57	0,48
400	0,1340	0,0869	0,0813	0,0225	2,74E+03	2,90E+03	6,01E+02	6,25E+02	0,60	0,56	0,56	0,48
401	0,1440	0,0962	0,0871	0,0197	2,71E+03	2,91E+03	5,96E+02	6,22E+02	0,62	0,58	0,58	0,48
402	0,1340	0,0897	0,0806	0,0203	2,75E+03	2,81E+03	6,00E+02	6,06E+02	0,61	0,58	0,57	0,48
403	0,1310	0,0857	0,0795	0,0237	2,71E+03	2,91E+03	5,92E+02	6,26E+02	0,60	0,56	0,57	0,47
404	0,1400	0,0931	0,0852	0,0203	2,69E+03	3,00E+03	5,91E+02	6,37E+02	0,61	0,57	0,57	0,49
405	0,1370	0,0919	0,0820	0,0214	2,67E+03	2,74E+03	5,89E+02	5,95E+02	0,60	0,57	0,57	0,50
406	0,1260	0,0783	0,0806	0,0267	2,75E+03	2,85E+03	6,04E+02	6,19E+02	0,61	0,58	0,57	0,48

Evaluation Run CFD	AvMagoa [m/s]	Avxoa [m/s]	Avyoa [m/s]	Avzoa [m/s]	Thrust RR1 [N]	Thrust RR2 [N]	Torque RR1 [Nm]	Torque RR2 [Nm]	Uniformity VelMag_oa [-]	Uniformity Velx_oa [-]	Uniformity Vely_oa [-]	Uniformity Velz_oa [-]
407	0,1400	0,0894	0,0885	0,0240	2,76E+03	2,91E+03	6,08E+02	6,24E+02	0,63	0,60	0,58	0,49
408	0,1360	0,0863	0,0859	0,0251	2,75E+03	2,76E+03	6,06E+02	6,01E+02	0,62	0,59	0,58	0,48
409	0,1350	0,0843	0,0871	0,0235	2,74E+03	2,82E+03	5,97E+02	6,16E+02	0,62	0,59	0,58	0,47
410	0,1410	0,0915	0,0888	0,0202	2,73E+03	2,82E+03	5,99E+02	6,10E+02	0,63	0,61	0,58	0,48
411	0,1460	0,0935	0,0932	0,0210	2,72E+03	2,83E+03	5,98E+02	6,12E+02	0,63	0,60	0,58	0,48
412	0,1350	0,0832	0,0878	0,0235	2,70E+03	2,88E+03	5,92E+02	6,23E+02	0,61	0,58	0,57	0,47
413	0,1370	0,0888	0,0876	0,0201	2,68E+03	2,81E+03	5,89E+02	6,08E+02	0,63	0,61	0,58	0,49
414	0,1070	0,0711	0,0615	0,0201	2,73E+03	2,61E+03	5,95E+02	5,81E+02	0,63	0,62	0,54	0,44
415	0,1230	0,0736	0,0797	0,0265	2,82E+03	2,84E+03	6,16E+02	6,17E+02	0,61	0,60	0,57	0,47
416	0,1370	0,0851	0,0883	0,0242	2,83E+03	2,79E+03	6,21E+02	6,05E+02	0,63	0,62	0,58	0,48
417	0,1290	0,0812	0,0819	0,0235	2,76E+03	2,65E+03	6,07E+02	5,83E+02	0,63	0,62	0,58	0,46
418	0,1340	0,0827	0,0866	0,0238	2,74E+03	2,81E+03	5,99E+02	6,12E+02	0,63	0,62	0,58	0,47
419	0,1400	0,0886	0,0900	0,0206	2,72E+03	2,83E+03	5,93E+02	6,14E+02	0,65	0,63	0,59	0,47
420	0,1540	0,0963	0,0995	0,0222	2,74E+03	2,68E+03	6,00E+02	5,89E+02	0,64	0,62	0,59	0,47
421	0,1360	0,0823	0,0887	0,0248	2,72E+03	2,84E+03	5,95E+02	6,16E+02	0,62	0,60	0,57	0,45
422	0,1480	0,0926	0,0969	0,0208	2,68E+03	3,01E+03	5,91E+02	6,44E+02	0,64	0,62	0,59	0,48
423	0,1470	0,0910	0,0956	0,0238	2,68E+03	2,72E+03	5,91E+02	5,94E+02	0,64	0,61	0,59	0,50
424	0,1280	0,0761	0,0815	0,0282	2,77E+03	2,83E+03	6,08E+02	6,17E+02	0,61	0,60	0,56	0,47
425	0,1360	0,0830	0,0869	0,0245	2,78E+03	2,78E+03	6,10E+02	6,04E+02	0,63	0,62	0,58	0,47
426	0,1340	0,0811	0,0862	0,0240	2,78E+03	2,70E+03	6,10E+02	5,93E+02	0,62	0,61	0,58	0,45
427	0,1310	0,0802	0,0824	0,0256	2,76E+03	2,79E+03	5,99E+02	6,10E+02	0,63	0,63	0,57	0,46
428	0,1480	0,0919	0,0943	0,0217	2,71E+03	2,76E+03	5,95E+02	6,00E+02	0,65	0,64	0,59	0,47
429	0,1370	0,0866	0,0861	0,0215	2,57E+03	2,67E+03	5,71E+02	5,87E+02	0,65	0,64	0,58	0,44
430	0,1390	0,0837	0,0898	0,0251	2,70E+03	2,81E+03	5,91E+02	6,15E+02	0,62	0,60	0,57	0,45
431	0,1410	0,0879	0,0903	0,0214	2,65E+03	2,77E+03	5,83E+02	6,02E+02	0,64	0,63	0,59	0,45
432	0,1410	0,0870	0,0902	0,0226	2,69E+03	2,67E+03	5,92E+02	5,87E+02	0,64	0,62	0,59	0,50

Evaluation Run CFD	AvMagoa [m/s]	Avxoa [m/s]	Avyoa [m/s]	Avzoa [m/s]	Thrust RR1 [N]	Thrust RR2 [N]	Torque RR1 [Nm]	Torque RR2 [Nm]	Uniformity VelMag_oa [-]	Uniformity Velx_oa [-]	Uniformity Vely_oa [-]	Uniformity Velz_oa [-]
433	0,1310	0,0785	0,0817	0,0281	2,80E+03	2,76E+03	6,14E+02	6,06E+02	0,61	0,61	0,57	0,47
434	0,1330	0,0821	0,0829	0,0247	2,78E+03	2,74E+03	6,10E+02	5,98E+02	0,63	0,62	0,58	0,46
435	0,1320	0,0810	0,0829	0,0248	2,79E+03	2,72E+03	6,12E+02	5,95E+02	0,62	0,61	0,57	0,45
436	0,1410	0,0869	0,0879	0,0256	2,69E+03	2,77E+03	5,91E+02	6,08E+02	0,63	0,62	0,58	0,46
437	0,1460	0,0904	0,0921	0,0210	2,75E+03	2,71E+03	6,01E+02	5,95E+02	0,64	0,62	0,59	0,46
438	0,1420	0,0882	0,0904	0,0212	2,75E+03	2,67E+03	6,01E+02	5,89E+02	0,63	0,62	0,58	0,45
439	0,1330	0,0820	0,0836	0,0251	2,70E+03	2,79E+03	5,92E+02	6,11E+02	0,62	0,61	0,57	0,45
440	0,1360	0,0858	0,0846	0,0214	2,70E+03	2,70E+03	5,92E+02	5,93E+02	0,64	0,63	0,58	0,44
441	0,1340	0,0977	0,0977	0,0234	2,65E+03	2,63E+03	5,84E+02	5,81E+02	0,64	0,63	0,58	0,47

Appendix D

Ranking mixer settings out of the CFD study

Ranking	Evaluation Run CFD	AngleLRRR1 [°]	AngleLRRR2 [°]	TransRR1_Z [m]	TransRR2_Z [m]	ΣTBS	TB% (in relation to ideal score)
1	369	75	75	3,80	3,80	203	**74,91%**
2	306	60	75	3,80	3,80	191	**70,48%**
3	305	60	75	3,80	2,80	185	**68,27%**
4	239	45	75	2,80	2,80	184	**67,90%**
5	231	45	60	2,80	3,80	180	**66,42%**
6	222	45	45	2,80	3,80	178	**65,68%**
7	284	60	45	2,80	2,80	178	**65,68%**
8	243	45	75	3,80	3,80	177	**65,31%**
9	233	45	60	3,80	2,80	175	**64,58%**
10	241	45	75	3,80	1,80	175	**64,58%**
11	287	60	45	3,80	2,80	175	**64,58%**
12	353	75	60	1,80	2,80	175	**64,58%**
13	360	75	60	3,80	3,80	173	**63,84%**
14	171	30	60	3,80	3,80	171	**63,10%**
15	180	30	75	3,80	3,80	171	**63,10%**
16	188	30	90	3,80	2,80	171	**63,10%**
17	343	75	45	1,80	1,80	171	**63,10%**
18	352	75	60	1,80	1,80	171	**63,10%**
19	356	75	60	2,80	2,80	171	**63,10%**
20	365	75	75	2,80	2,80	170	**62,73%**
21	162	30	45	3,80	3,80	169	**62,36%**
22	236	45	75	1,80	2,80	169	**62,36%**
23	408	90	45	1,80	3,80	169	**62,36%**
24	179	30	75	3,80	2,80	167	**61,62%**
25	281	60	45	1,80	2,80	167	**61,62%**
26	291	60	60	1,80	3,80	167	**61,62%**
27	308	60	90	1,80	2,80	167	**61,62%**
28	315	60	90	3,80	3,80	167	**61,62%**
29	296	60	60	3,80	2,80	166	**61,25%**
30	240	45	75	2,80	3,80	165	**60,89%**
31	242	45	75	3,80	2,80	165	**60,89%**
32	286	60	45	3,80	1,80	165	**60,89%**
33	289	60	60	1,80	1,80	165	**60,89%**
34	300	60	75	1,80	3,80	165	**60,89%**
35	350	75	45	3,80	2,80	164	**60,52%**

Ranking	Evaluation Run CFD	AngleLRRR1 [°]	AngleLRRR2 [°]	TransRR1_Z [m]	TransRR2_Z [m]	ΣTBS	TB% (in relation to ideal score)
36	164	30	60	1,80	2,80	163	**60,15%**
37	177	30	75	2,80	3,80	163	**60,15%**
38	297	60	60	3,80	3,80	163	**60,15%**
39	351	75	45	3,80	3,80	163	**60,15%**
40	423	90	60	3,80	3,80	163	**60,15%**
41	302	60	75	2,80	2,80	162	**59,78%**
42	5	0	0	2,80	2,80	161	**59,41%**
43	234	45	60	3,80	3,80	161	**59,41%**
44	288	60	45	3,80	3,80	161	**59,41%**
45	366	75	75	2,80	3,80	161	**59,41%**
46	348	75	45	2,80	3,80	160	**59,04%**
47	252	45	90	3,80	3,80	159	**58,67%**
48	292	60	60	2,80	1,80	159	**58,67%**
49	299	60	75	1,80	2,80	159	**58,67%**
50	312	60	90	2,80	3,80	159	**58,67%**
51	377	75	90	3,80	2,80	159	**58,67%**
52	432	90	75	3,80	3,80	159	**58,67%**
53	368	75	75	3,80	2,80	158	**58,30%**
54	374	75	90	2,80	2,80	158	**58,30%**
55	1	0	0	1,80	1,80	157	**57,93%**
56	116	15	75	3,80	2,80	157	**57,93%**
57	373	75	90	2,80	1,80	157	**57,93%**
58	378	75	90	3,80	3,80	157	**57,93%**
59	428	90	75	2,80	2,80	157	**57,93%**
60	183	30	90	1,80	3,80	155	**57,20%**
61	211	45	30	2,80	1,80	155	**57,20%**
62	214	45	30	3,80	1,80	155	**57,20%**
63	294	60	60	2,80	3,80	155	**57,20%**
64	429	90	75	2,80	3,80	155	**57,20%**
65	436	90	90	2,80	1,80	155	**57,20%**
66	293	60	60	2,80	2,80	154	**56,83%**
67	4	0	0	2,80	1,80	153	**56,46%**
68	8	0	0	3,80	2,80	153	**56,46%**
69	166	30	60	2,80	1,80	153	**56,46%**
70	247	45	90	2,80	1,80	153	**56,46%**
71	301	60	75	2,80	1,80	153	**56,46%**
72	375	75	90	2,80	3,80	153	**56,46%**
73	376	75	90	3,80	1,80	153	**56,46%**
74	427	90	75	2,80	1,80	153	**56,46%**
75	441	90	90	3,80	3,80	153	**56,46%**
76	167	30	60	2,80	2,80	152	**56,09%**
77	230	45	60	2,80	2,80	152	**56,09%**

Ranking	Evaluation Run CFD	AngleLRRR1 [°]	AngleLRRR2 [°]	TransRR1_Z [m]	TransRR2_Z [m]	ΣTBS	TB% (in relation to ideal score)
78	101	15	60	1,80	2,80	151	**55,72%**
79	153	30	30	3,80	3,80	151	**55,72%**
80	237	45	75	1,80	3,80	151	**55,72%**
81	277	60	30	3,80	1,80	151	**55,72%**
82	295	60	60	3,80	1,80	151	**55,72%**
83	303	60	75	2,80	3,80	151	**55,72%**
84	313	60	90	3,80	1,80	151	**55,72%**
85	363	75	75	1,80	3,80	151	**55,72%**
86	409	90	45	2,80	1,80	151	**55,72%**
87	413	90	45	3,80	2,80	151	**55,72%**
88	221	45	45	2,80	2,80	150	**55,35%**
89	338	75	30	2,80	2,80	150	**55,35%**
90	359	75	60	3,80	2,80	150	**55,35%**
91	2	0	0	1,80	2,80	149	**54,98%**
92	99	15	45	3,80	3,80	149	**54,98%**
93	168	30	60	2,80	3,80	149	**54,98%**
94	216	45	30	3,80	3,80	149	**54,98%**
95	226	45	60	1,80	1,80	149	**54,98%**
96	280	60	45	1,80	1,80	149	**54,98%**
97	283	60	45	2,80	1,80	149	**54,98%**
98	314	60	90	3,80	2,80	149	**54,98%**
99	342	75	30	3,80	3,80	149	**54,98%**
100	345	75	45	1,80	3,80	149	**54,98%**
101	346	75	45	2,80	1,80	149	**54,98%**
102	362	75	75	1,80	2,80	149	**54,98%**
103	411	90	45	2,80	3,80	149	**54,98%**
104	420	90	60	2,80	3,80	149	**54,98%**
105	431	90	75	3,80	2,80	149	**54,98%**
106	357	75	60	2,80	3,80	148	**54,61%**
107	223	45	45	3,80	1,80	147	**54,24%**
108	225	45	45	3,80	3,80	147	**54,24%**
109	238	45	75	2,80	1,80	147	**54,24%**
110	244	45	90	1,80	1,80	147	**54,24%**
111	251	45	90	3,80	2,80	147	**54,24%**
112	276	60	30	2,80	3,80	147	**54,24%**
113	285	60	45	2,80	3,80	147	**54,24%**
114	304	60	75	3,80	1,80	147	**54,24%**
115	355	75	60	2,80	1,80	147	**54,24%**
116	358	75	60	3,80	1,80	147	**54,24%**
117	403	90	30	3,80	1,80	147	**54,24%**
118	407	90	45	1,80	2,80	147	**54,24%**
119	419	90	60	2,80	2,80	147	**54,24%**

Ranking	Evaluation Run CFD	AngleLRRR1 [°]	AngleLRRR2 [°]	TransRR1_Z [m]	TransRR2_Z [m]	ΣTBS	TB% (in relation to ideal score)
120	224	45	45	3,80	2,80	146	**53,87%**
121	213	45	30	2,80	3,80	145	**53,51%**
122	220	45	45	2,80	1,80	145	**53,51%**
123	227	45	60	1,80	2,80	145	**53,51%**
124	290	60	60	1,80	2,80	145	**53,51%**
125	311	60	90	2,80	2,80	145	**53,51%**
126	344	75	45	1,80	2,80	145	**53,51%**
127	364	75	75	2,80	1,80	145	**53,51%**
128	425	90	75	1,80	2,80	145	**53,51%**
129	434	90	90	1,80	2,80	145	**53,51%**
130	437	90	90	2,80	2,80	145	**53,51%**
131	249	45	90	2,80	3,80	143	**52,77%**
132	361	75	75	1,80	1,80	143	**52,77%**
133	416	90	60	1,80	2,80	143	**52,77%**
134	27	0	30	3,80	3,80	141	**52,03%**
135	159	30	45	2,80	3,80	141	**52,03%**
136	170	30	60	3,80	2,80	141	**52,03%**
137	271	60	30	1,80	1,80	141	**52,03%**
138	307	60	90	1,80	1,80	141	**52,03%**
139	336	75	30	1,80	3,80	141	**52,03%**
140	418	90	60	2,80	1,80	141	**52,03%**
141	440	90	90	3,80	2,80	141	**52,03%**
142	347	75	45	2,80	2,80	140	**51,66%**
143	45	0	60	3,80	3,80	139	**51,29%**
144	187	30	90	3,80	1,80	139	**51,29%**
145	215	45	30	3,80	2,80	139	**51,29%**
146	232	45	60	3,80	1,80	139	**51,29%**
147	310	60	90	2,80	1,80	139	**51,29%**
148	330	75	15	2,80	3,80	139	**51,29%**
149	337	75	30	2,80	1,80	139	**51,29%**
150	371	75	90	1,80	2,80	139	**51,29%**
151	405	90	30	3,80	3,80	139	**51,29%**
152	410	90	45	2,80	2,80	139	**51,29%**
153	438	90	90	2,80	3,80	139	**51,29%**
154	161	30	45	3,80	2,80	138	**50,92%**
155	212	45	30	2,80	2,80	138	**50,92%**
156	52	0	75	3,80	1,80	137	**50,55%**
157	63	0	90	3,80	3,80	137	**50,55%**
158	228	45	60	1,80	3,80	137	**50,55%**
159	250	45	90	3,80	1,80	137	**50,55%**
160	279	60	30	3,80	3,80	137	**50,55%**
161	367	75	75	3,80	1,80	137	**50,55%**

Ranking	Evaluation Run CFD	AngleLRRR1 [°]	AngleLRRR2 [°]	TransRR1_Z [m]	TransRR2_Z [m]	ΣTBS	TB% (in relation to ideal score)
162	370	75	90	1,80	1,80	137	**50,55%**
163	412	90	45	3,80	1,80	137	**50,55%**
164	433	90	90	1,80	1,80	137	**50,55%**
165	185	30	90	2,80	2,80	136	**50,18%**
166	278	60	30	3,80	2,80	136	**50,18%**
167	339	75	30	2,80	3,80	136	**50,18%**
168	10	0	15	1,80	1,80	135	**49,82%**
169	19	0	30	1,80	1,80	135	**49,82%**
170	36	0	45	3,80	3,80	135	**49,82%**
171	44	0	60	3,80	2,80	135	**49,82%**
172	57	0	90	1,80	3,80	135	**49,82%**
173	217	45	45	1,80	1,80	135	**49,82%**
174	235	45	75	1,80	1,80	135	**49,82%**
175	298	60	75	1,80	1,80	135	**49,82%**
176	334	75	30	1,80	1,80	135	**49,82%**
177	31	0	45	2,80	1,80	133	**49,08%**
178	37	0	60	1,80	1,80	133	**49,08%**
179	113	15	75	2,80	2,80	133	**49,08%**
180	119	15	90	1,80	2,80	133	**49,08%**
181	125	15	90	3,80	2,80	133	**49,08%**
182	421	90	60	3,80	1,80	133	**49,08%**
183	424	90	75	1,80	1,80	133	**49,08%**
184	439	90	90	3,80	1,80	133	**49,08%**
185	104	15	60	2,80	2,80	132	**48,71%**
186	148	30	30	2,80	1,80	131	**48,34%**
187	152	30	30	3,80	2,80	131	**48,34%**
188	172	30	75	1,80	1,80	131	**48,34%**
189	174	30	75	1,80	3,80	131	**48,34%**
190	178	30	75	3,80	1,80	131	**48,34%**
191	229	45	60	2,80	1,80	131	**48,34%**
192	282	60	45	1,80	3,80	131	**48,34%**
193	349	75	45	3,80	1,80	131	**48,34%**
194	402	90	30	2,80	3,80	131	**48,34%**
195	422	90	60	3,80	2,80	131	**48,34%**
196	426	90	75	1,80	3,80	131	**48,34%**
197	149	30	30	2,80	2,80	130	**47,97%**
198	176	30	75	2,80	2,80	130	**47,97%**
199	11	0	15	1,80	2,80	129	**47,60%**
200	14	0	15	2,80	2,80	129	**47,60%**
201	22	0	30	2,80	1,80	129	**47,60%**
202	46	0	75	1,80	1,80	129	**47,60%**
203	51	0	75	2,80	3,80	129	**47,60%**

Ranking	Evaluation Run CFD	AngleLRRR1 [°]	AngleLRRR2 [°]	TransRR1_Z [m]	TransRR2_Z [m]	ΣTBS	TB% (in relation to ideal score)
204	108	15	60	3,80	3,80	129	**47,60%**
205	123	15	90	2,80	3,80	129	**47,60%**
206	275	60	30	2,80	2,80	128	**47,23%**
207	341	75	30	3,80	2,80	128	**47,23%**
208	6	0	0	2,80	3,80	127	**46,86%**
209	25	0	30	3,80	1,80	127	**46,86%**
210	34	0	45	3,80	1,80	127	**46,86%**
211	43	0	60	3,80	1,80	127	**46,86%**
212	50	0	75	2,80	2,80	127	**46,86%**
213	156	30	45	1,80	3,80	127	**46,86%**
214	175	30	75	2,80	1,80	127	**46,86%**
215	272	60	30	1,80	2,80	127	**46,86%**
216	273	60	30	1,80	3,80	127	**46,86%**
217	430	90	75	3,80	1,80	127	**46,86%**
218	435	90	90	1,80	3,80	127	**46,86%**
219	17	0	15	3,80	2,80	125	**46,13%**
220	54	0	75	3,80	3,80	125	**46,13%**
221	98	15	45	3,80	2,80	125	**46,13%**
222	106	15	60	3,80	1,80	125	**46,13%**
223	115	15	75	3,80	1,80	125	**46,13%**
224	169	30	60	3,80	1,80	125	**46,13%**
225	184	30	90	2,80	1,80	125	**46,13%**
226	186	30	90	2,80	3,80	125	**46,13%**
227	274	60	30	2,80	1,80	125	**46,13%**
228	41	0	60	2,80	2,80	123	**45,39%**
229	173	30	75	1,80	2,80	123	**45,39%**
230	322	75	0	3,80	1,80	123	**45,39%**
231	325	75	15	1,80	1,80	123	**45,39%**
232	328	75	15	2,80	1,80	123	**45,39%**
233	354	75	60	1,80	3,80	123	**45,39%**
234	390	90	15	1,80	3,80	123	**45,39%**
235	404	90	30	3,80	2,80	123	**45,39%**
236	417	90	60	1,80	3,80	123	**45,39%**
237	401	90	30	2,80	2,80	122	**45,02%**
238	160	30	45	3,80	1,80	121	**44,65%**
239	163	30	60	1,80	1,80	121	**44,65%**
240	246	45	90	1,80	3,80	121	**44,65%**
241	248	45	90	2,80	2,80	121	**44,65%**
242	264	60	15	1,80	3,80	121	**44,65%**
243	309	60	90	1,80	3,80	121	**44,65%**
244	9	0	0	3,80	3,80	119	**43,91%**
245	28	0	45	1,80	1,80	119	**43,91%**

Ranking	Evaluation Run CFD	AngleLRRR1 [°]	AngleLRRR2 [°]	TransRR1_Z [m]	TransRR2_Z [m]	ΣTBS	TB% (in relation to ideal score)
246	90	15	30	3,80	3,80	119	**43,91%**
247	107	15	60	3,80	2,80	119	**43,91%**
248	110	15	75	1,80	2,80	119	**43,91%**
249	117	15	75	3,80	3,80	119	**43,91%**
250	120	15	90	1,80	3,80	119	**43,91%**
251	124	15	90	3,80	1,80	119	**43,91%**
252	151	30	30	3,80	1,80	119	**43,91%**
253	181	30	90	1,80	1,80	119	**43,91%**
254	208	45	30	1,80	1,80	119	**43,91%**
255	245	45	90	1,80	2,80	119	**43,91%**
256	333	75	15	3,80	3,80	119	**43,91%**
257	335	75	30	1,80	2,80	119	**43,91%**
258	340	75	30	3,80	1,80	119	**43,91%**
259	400	90	30	2,80	1,80	119	**43,91%**
260	406	90	45	1,80	1,80	119	**43,91%**
261	35	0	45	3,80	2,80	117	**43,17%**
262	42	0	60	2,80	3,80	117	**43,17%**
263	102	15	60	1,80	3,80	117	**43,17%**
264	165	30	60	1,80	3,80	117	**43,17%**
265	210	45	30	1,80	3,80	117	**43,17%**
266	265	60	15	2,80	1,80	117	**43,17%**
267	268	60	15	3,80	1,80	117	**43,17%**
268	20	0	30	1,80	2,80	115	**42,44%**
269	60	0	90	2,80	3,80	115	**42,44%**
270	122	15	90	2,80	2,80	115	**42,44%**
271	155	30	45	1,80	2,80	115	**42,44%**
272	182	30	90	1,80	2,80	115	**42,44%**
273	207	45	15	3,80	3,80	115	**42,44%**
274	218	45	45	1,80	2,80	115	**42,44%**
275	318	75	0	1,80	3,80	115	**42,44%**
276	393	90	15	2,80	3,80	115	**42,44%**
277	415	90	60	1,80	1,80	115	**42,44%**
278	7	0	0	3,80	1,80	113	**41,70%**
279	18	0	15	3,80	3,80	113	**41,70%**
280	23	0	30	2,80	2,80	113	**41,70%**
281	24	0	30	2,80	3,80	113	**41,70%**
282	64	15	0	1,80	1,80	113	**41,70%**
283	67	15	0	2,80	1,80	113	**41,70%**
284	93	15	45	1,80	3,80	113	**41,70%**
285	189	30	90	3,80	3,80	113	**41,70%**
286	204	45	15	2,80	3,80	113	**41,70%**
287	253	60	0	1,80	1,80	113	**41,70%**

Ranking	Evaluation Run CFD	AngleLRRR1 [°]	AngleLRRR2 [°]	TransRR1_Z [m]	TransRR2_Z [m]	ΣTBS	TB% (in relation to ideal score)
288	372	75	90	1,80	3,80	113	**41,70%**
289	396	90	15	3,80	3,80	113	**41,70%**
290	399	90	30	1,80	3,80	113	**41,70%**
291	13	0	15	2,80	1,80	111	**40,96%**
292	48	0	75	1,80	3,80	111	**40,96%**
293	91	15	45	1,80	1,80	111	**40,96%**
294	103	15	60	2,80	1,80	111	**40,96%**
295	126	15	90	3,80	3,80	111	**40,96%**
296	270	60	15	3,80	3,80	111	**40,96%**
297	49	0	75	2,80	1,80	109	**40,22%**
298	62	0	90	3,80	2,80	109	**40,22%**
299	72	15	0	3,80	3,80	109	**40,22%**
300	81	15	15	3,80	3,80	109	**40,22%**
301	94	15	45	2,80	1,80	109	**40,22%**
302	100	15	60	1,80	1,80	109	**40,22%**
303	118	15	90	1,80	1,80	109	**40,22%**
304	146	30	30	1,80	2,80	109	**40,22%**
305	154	30	45	1,80	1,80	109	**40,22%**
306	209	45	30	1,80	2,80	109	**40,22%**
307	219	45	45	1,80	3,80	109	**40,22%**
308	395	90	15	3,80	2,80	109	**40,22%**
309	266	60	15	2,80	2,80	108	**39,85%**
310	16	0	15	3,80	1,80	107	**39,48%**
311	61	0	90	3,80	1,80	107	**39,48%**
312	65	15	0	1,80	2,80	107	**39,48%**
313	88	15	30	3,80	1,80	107	**39,48%**
314	96	15	45	2,80	3,80	107	**39,48%**
315	105	15	60	2,80	3,80	107	**39,48%**
316	121	15	90	2,80	1,80	107	**39,48%**
317	143	30	15	3,80	2,80	107	**39,48%**
318	145	30	30	1,80	1,80	107	**39,48%**
319	147	30	30	1,80	3,80	107	**39,48%**
320	157	30	45	2,80	1,80	107	**39,48%**
321	267	60	15	2,80	3,80	107	**39,48%**
322	269	60	15	3,80	2,80	107	**39,48%**
323	320	75	0	2,80	2,80	107	**39,48%**
324	387	90	0	3,80	3,80	107	**39,48%**
325	414	90	45	3,80	3,80	107	**39,48%**
326	26	0	30	3,80	2,80	105	**38,75%**
327	30	0	45	1,80	3,80	105	**38,75%**
328	53	0	75	3,80	2,80	105	**38,75%**
329	55	0	90	1,80	1,80	105	**38,75%**

Ranking	Evaluation Run CFD	AngleLRRR1 [°]	AngleLRRR2 [°]	TransRR1_Z [m]	TransRR2_Z [m]	ΣTBS	TB% (in relation to ideal score)
330	71	15	0	3,80	2,80	105	**38,75%**
331	78	15	15	2,80	3,80	105	**38,75%**
332	84	15	30	1,80	3,80	105	**38,75%**
333	89	15	30	3,80	2,80	105	**38,75%**
334	97	15	45	3,80	1,80	105	**38,75%**
335	206	45	15	3,80	2,80	105	**38,75%**
336	326	75	15	1,80	2,80	105	**38,75%**
337	332	75	15	3,80	2,80	105	**38,75%**
338	385	90	0	3,80	1,80	105	**38,75%**
339	394	90	15	3,80	1,80	105	**38,75%**
340	397	90	30	1,80	1,80	105	**38,75%**
341	86	15	30	2,80	2,80	104	**38,38%**
342	95	15	45	2,80	2,80	104	**38,38%**
343	3	0	0	1,80	3,80	103	**38,01%**
344	33	0	45	2,80	3,80	103	**38,01%**
345	58	0	90	2,80	1,80	103	**38,01%**
346	68	15	0	2,80	2,80	103	**38,01%**
347	87	15	30	2,80	3,80	103	**38,01%**
348	109	15	75	1,80	1,80	103	**38,01%**
349	111	15	75	1,80	3,80	103	**38,01%**
350	114	15	75	2,80	3,80	103	**38,01%**
351	144	30	15	3,80	3,80	103	**38,01%**
352	192	45	0	1,80	3,80	103	**38,01%**
353	198	45	0	3,80	3,80	103	**38,01%**
354	324	75	0	3,80	3,80	103	**38,01%**
355	331	75	15	3,80	1,80	103	**38,01%**
356	392	90	15	2,80	2,80	103	**38,01%**
357	83	15	30	1,80	2,80	101	**37,27%**
358	261	60	0	3,80	3,80	101	**37,27%**
359	327	75	15	1,80	3,80	101	**37,27%**
360	381	90	0	1,80	3,80	101	**37,27%**
361	384	90	0	2,80	3,80	101	**37,27%**
362	398	90	30	1,80	2,80	101	**37,27%**
363	329	75	15	2,80	2,80	100	**36,90%**
364	47	0	75	1,80	2,80	99	**36,53%**
365	59	0	90	2,80	2,80	99	**36,53%**
366	131	30	0	2,80	2,80	99	**36,53%**
367	199	45	15	1,80	1,80	99	**36,53%**
368	92	15	45	1,80	2,80	97	**35,79%**
369	135	30	0	3,80	3,80	97	**35,79%**
370	142	30	15	3,80	1,80	97	**35,79%**
371	195	45	0	2,80	3,80	97	**35,79%**

Ranking	Evaluation Run CFD	AngleLRRR1 [°]	AngleLRRR2 [°]	TransRR1_Z [m]	TransRR2_Z [m]	ΣTBS	TB% (in relation to ideal score)
372	205	45	15	3,80	1,80	97	**35,79%**
373	258	60	0	2,80	3,80	97	**35,79%**
374	323	75	0	3,80	2,80	97	**35,79%**
375	386	90	0	3,80	2,80	97	**35,79%**
376	391	90	15	2,80	1,80	97	**35,79%**
377	140	30	15	2,80	2,80	96	**35,42%**
378	32	0	45	2,80	2,80	95	**35,06%**
379	39	0	60	1,80	3,80	95	**35,06%**
380	82	15	30	1,80	1,80	95	**35,06%**
381	112	15	75	2,80	1,80	95	**35,06%**
382	137	30	15	1,80	2,80	95	**35,06%**
383	197	45	0	3,80	2,80	95	**35,06%**
384	201	45	15	1,80	3,80	95	**35,06%**
385	380	90	0	1,80	2,80	95	**35,06%**
386	15	0	15	2,80	3,80	93	**34,32%**
387	129	30	0	1,80	3,80	93	**34,32%**
388	141	30	15	2,80	3,80	93	**34,32%**
389	194	45	0	2,80	2,80	93	**34,32%**
390	196	45	0	3,80	1,80	93	**34,32%**
391	255	60	0	1,80	3,80	93	**34,32%**
392	260	60	0	3,80	2,80	93	**34,32%**
393	263	60	15	1,80	2,80	93	**34,32%**
394	29	0	45	1,80	2,80	91	**33,58%**
395	70	15	0	3,80	1,80	91	**33,58%**
396	128	30	0	1,80	2,80	91	**33,58%**
397	150	30	30	2,80	3,80	91	**33,58%**
398	190	45	0	1,80	1,80	91	**33,58%**
399	389	90	15	1,80	2,80	91	**33,58%**
400	79	15	15	3,80	1,80	89	**32,84%**
401	85	15	30	2,80	1,80	89	**32,84%**
402	130	30	0	2,80	1,80	89	**32,84%**
403	136	30	15	1,80	1,80	89	**32,84%**
404	200	45	15	1,80	2,80	89	**32,84%**
405	257	60	0	2,80	2,80	89	**32,84%**
406	316	75	0	1,80	1,80	89	**32,84%**
407	321	75	0	2,80	3,80	89	**32,84%**
408	388	90	15	1,80	1,80	89	**32,84%**
409	203	45	15	2,80	2,80	88	**32,47%**
410	12	0	15	1,80	3,80	87	**32,10%**
411	73	15	15	1,80	1,80	87	**32,10%**
412	74	15	15	1,80	2,80	87	**32,10%**
413	75	15	15	1,80	3,80	87	**32,10%**

Ranking	Evaluation Run CFD	AngleLRRR1 [°]	AngleLRRR2 [°]	TransRR1_Z [m]	TransRR2_Z [m]	ΣTBS	TB% (in relation to ideal score)
414	76	15	15	2,80	1,80	87	**32,10%**
415	132	30	0	2,80	3,80	87	**32,10%**
416	134	30	0	3,80	2,80	87	**32,10%**
417	139	30	15	2,80	1,80	87	**32,10%**
418	202	45	15	2,80	1,80	87	**32,10%**
419	259	60	0	3,80	1,80	87	**32,10%**
420	383	90	0	2,80	2,80	87	**32,10%**
421	21	0	30	1,80	3,80	85	**31,37%**
422	69	15	0	2,80	3,80	85	**31,37%**
423	127	30	0	1,80	1,80	85	**31,37%**
424	138	30	15	1,80	3,80	85	**31,37%**
425	191	45	0	1,80	2,80	85	**31,37%**
426	262	60	15	1,80	1,80	85	**31,37%**
427	77	15	15	2,80	2,80	84	**31,00%**
428	40	0	60	2,80	1,80	83	**30,63%**
429	56	0	90	1,80	2,80	83	**30,63%**
430	133	30	0	3,80	1,80	83	**30,63%**
431	193	45	0	2,80	1,80	83	**30,63%**
432	319	75	0	2,80	1,80	83	**30,63%**
433	80	15	15	3,80	2,80	81	**29,89%**
434	317	75	0	1,80	2,80	81	**29,89%**
435	66	15	0	1,80	3,80	79	**29,15%**
436	254	60	0	1,80	2,80	79	**29,15%**
437	379	90	0	1,80	1,80	79	**29,15%**
438	158	30	45	2,80	2,80	77	**28,41%**
439	38	0	60	1,80	2,80	75	**27,68%**
440	256	60	0	2,80	1,80	75	**27,68%**
441	382	90	0	2,80	1,80	75	**27,68%**

Appendix E

List of Publications

WIEDEMANN, L., CONTI, F., JANUS, T., SONNLEITNER, M., ZÖRNER, W., GOLDBRUNNER, M., (2017a). Mixing in biogas digesters and development of an artificial substrate for laboratory-scale mixing optimization. Chem. Eng. Technol. 40, 238-247.

WIEDEMANN, L., CONTI, F., JANUS, T., SONNLEITNER, M., ZÖRNER, W., GOLDBRUNNER, M., (2017b). Investigation of fluid dynamic in a scale-down laboratory digester. Proceeding of International Conference Progress in Biogas IV, Stuttgart, ISBN: 978-3-940706-09-6, 112.

WIEDEMANN, L., CONTI, F., JANUS, T., SONNLEITNER, M., ZÖRNER, W., GOLDBRUNNER, M., (2017c). Optimization of the mixing system in biodigesters with computational fluid dynamics (CFD). Proceeding of International Conference Progress in Biogas IV, Stuttgart, ISBN: 978-3-940706-09-6, 147.

WIEDEMANN, L., CONTI, F., SONNLEITNER, M., SAIDI, A., GOLDBRUNNER, M., (2017d). Investigation and optimization of the mixing in a biogas digester with a laboratory experiment and an artificial model substrate. Proceeding of 25th European Biomass Conference and Exhibition EUBCE, Stockholm, in press.

CONTI, F., WIEDEMANN, L., JANUS, T., SONNLEITNER, M., ZÖRNER, W., GOLDBRUNNER, M., (2016). Mixing in biogas digesters: correlation between laboratory experiments on artificial substrate and simulations with computational fluid dynamics. Proceeding of 10. Rostock Bioenergy Forum, Rostock, ISBN: 978-3-86009-433-4, 58, 445-450.

CONTI, F., WIEDEMANN, L., SAIDI, A., SONNLEITNER, M., GOLDBRUNNER, M., (2018). Mixing of a model substrate in a scale-down laboratory digester and processing with a computational fluid dynamics model. Proceeding of 26th European Biomass Conference and Exhibition EUBCE, Copenhagen, Denmark.

CONTI, F., WIEDEMANN, L., SONNLEITNER, M., GOLDBRUNNER, M., (2018). Thermal behaviour of viscosity of aqueous cellulose solutions to emulate biomass in anaerobic digesters NewJ.Chem., 2018, 42, 1099, DOI: 10.1039/c7nj03199h

CONTI, F., WIEDEMANN, L., SONNLEITNER, M., SAIDI, A., GOLDBRUNNER, M., (2018). Monitoring the mixing of an artificial model substrate in a scale-down laboratory digester, Elsevier Ltd. Renewable Energy, Volume 132, 2019, Pages 351-362